

①

[REDACTED]

AD C 027914

ROSENSTIEL SCHOOL OF MARINE AND ATMOSPHERIC SCIENCE

UNIVERSITY OF MIAMI

4600 RICKENBACKER CAUSEWAY

MIAMI, FLORIDA 33149

THE M7 COMMUNICATION SYSTEM [REDACTED]

FINAL REPORT OF CONTRACT

NO. N00014-80C-0418

CLASSIFIED BY: NAVINST C5511.5 OF 1 OCT 74
~~EXEMPT FROM GDS OF EO 11652~~
~~EXEMPTION CATEGORY: 3~~
DECLASSIFY ON: 31 DECEMBER 2007

DECLASSIFIED BY: Chief of Naval Research
DATE: 7 April 2021

CHRISTOPHER V. KIMBALL

26 JULY 1979

DTIC ELECTE
S D
APR 20 1982
A

DTIC FILE COPY

COPY NUMBER:

3 of 44

[REDACTED]

[REDACTED]

82 9 12 521

[REDACTED]

ROSENSTIEL SCHOOL OF MARINE AND ATMOSPHERIC SCIENCE

UNIVERSITY OF MIAMI
4600 RICKENBACKER CAUSEWAY
MIAMI, FLORIDA 33149

THE M7 COMMUNICATION SYSTEM [REDACTED]

FINAL REPORT OF CONTRACT

NO. N00014-80C-0418

CHRISTOPHER V. KIMBALL

26 JULY 1979

[REDACTED]

REPORT DOCUMENTATION PAGE		READ INSTRUCTIONS BEFORE COMPLETING FORM	
1. REPORT NUMBER	2. GOVT ACCESSION NO. AD-C027914	3. RECIPIENT'S CATALOG NUMBER	
4. TITLE (and Subtitle) THE M7 COMMUNICATION SYSTEM FINAL REPORT OF CONTRACT NO. N00014-80-C-0418		5. TYPE OF REPORT & PERIOD COVERED FINAL REPORT	
		6. PERFORMING ORG. REPORT NUMBER	
7. AUTHOR(s) Christopher V. KIMBALL		8. CONTRACT OR GRANT NUMBER(s) N00014-80C-0418	
9. PERFORMING ORGANIZATION NAME AND ADDRESS Rosenstiel School of Marine and Atmospheric Science University of Miami, 4600 Rickenbacker Causeway Miami, Florida 33149		10. PROGRAM ELEMENT, PROJECT, TASK AREA & WORK UNIT NUMBERS 531221	
11. CONTROLLING OFFICE NAME AND ADDRESS ONR Research Representative, Georgia Institute of Technology, Room 325, Finman Research Building Atlanta, Georgia 30332		12. REPORT DATE 26 July 1979	
		13. NUMBER OF PAGES 183	
14. MONITORING AGENCY NAME & ADDRESS (if different from Controlling Office) Director Sensor and Control Technology Division, Technology Programs, Office of Naval Research, 800 N. Quincy Street. Arlington, Virginia 22217		15. SECURITY CLASS. (of this report) [REDACTED]	
		15a. DECLASSIFICATION/DOWNGRADING SCHEDULE NAVINST C5511.6; DECL: 31 Dec 2007	
15. DISTRIBUTION STATEMENT (of this Report) "Distribution shall be only as prescribed by the Scientific Officer."			
17. DISTRIBUTION STATEMENT (of the abstract entered in Block 20, if different from Report)			
18. SUPPLEMENTARY NOTES			
19. KEY WORDS (Continue on reverse side if necessary and identify by block number) Acoustic Communication Studies Summary Acoustic Fluctuations			
20. ABSTRACT (Continue on reverse side if necessary and identify by block number) The M7 underwater acoustic communication system developed by the Acoustic Communication Studies Project of the University of Miami as described. This system is designed to reduce the transmitted energy per received bit and to reduce the vulnerability of the transmitting platform to detection by hostile receivers. Three techniques are used to accomplish these objectives: a freely randomisable pseudo-noise transmission format, true matched filter reception, and coherent integration.			

ITEM 20 CONTINUED

Five independently written papers follow a brief introduction in this report. These papers provide an overview of system objectives and techniques, followed by more detailed explanation of actual receiver operation. Finally, a discussion of the relevance of the Mobile Acoustic Communication Study (MACS) results available to date is included.

ABSTRACT

The M7 underwater acoustic communication system developed by the Acoustic Communication Studies Project of the University of Miami as described. This system is designed to reduce the transmitted energy per received bit and to reduce the vulnerability of the transmitting platform to detection by hostile receivers. Three techniques are used to accomplish these objectives: a freely randomizable pseudo-noise transmission format, true matched filter reception, and coherent integration.

Five independently written papers follow a brief introduction in this report. These papers provide an overview of system objectives and techniques, followed by more detailed explanation of actual receiver operation. Finally a discussion of the relevance of the Mobile Acoustic Communication Study (MACS) results available to date is included.



Accession For	
NTIS GRA&I	<input type="checkbox"/>
DTIC TAB	<input checked="" type="checkbox"/>
Unannounced	<input type="checkbox"/>
Justification	
By _____	
Distribution/ _____	
Availability Codes	
Dist	Avail and/or Special
9	

FORWARD

■ The University of Miami Acoustic Communication Studies project has been terminated without the sea evaluation recommended by both ONR and NOSC. Consequently, this final report is presented without any at sea performance data. Earlier experimental results and recent simulation data suggest the system would provide significant (~ 10dB) performance advantages relative to a comparable incoherent tonal system, but a side-by-side evaluation of the two systems proposed for the summer of 1979 was denied. The Navy's failure to evaluate the M7 system either independently or in comparison with the tonal system has been a disappointment to the author.

■ Five papers have been bound together for this report. The first gives a brief overview of the system goals, techniques and capabilities. The second provides a detailed description of the signal format and receiver operation. In the third paper, the results of an extensive simulation of receiver operation under realistic operating conditions is presented. In the fourth paper, the hardware requirements for implementation of the system are described. Finally, the fifth paper comments on the coherence time results obtained by the Mobile Acoustic Communication Studies (MACS) project and their relevance to large time bandwidth product systems such as M7.

ACKNOWLEDGEMENTS

The determined support of Dr. A. O. Sykes of the Office of Naval Research (Code 222) and Mr. Darrell E. Marsh of the Naval Ocean Systems Center (Code 7123) is gratefully acknowledged. Important contributions to the project were made by Dr. Chester A. Jacewitz.

TABLE OF CONTENTS ■

ABSTRACT

FOREWORD

ACKNOWLEDGEMENTS

- PART 1: THE M7 COMMUNICATION SYSTEM: AN OVERVIEW ■
- PART 2: A GUIDE TO THE PARAMETERS AND OUTPUT OF THE M7 COMMUNICATION SYSTEM ■
- PART 3: PERFORMANCE OF THE M7 SYSTEM SIMULATION ■
- PART 4: COMPUTER REQUIREMENTS FOR THE M7 COMMUNICATION SYSTEM
- PART 5: COMMENTS ON THE MACS COHERENCE TIME MEASUREMENTS ■

DISTRIBUTION LIST

DD FORM 1473



LIST OF FIGURES ■

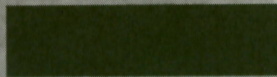
<u>Figure</u>	<u>Title</u>	<u>Page</u>
1	M7B Computer Programs	3
2	M7BX2 Transmission Example	8
3	Digit Modulation Alternatives	10
4	Block Summary: Identifying Labels	14
5	Receiver Operation Overview	16
6	Search Procedure	20
7	Block Summary: Synchronization Outputs	24
8	Demodulation Flow Chart	26
9	Block Summary: Initial Demodulation Outputs	32
10	Block Summary: Bootstrap Demodulation	35
11	Page and Line Summaries	38
12	Teleprinter Output	41



PART 1

THE M7 COMMUNICATION SYSTEM:
AN OVERVIEW

26 JULY 1979



[REDACTED]

The M7 Communication System: An Overview [REDACTED]

[REDACTED] The M7 communication system is the seventh experimental underwater acoustic communication system developed at the Universities of Miami and Michigan during the interval 1967-1979. It is distinctly different from the incoherent, tonal signalling systems currently in use or proposed. The two major considerations in its design were the minimization of transmitted energy per information bit and the reduction of the vulnerability of the transmitting platform to hostile detection. With appropriate choice of parameters the system can be configured for either tactical or strategic applications, the example presented below is on the borderline between these two applications. The M7 system has been ready for evaluation at sea since June 1978, an opportunity perform the evaluation is still being sought.

[REDACTED] The fundamental technique of the M7 system is based on classical signal detection theory for a signal known exactly in added white Gaussian noise. Under such conditions, the optimum (likelihood) receiver is a filter matched to the received signal followed by a threshold detector. Since a practical acoustic channel does not yield a response known a priori, the M7 system performs a measurement of the channel impulse response prior to the information processing. Although the details of the signal processing and parameter values are different, the operation of the system is analogous to the "RAKE" HF modern described by Price and Green in 1958.

[REDACTED] In order for the above technique to be applicable, the acoustic channel must be linear and time-invariant over the channel measurement time. For fixed site channels and center frequencies below 500 Hz, this result has been established for measurement times of the order of minutes. Experiment with towed sources conducted off Eleuthera (400 Hz, 1974) Bermuda (313 Hz, 1976) indicated measurement times of the order of a minute would be satis-

[REDACTED]

[REDACTED]

factory. As the system center frequency is decreased, these times can be expected to increase further.

■ To reduce the detectability of the transmitted signal by hostile receivers, a pseudo-noise transmission format was selected. This makes detection by narrow band spectral analysis futile, particularly when the received signal level is low (below 0 dB), which is the system's intended operating condition. For the hostile detector the problem becomes one of detecting noise-like signals in the fluctuating ambient noise of the ocean.

■ The pseudo-noise transmission format is also an excellent one for purely communication purposes, as the signal is uniformly distributed over the available bandwidth. Equivalently, the pseudo-noise format can be considered to offer a very large degree of frequency diversity.

■ Three basic features are incorporated into the M7 system: freely randomizable choice of pseudo-noise wave form, true matched filter processing, and coherent integration. Other included features such as the synchronization/Doppler removal algorithms and the provision for m -ary biorthogonal signalling are beyond the scope of this paper.

■ The transmitted waveform in the M7 system is based on a binary sequence known to both the transmitter and intended receiver. This sequence must have the statistical properties (particularly bias and auto correlation properties) of a random bit stream and could be conveniently be provided by an approved cryptologic generator and changed on a code-of-the-day basis. The sequence need not obey any deterministic mathematical law, such as the linear maximal sequences commonly employed in scientific channel measurement programs. Further, the randomness of the transmission is unaffected by the particular message being sent. With

[REDACTED]

[REDACTED]

this freely randomizable design, the system satisfies the "cryptologic postulate" in that an interceptor equipped with the same receiving equipment as the intended receiver has no detection advantage unless he knows the prescribed bit stream.

■ The second feature of the M7 system is its measurement of the channel impulse response with each transmission. This measurement is possible because the transmission includes a known component, called the probe, which also is used for time and frequency synchronization. The channel impulse response is extracted from the received signal through a correlation and filtering algorithm. Then filters for each of the information-bearing symbols are constructed through the assumed linearity of the channel and the knowledge of the symbol alphabet. Because both probe and information components pass through the channel at the same time, the exact instant for sampling the symbol filter outputs is known and no "soft decoding" algorithm need be applied.

■ The sharp contrast in approaches to channel variations between the M7 system and conventional incoherent tonal systems must be noted. A typical tonal system represents a compromise in design parameters to allow operation at different ranges and locations. Extensive statistical studies of channel responses have been made to facilitate this compromise. The M7 system, through its on-the-spot channel measurement, designs its receiving filters for exactly the channel at hand.

■ Finally, the M7 system uses coherent integration for synchronization, channel measurement and information processing. This allows useful operation at signal to noise ratios well below 0 dB.

[REDACTED]

[REDACTED]

■ To provide a tangible example of the M7 system, consider the most recent version, M7BX3. The transmission for this version occupies a 51.2 Hz (at 4 dB points) bandwidth centered on 204.8 Hz, so that each burst has a time-bandwidth product of 4096. Sixty information bits are contained in each burst, yielding a bit rate of .75 bits/sec. Simulation results based on a measured 350 nm channel and worst case (21.5 kt) Doppler conditions show the system does not miss any bursts (out of 512) at -10 dB signal to noise ratio. The probability of a symbol error at this signal to noise ratio is .0078, which is equivalent to a bit probability of error of .0016. At an input signal to noise ratio of -7 dB, the probability of a symbol error falls to .000173, which is equivalent to a bit probability of error of .000029. Note that these error probabilities are obtained at the receiver filter output and have not been enhanced through error correcting codes. When compared with theoretical values for a competitive incoherent tonal system, these results indicate a 10 dB advantage for the M7 system.

■ The issue of hardware implementation of the M7 system is an important one because the M7 does place different requirements on the hardware, specifically in terms of calculational speed and memory size. Nevertheless satisfactory hardware is currently available based on a military-qualified version of the PDP-11 computer and an array processor built to be in compliance with military standards. This hardware occupies 3.52 cubic feet (4 ATR modules) including space for interface electronics. The cost per unit (based on a 4 unit purchase) is \$313,000 with delivery within 6 months. These costs do not include that for the interface circuitry which is application dependent. With this hardware the M7BX3

[REDACTED]

[REDACTED]

version could be operated with at least a \pm kt Doppler uncertainty in a single channel mode or a low-Doppler strategic System could be operated on eight channels.

References [REDACTED]

1. R. Price and P. E. Green, "A Communication Technique for Multi-path Channels," Proceedings of the IRE, March 1958.
2. C. V. Kimball, "Acoustic Communication Studies [REDACTED]," Journal of Defense Research, Series B: Tactical Warfare, Summer 1975 [REDACTED].
3. C. V. Kimball, letter to Dr. A. O. Sykes, Office of Naval Research (Code 222), dated 19 February 1979 [REDACTED].
4. C. V. Kimball, letter to Dr. Daniel M. Viccione, Naval Underwater Systems Center, New London Laboratory (Code TC), dated 13 March 1979 [REDACTED].

PART 2

A GUIDE TO THE PARAMETERS AND
OUTPUT OF THE M7 COMMUNICATION SYSTEM ■

ORIGINAL VERSION: 6 JUNE 1978

REVISED: 6 June 1979

CONTENTS ■

	Page
1. Introduction	1
2. General System Operation	2
3. Transmission Format	4
4. Receiver Operation and Results	12
4.1 General Operation	12
4.2 Synchronization	17
4.3 Demodulation	25
4.3.1 Initial Demodulation	25
4.3.2 Bootstrap Demodulation	33
4.4 Other Receiver Outputs	37
4.4.1 General	37
4.4.2 Line Summaries	37
4.4.3 Page Summaries	39
4.4.4 Teleprinter Output	40
4.4.5 Oscilloscope Display	40
4.4.6 Magnetic Tape	42

[REDACTED]

Preface to the Revision of 6 June 1979

Three minor changes were made in the year since the original report was written.

First, a limit, ZSHLIM, on the magnitude of the fine-grain frequency shift performed by ZSHIFT was incorporated. This prevents the ZSHIFT algorithm from radically modifying the signal frequency when the signal to noise ratio is too low for a correct fine-grain frequency measurement.

Second, the search algorithm has been applied after the ZSHIFT in the initial demodulation. This post-ZSHIFT search improves the frequency synchronization on the initial demodulation and leads to better initial symbol decisions.

Third, the nomenclature for the statistical output variables has been improved. Appendix A gives translation tables between versions. The new nomenclature for an output variable XXN tells which stage N the variable XX was computed:

<u>N</u>	<u>Stage</u>
0	Primary Search
1	Secondary Search
2	Initial Demodulation
3	Bootstrap Demodulation

This change does not apply to input variables, i.e., R2CUT ϕ is used on all applications of the ZSHIFT algorithms, not to the primary search.

[REDACTED]

1. Introduction

The objective of this paper is to provide a guide for the interpretation of results from the M7 receiver, so that its capabilities can be understood prior to an experiment at sea. Although no attempt is made to explain the theoretical and engineering considerations behind the M7 system, sufficient background to understand the various parameters is provided. After a quick overview of system operation, a detailed description of the transmission format is given. This is followed by a description of the outputs corresponding to both synchronization and information processing stages of the receiver.

2. General System Operation

The operation of the M7 communication system is based on a random bit stream known only to the transmitter and receiver. Such a bit stream, along with identifying labels, is referred to as a KFILE, where the "K" is for "key stream". Specific KFILES are generated by undersampling a laboratory thermal noise source. Since no communication is possible if the transmitter and receiver are using different KFILES, great care is taken to avoid mixed usage!

The M7 transmitter generates the M7 communication signal, as well as a number of classical channel measurement signals such as CW, coherent pulses and periodic pseudo-random sequences. In the M7 mode, the KFILE and receiver parameters are entered by the operator. Errors in the KFILE or between the KFILE parameters and those specified by the operator are automatically indicated. The operator also enters the message in either hexadecimal or radix 40 (A-Z, 0-9, ?/*-) notation and starts the transmission. Transmissions can be sent either one at a time or periodically at a specified

[REDACTED]

delay. Provision for a continuous carrier (CW) while in this mode is available, with the carrier to burst energy ratio adjustable from 1 to 0 (during the burst).

■ The M7 receiver is a flexible system for detecting and processing the transmission, the details of which are beyond the scope of this note. Because a particular version of the M7 system requires the specification of 27 parameters, a set of parameters and an identifying label for a particular version of the system are placed in a file, called the RFILE (R for "receiver") for use when required. Operation of the receiver requires the presence of precomputed vectors on another file. These vectors are calculated from the parameters and the specific KFILE in use; the file that contains them is called the VFILE (V for "vector"). When the receiver is started, the correspondence between the parameters of the RFILE and the VFILE is verified. The interrelation of the various files and the programs that generate them is shown in Figure 1.

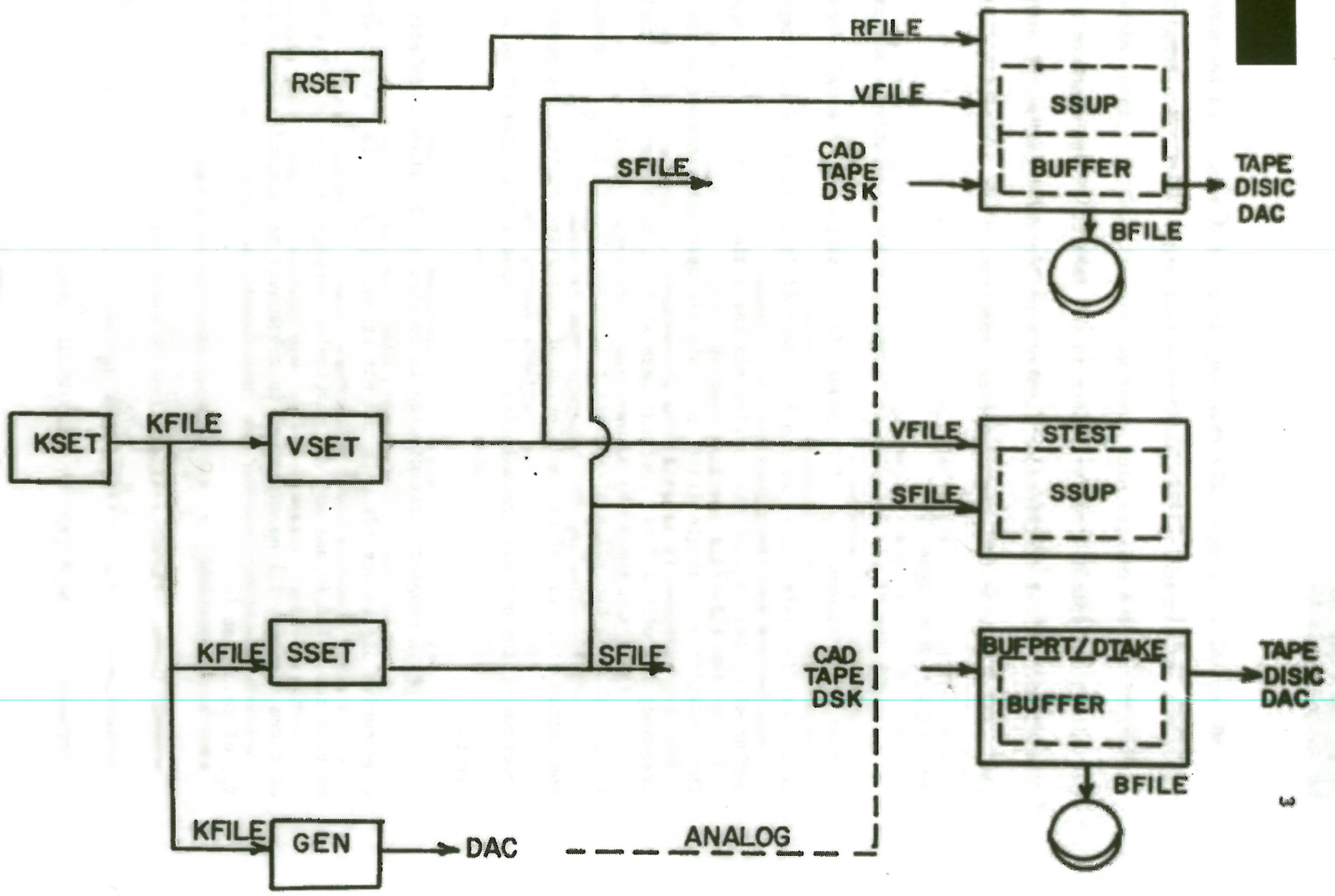
■ Many outputs are available during the operation of the receiver. If the input is from an analog source, an industry-compatible (IBM) tape can be written, containing all the unprocessed input samples. Approximately 24 hours can be placed on one tape, which can then be reprocessed by the receiver with different parameters (i.e. a different RFILE). A conventional teleprinter allows operator control and provides a single line containing the time and information content (in both hexadecimal and radix 40 notation) for each burst received. A line printer provides more detailed information in several forms. First, a single line is typed for each burst, giving 10 different measurements on that burst, including time. Second, at the end of each page, (typically 1/2 hour/page) a statistical summary (mean and standard deviation)

[REDACTED]

Figure 1: M7B COMPUTER PROGRAMS

(This figure [redacted])

Figure 1: M7B Computer Programs
(This figure [redacted])



for 50 variables averaged over that page is printed along with the number of bursts and characters received during that page. Finally, a complete summary of all the results plus error measurements can be printed either periodically (typically every 4 hours in the lab) or at the operator's discretion. An X-Y oscilloscope display provides the magnitude of either the channel impulse response or channel spectrum at the operator's choice.

3. Transmission Format

The M7 transmission is formed by phase modulating a sinusoidal carrier at a frequency f_T . This modulation is performed on small pieces of the carrier referred to as digits. Each digit consists of an integer number of cycles, N_Q , of the carrier and has a time duration, $T_D = N_Q/f_T$. The bandwidth of a single digit has a $\sin x/x$ spectrum centered on the carrier frequency and with a first spectral zero at f_T/N_Q on either side. Equivalently, the 4dB bandwidth of the digit spectrum, W_D , is f_T/N_Q . Because of the random structure of the modulation of successive digits, the power spectrum of the overall transmission is (in expectation) that of an individual digit.

A complete transmission is constructed by phase modulating N_B consecutive digits according to two bit streams $\{a_i\}$ and $\{b_i\}$ which are based on both the KFILE in use and the particular message being sent. The derivation of these streams will be explained in subsequent paragraphs. The total duration, T_B , of the burst is

$$T_B = N_B \cdot T_D \quad (1)$$

$$= N_B \cdot N_Q / f_T \quad (2)$$

Taking the 4 dB digit bandwidth, W_D , as the system bandwidth yields the following result for the transmission TW product:

$$T_B \cdot W_D = N_D \cdot N_Q / f_T \quad f_T / N_Q \quad (3)$$

$$= N_B \quad (4)$$

Thus, the transmission TW product equals the number of digits in the burst, N_B . In current versions of the system, N_B is constrained to be a power of 2.

N_A -ary biorthogonal signalling is used to impose the information on each burst. Although the name sounds esoteric, the technique is not difficult to understand. The parameter N_A is the number of different symbols which can be transmitted in a given symbol position. For example, in dialing a telephone $N_A = 10$ as only the integers 0...9 can be used. In order to facilitate the conversion between bit patterns and symbols, N_A is required to be a power of 2 in the current system. This means N_L bits are contained in each symbol, where

$$N_L = \log_2 N_A \quad (5)$$

will always be an integer. The symbols are biorthogonal in signal space in that for any two different symbols, either the symbols are orthogonal to each other or the symbols are the negative of each other. The reason for this choice is beyond the scope of the present paper.

Each burst of N_B digits is divided into N_C symbol positions, that is, there are N_C symbols per burst. To maintain homogeneity among the symbols in error performance, the number of digits in each of the N_C symbol positions should be nearly constant. Because N_C may not divide N_B perfectly, the number of digits per symbol position can't always be made equal for a given

choice of N_B and N_C . In the current system, the N_B digits are divided into N_C-1 symbol positions of N_S digits each, plus one slightly longer final symbol of $N_{S(LAST)}$ digits. Because of the structure of the current system, N_S must also be a multiple of 16. The equations for N_S and $N_{S(LAST)}$ are then

$$N_S = \text{INT} \left[\frac{N_B}{16 \cdot N_C} \right] \cdot 16 \quad (6)$$

$$N_{S(LAST)} = N_B - (N_C-1) \cdot N_S \quad (7)$$

where $\text{INT}[x]$ is the "integer part of x " function, i.e. $\text{INT}[8/3] = 2$.

If N_C happens to be a power of 2, then $N_S = N_{S(LAST)}$ and the symbol positions have the same number of digits. In practical cases considered to date, N_S and $N_{S(LAST)}$ differ only slightly (i.e. 5%).

As indicated above, the phase modulation of the N_B digits is based on two bit streams $\{a(i)\}$ and $\{b(i)\}$. Both streams are derived from the random bit stream, $\{k(i)\}$ contained in the KFILE. The random bit stream $\{k(i)\}$ must contain $N_B \cdot (1 + (N_A/2))$ bits. The stream $\{a(i)\}$ is called the probe bit stream and is simply the first N_B bits from $\{k(i)\}$:

$$a(i) = k(i) \quad i = 0 \dots N_B-1 \quad (8)$$

where each $k(i)$ is either zero or one.

The second bit stream, $\{b(i)\}$, is called the information stream and is derived from the information being transmitted as well as the bit stream $\{k(i)\}$. Let $\{I(k)\}$ be the information bits to be transmitted where $I(k)$ is either zero or one. The sequence $\{I(k)\}$ has $N_C \cdot N_L$ bit values as there are N_C symbol positions capable of conveying N_L bits each. From $\{I(k)\}$ two N_C long sequences can be derived which are useful in subsequent work:

$$\text{SYM}(\ell) = \sum_{r=0}^{N_L-2} 2^{(N_L-2)-r} I(N_L \cdot \ell + r),$$

$$\ell = 0 \dots N_G - 1 \quad (9)$$

$$\text{SYMSGN}(\ell) = I(N_L \cdot \ell + N_L - 1),$$

$$\ell = 0 \dots N_G - 1 \quad (10)$$

$\text{SYM}(\ell)$ is simply the usual integer representation of the first $N_L - 1$ bits of the ℓ -th symbol position. For example, if $N_L = 4$, $N_G = 2$ and $\{I(k)\} = 1, 0, 1, 1, 0, 0, 1, 0$, then $\{\text{SYM}(\ell)\} = 5, 1$. $\text{SYMSGN}(\ell)$ is the N_L th bit in the ℓ -th symbol position. In the preceding example, $\{\text{SYMSGN}(\ell)\} = 1, 0$.

The information stream $\{b(i)\}$ may be derived based on $\text{SYM}(\ell)$ and $\text{SYMSGN}(\ell)$. Define $\tilde{\ell}$ as follows:

$$\tilde{\ell}(i) = \text{INT}[i/N_S] \quad 0 \leq (N_S \cdot N_G) - 1 \quad (11)$$

$$= N_G \quad \text{otherwise} \quad (12)$$

Thus, $\tilde{\ell}(i)$ is the index of the symbol position to which the i -th digit belongs. The condition in Equations 11 and 12 is necessary because $N_{S(\text{LAST})} > N_S$, which could yield $\tilde{\ell}(i) > N_G - 1$ if it were not imposed. The information sequence $\{b(i)\}$ can then be written:

$$b(i) = \text{SYMSGN}(\tilde{\ell}(i)) \oplus k(N_B + N_S \left[\left(\frac{N_A}{2} \right) \tilde{\ell}(i) + \text{SYM}(\tilde{\ell}(i)) \right] + 1)$$

$$i = 0 \dots N_B - 1 \quad (13)$$

Where \oplus indicates modulo 2 addition.

Equation 13 can best be understood in conjunction with Figure 2.

The first N_B bits of $\{k(i)\}$ are used to form the probe stream marked 'PROBE' in the figure. The next $N_A/2 * N_S$ bits form $N_A/2$ symbol waveforms for the first symbol position, where each symbol uses N_S bits. These symbols are represented by the rectangles marked 0 through 7 in the left column of the table. For $\tilde{\ell}(i) = 0$,

NA=16

CHARACTERS IN ALPHABET

NS = 340

NB = 4096

NG = 12 SYMBOLS

NSLAST = 356

+	INFO	-	0	-	8	16	24	-	32	40	48	56	64	72	80	88			
0	I		1		9	+	17	-	25	33	41	49	57	65	73	81	89		
2	3		2		10		18		26	34	42	50	58	66	74	82	90		
4	5		3		11		19		27	35	43	-	51	59	67	75	83	91	
6	7		4		12		20		28	36	-	44	52	+	60	68	76	84	92
8	9		5		13		21		29	37	45	53	61	69	+	77	85	93	
A	B		6		14		22		30	38	46	54	62	+	70	78	86	94	
C	D		7		15		23		31	39	47	55	63	71	79	-	87	+	95
E	F																		

← NA/2 = 8 ↑

INFORMATION

7	I	2	3	I	9	7	8	C	A	F	E
-3	-8	+17	-25	-32	-44	-51	+60	+70	+77	-87	+95
PROBE (CONSTANT)											

Figure 2:

M7BX2 TRANSMISSION EXAMPLE (INFO=7123 1978 CAFE)

(This figure [redacted])

the first symbol position, Equation 13 becomes:

$$b(i) = \text{SYMSGN}(0) \oplus k(N_B + N_S \cdot \text{SYM}(0) + i) \quad (14)$$

$$i = 0 \dots N_S - 1$$

That is, $b(i)$ is taken from the symbol specified by $\text{SYM}(0)$; then inverted or not inverted according to $\text{SYMSGN}(0)$. In the example, $\text{SYM}(0) = 3$, $\text{SYMSGN}(0) = 1$, thus the first N_S bits are the complement of those in the rectangle marked 3. This is indicated by -3 placed in the first symbol position. Other symbol positions are filled by moving $N_S \cdot N_A / 2 \cdot \tilde{i}(i)$ bits along the $\{k(i)\}$ stream and performing the same process.

Note that because of the random structure of $\{k(i)\}$ there is no relation between the probe and any of the rectangles marked 0...95 nor between the rectangles. This is a key point in the denial of signal processing gain to an interceptor who does not have $\{k(i)\}$ available.

Given the probe and information bit streams $\{a(i)\}$ and $\{b(i)\}$ of length N_B , the transmission can be easily constructed. First, however, these bit streams must be converted to bipolar form, that is have values of either plus one or minus one. Let

$$\tilde{a}(i) = 2a(i) - 1 \quad i = 0 \dots N_B - 1 \quad (15)$$

$$\tilde{b}(i) = 2b(i) - 1 \quad i = 0 \dots N_B - 1 \quad (16)$$

Further, define $p(t)$ to be a rectangular baseband pulse of duration equal to the digit duration, T_D . That is

$$p(t) = 1 \quad 0 \leq t < T_D \quad (17)$$

$$= 0 \quad \text{otherwise} \quad (18)$$

Then the M7 transmitter output, $m(t)$, is given by

$$m(t) = \sum_{i=0}^{N_B-1} p(t-i T_D) \left\{ \tilde{a}(i) \cos 2\pi f_T t - \tilde{b}(i) \sin 2\pi f_T t \right\} \quad (19)$$

Since $\tilde{a}(i)$ and $\tilde{b}(i)$ are bipolar, the i -th transmitted digit consists of a cosine component, whose sign is set by the probe stream, $\tilde{a}(i)$, plus a sine component, whose sign is set by the information stream, $\tilde{b}(i)$.

Figure 3 depicts these components, with the resultant vectors labelled $(\tilde{a}(i), \tilde{b}(i))$. Note that because of the symmetry of the modulation and the randomness underlying $\{\tilde{a}(i)\}$, $\{\tilde{b}(i)\}$, the average of the transmission over the burst will be zero. This means that the spectrum of the burst will have no discernible carrier.

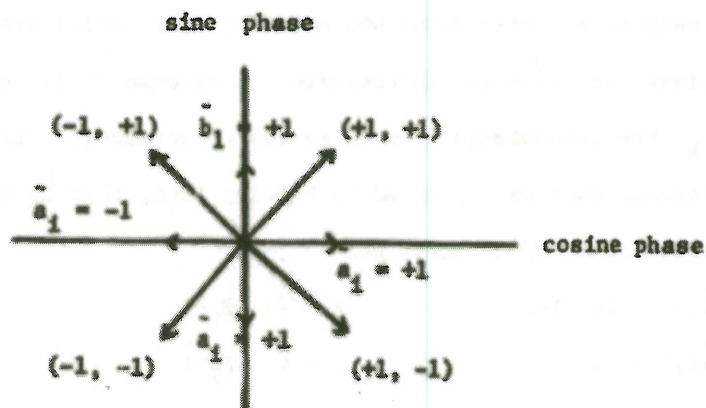


Figure 3: Digit modulation alternatives. ■

(This figure ■

Although the absence of a carrier line in the transmission spectrum is essential for a practical system, it prevents the concurrent processing of the signal by traditional (CW) methods. Since evaluation of the system must be done in cooperation with other (CW) studies, the existing transmitter has been designed to inject a specified amount of carrier if necessary. This allows the transmission to be processed both the M7 system and traditional CW methods without appreciably reducing either's performance. With this modification, Equation 19 becomes:

$$m(t) = \sum_{i=0}^{N_B-1} p(t-iT_D) \{ \bar{a}(i) \cos 2\pi f_T t - \bar{b}(i) \sin 2\pi f_T t \} + K_{CI} \cos 2\pi f_T t \quad (20)$$

where K_{CI} is the carrier injection coefficient. If $K_{CI} = 2$, then equal amounts of signal energy are contained in the burst and in the carrier while the burst is on.

4. Receiver Operation and Results

4.1 General Operation

An overview of the M7 receiver operation is presented in this section to enable the reader to understand the many results produced on-line and in real time by the receiver. Operation of the receiver can be considered in terms of two independent processes: synchronization and demodulation. Synchronization is the process by which the presence or absence of an M7 signal is determined; if the signal is present preliminary estimate of its time and frequency location is provided. If a signal is present, the demodulation process is initiated, which removes any residual Doppler from the signal and makes the necessary symbol decisions.

During operation, the receiver prints results on both the teleprinter and line printer; producing line summaries, page summaries and block summaries, as well as a printout of the message. The block summary is a single 8-1/2 x 11 sheet summarizing all results over a selected period of time, typically several hours. Although the block summary has the most densely packed results, it is the best one on which to learn to interpret the system outputs. Consequently, the discussion of line summaries, page summaries and message printouts will be deferred until later.

Figure 4 depicts a typical block summary, along with hand annotation of relevant outputs. The top-most encircled line identifies the receiver date and the time interval over which the data is summarized. The quantities in parentheses give the duration of the interval in HOUR:MIN format. When using the receiver, the computer program date should be verified to be that of the latest revision. The times are indicated in the format DAY:HOURL:MIN, where DAY is the day of the year.

■ The second block from the top identifies the particular version of the receiver in use, as specified by the contents of the RFILE. All of the parameters associated with the version are printed. The parameters NA, NB, NC, NL, NQ, NS and $NSL = N_{S(LAST)}$ were defined in the preceding section, the remaining parameters will be defined later.

■ The third block from the top defines the VFILE in use. Because of an interlock, the parameters of this VFILE necessarily correspond to those of the RFILE. The first 4 lines in this block are the VFILE identification, which is identical to the KFILE identification. The quantity N_K is the decimation factor used in generating the sequence $\{k(i)\}$ in the KFILE, the quantities NIV, NOV are parameters dealing with the construction of the VFILE and will be described later.

■ The fourth block from the top describes the data being applied to the receiver. If the input is analog, the data header is entered by the operator, if the input is from tape, the data header is taken from the tape. The data header contains the starting time of the data and the receiver center frequency, f_R and N_Q . While the value of N_Q placed in the data header by the operator must agree with that of the RFILE, the center frequency can be adjusted to meet particular operating conditions. Also included in the data header is the frequency of the sampling clock, which is always equal to $4*f_R$.

■ Finally, in the lower right hand corner is a block labeled NDBV(X) with two numbers below it. This represents the average input level in dB relative to one volt, as measured at periodic intervals. The quantity X is the number of such measurements taken, the first number below it is the mean value, the second below it is the standard deviation. The measurement NDBV

Figure 4: Block Summary: Identifying Labels
(this figure classified)

RECVR : 11 FEB 79A - BLOCK SUMMARY : 50: 8: 33 TO 51: 22: 18 (37: 45)

'BX3A - SPECIAL HIGH RATE VERSION FOR '78 NSUA
 NH0 = 16 , INFO = NSUA-NUSC780 **RFILE**

30 OCT 78 AT 1109 HR (RETYPED 05 JAN 78 AT 0757 HR)

NA	NB	ND	NE	NG	NH0	NH1	NI	NL	NM	NO	NO	NS	NSL	NT0	NT1	NA
64	4096	15	2048	10	16	256	512	6.240	32	4	409	415	2	5	16	

ISHLIM	FTHRS0	FTHRS1	R2CUT0	R2CUT1	R2CUT2	DF1	DF2	NE1	INVFL0
0.200	3.235	3.730	0.100	0.100	0.100	1.000	1.000	4096	0

K12013 K STREAM FOR M7BX5 **RFILE / VFILE**

12 OCT 78 AT 1330 HR
 NI : 4 NIV : 512 NOV : 32

M7BX5 THROUGH CELTHRA CHANNEL AT -8.0 DB
 TWIST = 119. (21.5 KT) , INFO = NSUA-NUSC78 **DATA**

15 FEB 79 AT 0833 HR
 STARTING TIME : 50 : 8 : 33 : 0 NO = 4
 CENTER FREQUENCY : 204.800 CLOCK FREQUENCY : 0 819. 200

583. BURSTS	5830. SYMBOLS	34980. BITS
-------------	---------------	-------------

2. SYMBOL ERRORS 0.000343/ 0.000343 PE(SYM)

SYMBOL ERRORS BY LOCATION :

1.	0.	0.	0.	0.	0.	0.	1.
C.	0.						
1.	0.	0.	0.	0.	0.	0.	1.
0.	0.						

L0	L1	L2	L3	TS0	TS1	TS2	TS3
5.38	8.13	13.85	26.43	-28.	0.	-0.	1.
1.33	0.76	1.12	1.49	1483.	2.	2.	2.

FS0	FS1	FS2	FS3	F2	F2A	F2B	F3	F3A	F3B
118.64	118.64	118.68	118.96	118.65	118.97	118.97	118.98	118.98	118.98
0.32	0.24	0.08	0.08	0.24	0.05	0.05	0.06	0.08	0.01

R2	R2A	R2B	R3	R3A	R3B	A2	A2A	A2B	A3	A3A	A3B
0.746	0.697	0.762	0.918	0.858	0.885	0.153	0.000	0.001	0.000	0.000	0.001
0.111	0.105	0.075	0.042	0.057	0.046	0.118	0.018	0.009	0.016	0.003	0.008

TP2A	TP2B	TP3A	TP3B	NZ2A	NZ2B	NZ3A	NZ3B	SNR2A	SNR2B	SNR3A	SNR3B
143.	-359.	137.	-368.	5.	4.	4.	4.	-12.2	-12.2	-9.3	-9.2
51.	51.	58.	59.	1.	1.	1.	1.	0.7	0.7	0.5	0.5

INF2A	INF2B	INF3A	INF3B	SS	L0N(1065.)	L1N(228.)	NDBV(75.)
13.1	13.0	13.3	13.2	-3.1	2.73	2.28	-3.6
0.7	0.7	0.6	0.7	0.0	0.15	0.15	0.3

SPEED : 21.5 (0.02) KTS OFFSET : 1.487294 (0.001059) HZ

* * * [REDACTED] * * *

is taken independently of whether signal or noise is present and hence may contain portions of both signal and noise. The primary purpose of computing NDBV is to assure that the input of the A/D converter is not overloaded, which occurs roughly at NDBV = + 3 dBV.

The objective of the synchronization procedure is to determine the presence or absence of the M7 signal; if it is present, a preliminary estimate of its time and frequency location must be produced. Each input complex sample $x(i)$ is assigned an index number and rotated through a disk buffer file called the BFILE (B for 'buffer'). The primary synchronization search is performed on successive N_B -long vectors $\bar{X}_0(i)$ separated by N_E complex samples.

$$\bar{X}_0(i) = [x(i \cdot N_E), \dots, x(i \cdot N_E + N_B - 1)] \quad (21)$$

If $N_E < N_B$, as is usually the case, the vectors $\bar{X}_0(i)$ overlap. When the primary search indicates a signal may be present in $\bar{X}_0(i)$, a secondary search is initiated to better resolve the time and frequency location of the signal. If the results of the secondary search confirm that a signal is present, the demodulation procedure described in the next section is initiated; if the secondary search fails, the receiver continues with a primary search of $\bar{X}_0(i + 1)$. Figure 5 is helpful in visualizing the synchronization process.

If the receiver enters the information processing procedure, the data is displaced by an additional amount N_{E1} to make up for the additional time spent in information processing.

$$\bar{X}_0(i + 1) = [x(i \cdot N_E + N_E + N_{E1}) \dots x(i \cdot N_E + N_E + N_{E1} + N_B - 1)]$$

(Post Demodulation) (22)

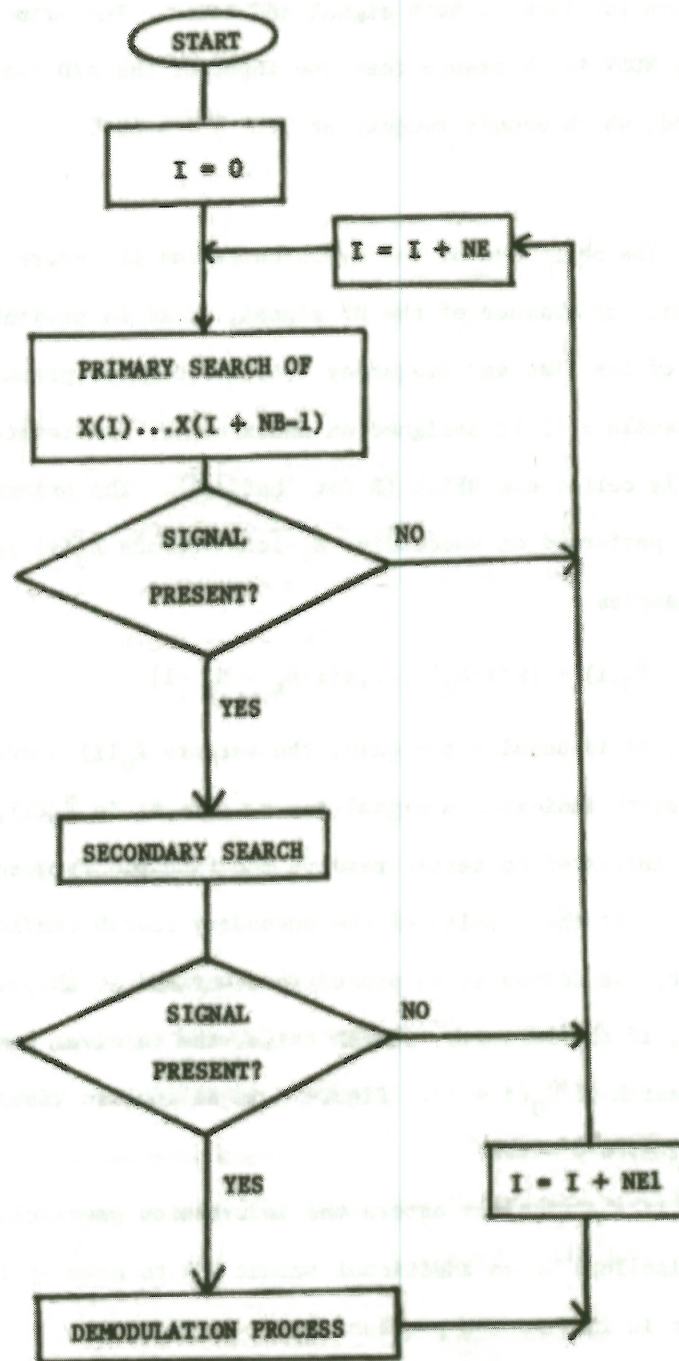


Figure 5. Receiver operation overview. (This figure

This gives rise to a period of receiver blanking of duration $N_E + N_{E1}$ after every entry (false alarms too!) into the information procedure. Consequently, messages that are sent too close together or which follow a false alarm may be missed. Current values of N_E and N_{E1} are sufficient to assure that signals sent at a 50% or less duty factor will not be missed because of receiver blanking unless a false alarm occurs.

4.2 Synchronization

All the details of the primary search will not be presented here, however, meaning of the parameters related to it will be given. The objective of the primary search is to determine whether signal is present within the vector of input samples, $X_0(i)$, presented to it. Because the signal may start or end at any point in the vector and may be located at a substantial Doppler offset from the receiver center frequency, f_R , the primary synchronization task is formidable. The search is performed over several Doppler offsets and effectively all possible time offsets, to obtain the primary search output, $L\phi$, and the estimated time and frequency locations of the signal $TS\phi$ and $FS\phi$.

The structure of the frequency search is worth noting. For convenience, frequency offsets are considered in terms of line spacings of the Fourier transform of the N_B output points rather than in Hertz. This makes interpretation of the frequency offsets independent of frequency and system Q , N_Q . The spacing between spectral lines in Hertz is the reciprocal of the N_B -long block duration.

$$DFLINE = \frac{f_R}{N_Q N_B} \quad (23)$$

A frequency shift of DF_{Hz} Hertz is then equal to the following offset in terms of spectral lines:

$$DF = \frac{DF_{Hz}}{DF_{LINE}} \quad (24)$$

Unless explicitly labelled as being in Hertz, the output results of the receiver are in terms of spectral line spacings as indicated by Equation 22 above. Because of the structure of subroutines internal to the receiver, the sign of all frequency offsets is inverted from the usual notion. That is, a signal received at $DF = +10$ actually is below the receiver frequency f_R , not above it.

For small amounts of Doppler, Doppler on a wideband signal can be considered as a frequency shift. The Doppler search can then be conducted by simply offsetting the transform of the input by an integer number of spectral lines, k . In order to increase the detectability of the signal, however, a finer grain search may be called for. The search algorithm in the receiver provides for this by permitting $N_{T\phi}$ searches within a given line width. Thus, the resolution in Hertz of the search process is

$$DF_{RESOLUTION}(Hz) = \frac{f_R}{N_Q \cdot N_B \cdot N_{T\phi}} \quad (25)$$

Let the total width of the search be N_W spectral lines ($\pm NW/2$ lines) or

$$DF_{RANGE}(Hz) = \frac{f_R}{N_Q \cdot N_B} \cdot N_W \quad (26)$$

Thus for small amounts of Doppler, N_W specifies the Doppler range being searched, whereas $N_{T\phi}$ indicates the spacing of the search.

For non-trivial amounts of Doppler (± 8 spectral lines), the time dilation effects of Doppler must be taken into account or

dramatically reduced performance results. This is handled in the M7 receiver by generating N_D -time dilated waveforms separated by N_W spectral lines. A search of $\pm N_W/2$ spectral lines is performed about each waveform, so that the Doppler offset between the input and the correlator waveform is at most $N_W/2$ spectral lines. The frequency interval of width N_W centered on a time dilated correlator waveform is called a time dilation bin. This yields a total search range of N_M spectral lines where

$$N_M = N_W \cdot N_D \quad (27)$$

The total search range in Hertz is:

$$DF_{\text{RANGE}}(\text{Hz}) = \frac{f_R}{N_Q \cdot N_B} \cdot N_M \quad (28)$$

For convenience, N_D is constrained to be odd by the current version of the receiver. This assures that one of the correlator waveforms is un-dilated (i.e., at zero Doppler). Figure 6 is helpful in visualizing the parameters N_W , $N_{T\phi}$, and N_M .

At each Doppler offset, the receiver calculates the cross-correlation of the input vector $\bar{X}(i)$ with the transmitted probe waveform. Since the spectrum of the probe waveform is nearly white because of the randomness of the $\{a_i\}$ stream, the cross correlator output approximates the impulse response of the channel. The correlator output is squared to provide an energy measurement, and then summed over $N_{H\phi}$ samples starting at each possible time offset, i , $0 \leq i < N_B$. Let $y(i,k)$ be the (complex) correlator output, $0 \leq i < N_B$ at the k th Doppler offset. Then the summer output $z(j,k)$ for a time offset j and Doppler offset k is simply:

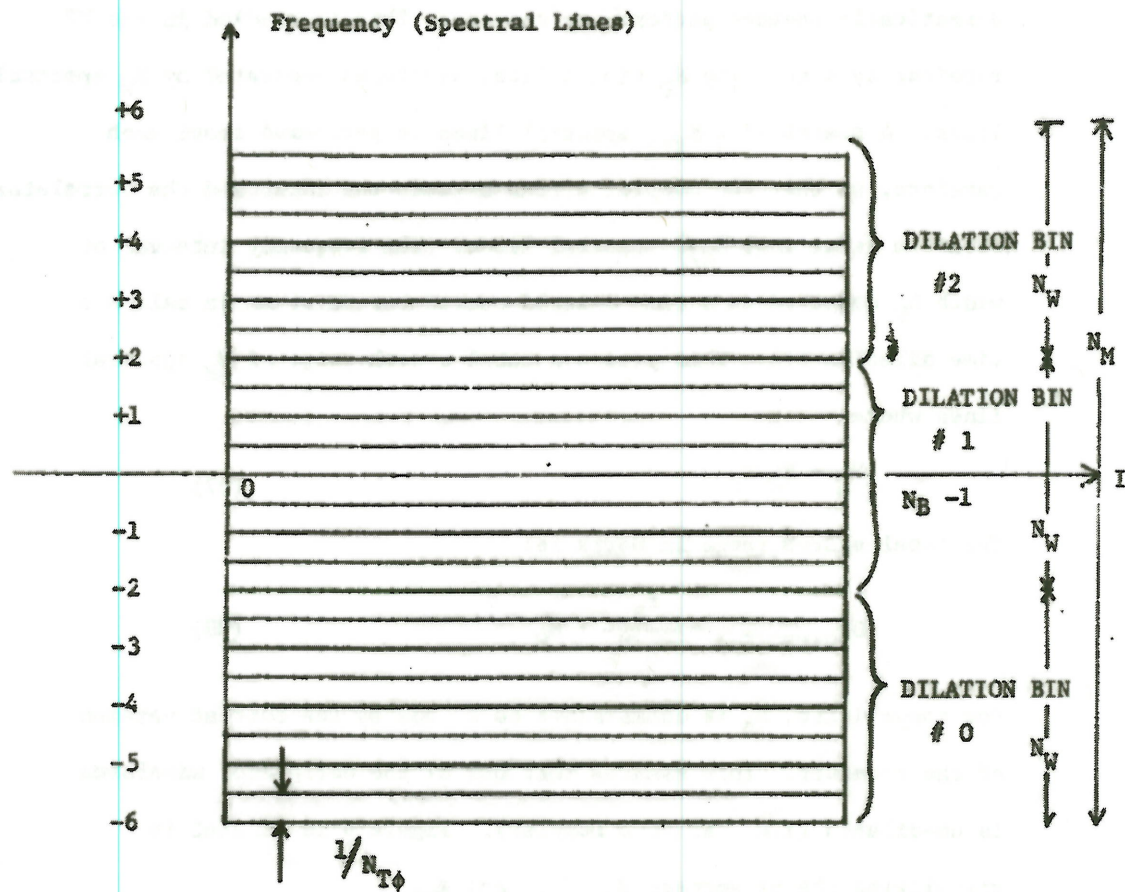


Figure 6: Search Procedure ($N_D = 3$, $N_W = 4$, $N_{T0} = 2$, $N_M = 12$)

(This figure [redacted])

$$z(j, k) = \sum_{i=j}^{j + (N_{H\phi} - 1)} |y(i, k)|^2 \quad (29)$$

where the index is calculated modulo N_B . Because of the excellent ambiguity function (in expectation) of the transmitted probe waveform, $z(j, k)$ can be expected to reach a maximum when k^* is the Doppler offset closest to the received signal. Likewise $z(j, k^*)$ can be expected to reach a maximum when the index j^* specifies the start of the most energetic segment of the channel impulse response. The output of the primary synchronization procedure l_0 , is then

$$l_\phi = \frac{1/N_{H\phi} \max_k \{ \max_{0 \leq j < N_B} z(j, k) \}}{1/N_B \sum_{i=0}^{N_B - 1} |x(i)|^2} \quad (30)$$

Here the factor $1/N_{H\phi}$ and the denominator serve to normalize the output against changes in input level. If the channel is ideal and no noise is present, l_0 takes on the value $N_B/N_{H\phi}$. Let j^* , k^* represent the time and Doppler indices for which the maximum is attained.

The final step of the primary synchronization is to compare l_0 with a prescribed threshold, $FTHRS_\phi$. If l_0 is below the threshold, a "signal not present" decision is made and the search is initiated over a later data vector. The synchronization output, l_0 , is saved as the result $L_\phi N$. If l_0 exceeds the threshold, $FTHRS_\phi$, the secondary search is initiated. Furthermore, the following results are saved: $L_\phi = l_0$, $TS_\phi = j^*$, and $FS_\phi = k^*$. The indices of the maximum, j^* , k^* are passed to the secondary search.

At first glance, a secondary search does not seem necessary as an estimate of the time and frequency location (j^*, k^*) are available at the conclusion of the primary search. In fact, a secondary search is necessary for two reasons. First, the primary synchronization output, l_0 , could have been obtained as a result of a signal starting at either $i_0 + j^*$ or at $i_0 + j^* - N_B$, where i_0 is the index of the first complex sample of the vector $\bar{X}_0(k)$ processed in the primary synchronization. This ambiguity of N_B complex points must certainly be resolved. Second, better overall performance can be achieved if the search is repeated with the input vector more closely aligned with the input signal and with a finer resolution in the frequency search.

The secondary synchronization search involves the same calculation performed in the primary search, but acts on different vectors and with a different Doppler search range. Two input vectors are searched, one beginning ahead of $\bar{X}_0(i)$, $\bar{X}_1^-(i)$ and one behind $\bar{X}_0(i)$, $\bar{X}_1^+(i)$.

$$\bar{X}_1^-(i) = [x(i \cdot N_E + j^* - N_B), \dots, x(i \cdot N_E + j^* - 1)] \quad (31)$$

$$\bar{X}_1^+(i) = [x(i \cdot N_E + j^*), \dots, x(i \cdot N_E + j^* + N_B - 1)] \quad (32)$$

In order to save computation time, the search is limited to a range of $\pm DF1$ spectral lines centered on the estimated Doppler offset k^* . To provide better frequency resolution, the number of interline searches is taken as N_{T1} instead of N_{T0} as in the primary search. This yields two secondary synchronization outputs l_1^- , corresponding to the older data and l_1^+ , corresponding to the more recent data. With each of these outputs are estimates of the time and frequency locations of the signal, $j_1^-, j_1^+, k_1^+, k_1^-$.

The secondary synchronization outputs l_1^+, l_1^- are compared against the secondary threshold, $FTHRS1$. If both outputs are below $FTHRS1$, then the statistic LIN is updated by each value. If one of the values exceeds $FTHRS1$,

say ℓ_1^{\pm} , then information procedure is initiated, and a "signal present" indication is made. The following statistics are set: $L1 = \ell_1^{\pm}$, $TS1 = \frac{\ell_1^{\pm}}{J_1}$, $FS1 = k_1^{\star\pm}$. The instance where both outputs exceed the threshold is extremely unlikely. The current program processes the earliest segment and then skips over the second.

To facilitate evaluation of the synchronization performance, bursts are usually transmitted at a specified duty cycle so that the number of complex samples between successive bursts is known. The receiver calculates the difference in complex samples between detection and designates it as the result DT. For bursts sent at a 50% duty cycle and zero Doppler the difference DT should be simply $2N_B$. If DT is found to be $4N_B$, a burst has been missed and synchronization performance can be scored appropriately.

Figure 7 depicts the same block summary sheet as in Figure 4, but with parameters and results pertaining to synchronization annotated. In the RFILE header, the parameters related to synchronization are underlined. The first encircled line gives the number of bursts detected, that is the number of times, N_{BURST} , the information procedure was initiated. Also given are the total number of symbols ($N_G \cdot N_{BURST}$) and bits ($N_G \cdot N_L \cdot N_{BURST}$) contained in these bursts. The variables labelled $L\phi$, $L1$ are the primary and secondary synchronization outputs given that the thresholds were exceeded. The numbers directly below the labels are the means, the numbers below the means are the standard deviations. The time and frequency estimates for the primary and secondary searches ($TS\phi$, $TS1$, $FS\phi$, $FS1$) are also given. Finally, $L\phi N(NN)$ and $L1 N(NN)$ give the primary and secondary synchronization outputs given that the thresholds were not exceeded. The numbers in parentheses indicate the number of points on which the means and standard deviations are based.

Figure 7: Block Summary: Synchronization Outputs
 (This figure classified [redacted])

RECVR : 11 FEB 79A - BLOCK SUMMARY : 50: 8: 33 TO 51: 22: 18 (37: 45)

EXSA - SPECIAL HIGH RATE VERSION FOR '78 NSUA
 NH0 = 16 , INFO = NSUA-NUSC780

30 OCT 78 AT 1105 HR (RETYPED 05 JAN 78 AT 0757 HR)

NA	NE	ND	NE	NG	NH0	NH1	NI	NL	NH	NO	NO	NS	NSL	NT0	NT1	NW
54	4096	15	2048	10	16	256	512	6	240	32	4	409	415	2	5	16

DSHLIM	FTHRS0	FTHRS1	R2CUT0	R2CUT1	R2CUT2	DF1	DF2	NE1	INVFLG
0.200	3.235	3.730	0.100	0.100	0.100	1.000	1.000	4096	0

*12012
 K STREAM FOR M7BYS

12 OCT 78 AT 1930 HR
 NA : 4 NIV : 512 NOV : 32

M7BYS THROUGH CELTHRA CHANNEL AT -6.0 DB
 TWIST = 119. (21.5 KT) , INFO = NSUA-NUSC78

19 FEB 79 AT 0833 HR
 STARTING TIME : 50 : 8 : 33 : 0 NO = 4
 CENTER FREQUENCY : 204.800 CLOCK FREQUENCY : 9 819. 200

583. BURSTS 5830. SYMBOLS 34980. BITS

2. SYMBOL ERRORS 0.000343/ 0.000343 PE(SYM)

SYMBOL ERRORS BY LOCATION :

1.	0.	0.	0.	0.	0.	0.	1.
0.	0.						
1.	0.	0.	0.	0.	0.	0.	1.
0.	0.						

L0	L1	L2	L3	TS0	TS1	TS2	TS3
5.38	8.13	13.85	26.43	-28.	0	-0.	1.
1.33	0.78	1.12	1.49	1483.	2.	2.	2.

F50	F51	F52	F53	F2	F2A	F2B	F3	F3A	F3B
118.14	118.64	118.98	118.98	118.65	118.97	118.97	118.98	118.98	118.99
0.32	0.24	0.08	0.08	0.24	0.05	0.05	0.06	0.08	0.01

R2	R2A	R2B	R3	R3A	R3B	A2	A2A	A2B	A3	A3A	A3B
0.741	0.687	0.762	0.818	0.858	0.889	0.152	0.000	0.001	0.000	0.000	0.001
0.111	0.105	0.075	0.042	0.057	0.046	0.118	0.018	0.005	0.016	0.003	0.008

TP2A	TP2B	TP3A	TP3B	N22A	N22B	N23A	N23B	SNR2A	SNR2B	SNR3A	SNR3B
143.	-359.	137.	-366.	5.	4.	4.	4.	-12.2	-12.3	-9.2	-9.2
61.	61.	58.	59.	1.	1.	1.	1.	0.7	0.7	0.5	0.5

INF2A	INF2B	INF3A	INF3B	SS	LINK (1088.)	LINK (228.)	NDBV (75.)
13.1	13.0	13.3	13.2	-3.1	2.73	2.26	-3.8
0.7	0.7	0.6	0.7	0.0	0.15	0.15	0.3

WFEEL : 21.5 (0.02) KTS OFFSET : 1.487294 (0.001059) HZ

*** [redacted] ***

4.3 Demodulation

At the conclusion of the synchronization process, the demodulation process is initiated if a "signal present" decision was made. Estimates of the signal's time and Doppler location are available when demodulation begins. The demodulation process consists of 2 steps: an initial demodulation to determine the symbols transmitted followed by a bootstrap demodulation based on a higher quality channel measurement. Figure 8 provides a flow chart for the overall demodulation process. Note that each demodulation step consists of 5 operations: frequency shifting, a search, further frequency shifting, channel impulse response measurement and symbol decision making.

4.3.1 Initial demodulation

The first step in either the initial or final demodulation is to shift the signal to zero frequency via the ZSHIFT algorithm. This algorithm is applied to the data six times throughout the demodulation process. The ZSHIFT algorithm takes the time dilation effects of Doppler into account. This is done by interpolating the data at a rate corresponding to the Doppler offset found during synchronization. In the current program, a sinc/x interpolation function is used with N_0 -th order interpolation. Because the calculation of the requisite sinc/x function is time consuming for the $N_B \cdot N_0$ points required for the interpolation, the sinc/x function is calculated from tabular values. In the current program, the table values have N_I points between zeros. Since the function is symmetric, only $N_0 \cdot N_I/2$ points of sinc/x need be computed, a considerable savings in time. The use of tabular values for sinc/x results in a trivial increase in interpolation error.

Figure 8: Demodulation Flow Chart

(This figure classified [redacted])

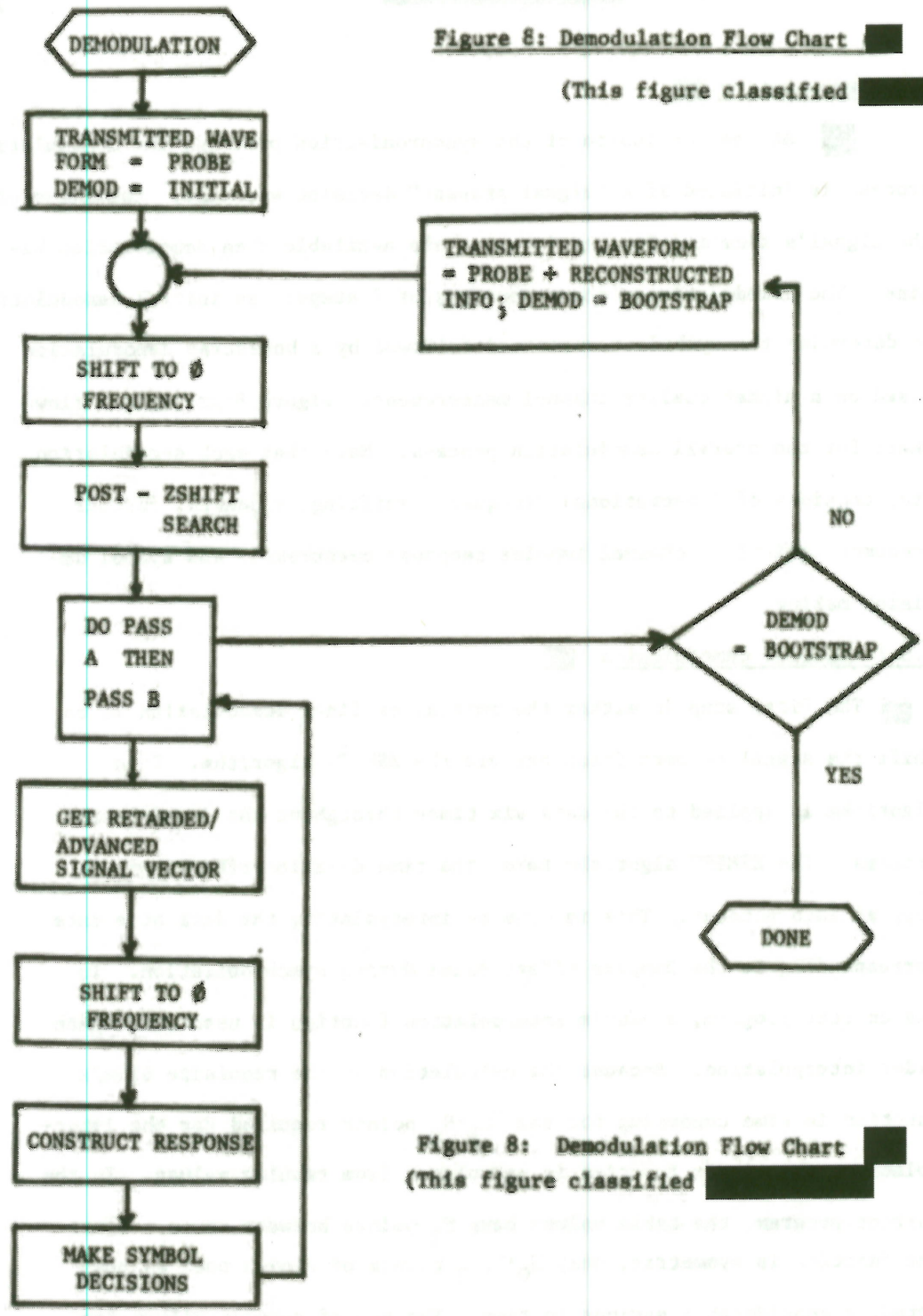


Figure 8: Demodulation Flow Chart

(This figure classified [redacted])

Before continuing the description of the shift to zero Doppler, note that the variables NIV, NOV in the VFILE header have the same roles as N_I , N_O in the construction of the VFILE. They are used to construct the N_D time-dilated representations of the probe component, as required by the synchronization procedure. Although N_{IV} , N_I and N_{OV} , N_O are equal in current versions, no interlock is enforced. Thus the quality of interpolation for the synchronization vectors can be different from that in the demodulation process.

The shift to zero Doppler is not complete after the above mentioned interpolation, as some slight residual phase shift across the input vector might remain. Since the sign of filter outputs is important in determining the symbol values, such a phase shift must be minimized. This is accomplished by partitioning the signal into two halves and construction the channel impulse response from each half. To improve the quality of these responses, they are filtered in the time domain by a procedure described under the channel measurement operation below. Two parameters involved in this filtering are N_{HI} , the width of the time window and R2CUT θ , the threshold on magnitude squared. The complex correlation between the two halves is then calculated and the angle of the correlation yields the final frequency shift required to achieve zero Doppler. To preclude excessive final frequency shifts at low S/N, the magnitude of the final frequency shift is constrained to be less than the parameter ZSH.IM.

■ The results of the shift to zero Doppler is expressed in the measurement of the frequency of the incoming transmission, designated F_2 . At the conclusion of the shift, the complex correlation coefficient is recomputed, to give an indication of any residual Doppler. This yields two additional measurements: R_2 which is the magnitude of the normalized correlation coefficient and A_2 which is the angle, in revolutions ($360^\circ = 1$), of the coefficient.

■ Each application of the ZSHIFT algorithm yields three variables: the frequency measured F_N , the magnitude of the correlation coefficient, R_N , and the angle of the correlation coefficient A_N .

■ The second step in either demodulation process is to re-apply the SEARCH algorithm to the signal which is presumably at zero frequency. This seemingly needless function is in fact important because the frequency estimate from the earlier search is subject to distortion due to time dilation effects. The ZSHIFT routine brings the signal close enough to zero frequency that the frequency estimate from this search, designated the post-ZSHIFT search, is of high quality. The results of the post-ZSHIFT search are given in the statistical outputs L_2 , TS_2 and FS_2 , which are the output level, time estimate and frequency estimate, respectively.

■ When a burst of N_B complex samples is transmitted through the ocean, multipath increases the duration of the received signal beyond N_B samples. The time location found by the synchronization process effectively locates the start of the most energetic N_B -long interval containing the signal. In so doing, a portion of either the first symbol

or last symbol may fall outside the interval specified by the synchronization process, which will lead to errors on these symbols. To counter this problem, the receiver processes the signal in two passes: In the first pass, designated the A pass, it acts on a signal retarded by N_{H1} complex points to determine the first $N_{G/2}$ symbols. This retarded signal certainly contains all of the first symbol energy, but may miss much of the last symbol. In the second pass, designated the B pass, it acts on a signal advanced by N_{H1} complex points to determine the last $N_{G/2}$ symbols. This advanced signal certainly contains all of the last symbol energy but may miss much of the first symbol. Because N_{H1} is small relative to N_B , the offsetting process does not significantly effect the subsequent processing of the probe component.

First, the input to the pass is shifted to zero Doppler via the ZSHIFT algorithm. This yields the statistical outputs F2A, F2B, R2A, R2B and A2A, AZB. Because the frequency estimate provided to the ZSHIFT algorithm has been improved by the post-ZSHIFT search, the frequency estimates F2A, F2B are generally better than the earlier estimate F2.

The next operation is to measure the channel impulse response for construction of the symbol matched filters. This is accomplished by crosscorrelating the transmitted probe waveform with the input signal (now at zero Doppler). Two filtering operations in the time domain are applied to the measured response to improve the quality of the estimate.

First, the most energetic contiguous segment of N_{HI} points is located and all points outside that segment are zeroed. Second, the maximum value of magnitude squared for points within the segment is computed and points within the segment below $R2CUT1$ times the maximum in magnitude squared are zeroed. This leaves a response with only significant points non zero.

■ Several important statistics are computed while deriving the channel impulse response estimate. Prior to the filtering operations, the ratio of the energy in the selected N_{HI} -long interval to that in an interval $N_B/2$ points away is computed. This forms the basis for the calculation of the estimates of input signal to noise ratio, $SNR2A$, $SNR2B$, in dB. Because of the equation employed, these estimates are 3 dB below the actual S/N. Further, the equation employed is applicable only for S/N's below -3 dB. The starting index of the N_{HI} long interval is saved statistically as $TP2A$ and $TP2B$. Also the number of non-zero points in the channel impulse response is saved as $NZ2A$ and $NZ2B$. The latter quantities provide a good measure of the severity of multipath.

■ The third operation in the initial demodulation is to make the decisions on the received symbols. This is done by applying matched filters corresponding to each possible symbol. The channel impulse response measurement is used to construct each filter, so that the filters are matched to the received symbol waveform. Because of the way the filters are constructed the correct sampling instant for each filter decision is known. Consequently, there are $N_C \cdot N_A/2$ signed real numbers corresponding to the outputs of the symbol filters. Symbol decisions are made by choosing the filter output having the largest magnitude (out of $N_A/2$ filter outputs) for each of the N_C symbol positions. The sign of the filter output along with the identity of

[REDACTED]

that filter sets the symbol value.

■ For non-binary signalling ($N_A > 2$), an interesting statistic based on the symbol filter outputs is computed. Suppose $N_A = 16$, then there are 8 filter outputs, 1 which is the maximum which corresponds to the correct symbol and 7 that correspond to the other, presumably incorrect symbols. The ratio in dB of the maximum filter output to the average non-maximum symbol output is calculated for each of N_C symbol positions. This result is then averaged over N_C symbol positions and saved as the statistics INF2A, INF2B, providing a good measure of the quality of the symbol decisions. When $N_A = 2$ (binary signalling) this statistic cannot be computed as there is only one filter output, and INF2A, INF2B are set to zero.

■ When an RFILE is generated a correct message is specified to be used in evaluating the system error performance. After each demodulation the symbol decisions are scored against this message. A count of errors by symbol position is maintained to aid in locating anomalies in the processing. A total error count is also maintained and an overall probability of a character error PE(CHAR) is computed. The correct message contained in the RFILE effects only the receiver scoring, arbitrary messages are processed and printed without prejudice.

■ Figure 9 depicts a block summary with the variables in the RFILE header pertaining to initial demodulation underlined and with results from the initial demodulation circled. The meaning of the parameters N_{H1} , N_I , N_O , ZSHLIM, R2CUT0 and R2CUT1 has been given above. The circled results have also been explained above. Note, however, the adjacent results of similar annotation appear on the summary. They arise from the bootstrap

[REDACTED]

Figure 9: Block Summary: Initial Demodulation Outputs

(This figure classified)

RECVR : 11 FEB 79A - BLOCK SUMMARY : 50: 8: 33 TO 51: 22: 18 (37: 45)

MEX3A - SPECIAL HIGH RATE VERSION FOR 78 NSUA
 NH0 = 16 , INFO = NSUA-NUSC780

30 OCT 78 AT 1109 HR (RETYPED 05 JAN 78 AT 0757 HR)

NA	NB	ND	NE	NG	NH0	NH1	NI	NL	NM	NO	NC	NS	NSL	NT0	NT1	NW
64	4096	15	2048	10	16	256	512	6	240	32	4	405	415	2	5	16

ZSHLIM	FTHRS0	FTHRS1	RZCUT0	RZCUT1	RZCUT2	DF1	DF2	NE1	INVFLG
0.200	3.235	3.730	0.100	0.100	0.100	1.000	1.000	4096	0

M12013

K STREAM FOR M78X5

12 OCT 78 AT 1330 HR

NK : 4 NIV : 512 NOV : 32

M78X3 THROUGH CELTHRA CHANNEL AT -8.0 DB
 TWIST = 115. (21.5 KT) , INFO = NSUA-NUSC78

15 FEB 79 AT 0823 HR

STARTING TIME : 50 : 8 : 33 : 0 NO = 4
 CENTER FREQUENCY : 204.800 CLOCK FREQUENCY : 0 819.200

583. BURSTS

5830. SYMBOLS

34980. BITS

2. SYMBOL ERRORS

0.000343 0.000343 PER(SYM)

SYMBOL ERRORS BY LOCATION :

1.	0.	0.	0.	0.	0.	0.	1.
1.	0.	0.	0.	0.	0.	0.	1.
0.	0.						

L0	L1	L2	L3	T50	T51	T52	T53
8.38	8.13	13.85	26.43	-28.	0.	-0.	1.
1.33	0.75	1.12	1.49	1483.	2.	2.	2.

F50	F51	F52	F53	F2	F2A	F2B	F3	F3A	F3E
118.84	118.64	118.98	118.98	118.65	118.97	118.97	118.98	118.98	118.99
0.32	0.24	0.08	0.08	0.24	0.05	0.05	0.06	0.08	0.01

R2	F2A	R2B	R3	R3A	R3B	A2	A2A	A2B	A3	A3A	A3B
0.745	0.897	0.762	0.915	0.855	0.885	0.153	0.009	0.001	0.000	0.000	0.001
0.111	0.105	0.075	0.042	0.057	0.046	0.116	0.018	0.005	0.016	0.003	0.008

TP2A	TP2B	TP3A	TP3B	NZ2A	NZ2B	NZ3A	NZ3B	SNR2A	SNR2B	SNR3A	SNR3B
143.	-359.	137.	-366.	5.	4.	4.	4.	-12.2	-12.2	-9.3	-9.2
52.	51.	56.	59.	1.	1.	1.	1.	0.7	0.7	0.5	0.5

INF2A	INF2B	INF3A	INF3B	SE	LEN(1068.)	L1N(228.)	NDBV(75.)
13.1	13.0	13.2	13.2	-3.1	2.73	2.28	-3.8
0.7	0.7	0.6	0.7	0.0	0.15	0.15	0.3

SPEED : 21.5 (0.02) KTS

OFFSET : 1.487294 (0.001053) HZ

*** [REDACTED] ***

[REDACTED]

demodulation described later. Thus, only the first of the error results and those statistical results with a 2 in their label arise from the initial demodulations.

4.3.2 Bootstrap Demodulation [REDACTED]

[REDACTED] The error performance of the M7 system depends on the quality of the channel impulse response measurement. A better response measurement will yield better error performance. Only one half of the transmitted energy (the probe) is known exactly to the receiver and can be used in the response measurement during the initial demodulation. After the initial demodulation, however, the symbol decisions obtained in initial demodulation can be used to form an estimate of the total transmitted signal. If the symbol decisions are correct, this would increase by 3 dB the known part of the received signal, and a better response measurement would result. Bootstrapping is the process by which the decisions made in the initial demodulation are used to improve the quality of the information demodulation.

[REDACTED] In order for bootstrapping to be successful, the preliminary symbol decisions should be very nearly correct. Since the receiver is designed to operate with an initial probability of symbol error of .001, few symbol errors are expected in any single burst. Although no theoretical work on bootstrapping has yet been performed, empirical results indicate that it reduces the symbol error rate under normal operating conditions. Consequently, it has been included in the receiver. The difference in error performance and other parameters between initial and bootstrap operations indicates the sensitivity of these parameters to a 3 dB improvement in probe energy.

[REDACTED]

[REDACTED]

The bootstrap process reconstructs the transmitted waveform based on the symbol decisions from the initial demodulation. This reconstructed waveform is then used in subsequent applications of the zero shifting (ZSHIFT), search (SEARCH) and probe reconstruction (PROBE) algorithms. The order of application of these algorithms is exactly the same as for the initial demodulation. The resulting outputs are completely analogous to those of the initial demodulation, except they contain a 3 in their designation instead of a 2. The only exception occurs in SNR3A, SNR3B which measure the input S/N without the 3 dB offset of SNR2A, SNR2B.

To allow additional flexibility in the bootstrap process, different parameters for the search width DF2 (in place of DF1) and for the probe threshold R2CUT2 (in place of R2CUT1) may be specified. Current versions of the program do not make use of their capability and set the values the same for the initial and bootstrap processes.

Figure 10 depicts the block summary with the RFILE parameters dealing with bootstrapping underlined and with the bootstrap results circled. S3 is simply the energy in the input waveform prior to the bootstrap demodulation. The statistics L3, TS3, FS3, arise from the bootstrap search, the statistics F3, R3, A3 arise from the bootstrap zero shifting process, etc. At the bottom of the page, the frequency offset F3 is converted into both knots and Hertz for convenience. The quantities in parentheses are the standard deviations of the offsets in knots and Hertz. Note that the character error count, character error probability and character errors by location are given in the right most or lower position for the bootstrapping demodulation.

[REDACTED]

Figure 10: Block Summary: Bootstrap Demodulation
 (This figure classified [REDACTED])

35

RECVR : 11 FEB 78A - BLOCK SUMMARY : 50: 8: 33 TO 51: 22: 18 (37: 45)

7BX3A - SPECIAL HIGH RATE VERSION FOR 78 NSUA
 NH0 = 1E , INFO = NSUA-NUSC780

30 OCT 78 AT 1109 HR (RETYPED 05 JAN 78 AT 0757 HR)

NA	NE	ND	NE	NG	NH0	NH1	NI	NL	NM	NO	NO	NS	NSL	NT0	NT1	NH
64	4096	15	2048	10	1E	256	512	E	240	32	4	409	415	2	5	16
ZSHLIM	FTHRS0	FTHRS1	R2CUT0	R2CUT1	R2CUT2	DF1	DF2	NEI	INVFLG							
4.200	3.235	3.730	0.100	0.100	0.100	1.000	1.000	4096								

K12013

K STREAM FOR M7BX5

12 OCT 78 AT 1330 HR
 NK : 4 NIV : 512 NOV : 32

M7BX3 THROUGH CELTHRA CHANNEL AT -2.0 DB
 TWIST = 119. (21.5 KT) , INFO = NSUA-NUSC78

15 FEB 78 AT 0633 HF
 STARTING TIME : 50 : 8 : 33 : 0 NO = 4
 CENTER FREQUENCY : 204.800 CLOCK FREQUENCY : 9 819. 200

513. BURSTS 5630. SYMBOLS 34980. BITS

2. [REDACTED] 2. SYMBOL ERRORS 0.000343/ 0.000343 PE(SYM)

SYMBOL ERRORS BY LOCATION

1.	0.	0.	0.	0.	0.	0.	0.	1.
0.	0.	0.	0.	0.	0.	0.	0.	1.
0.	0.	0.	0.	0.	0.	0.	0.	1.

L0	L1	L2	L3	T0	T1	T2	T3
8.38	6.13	13.85	26.43	-28.	0.	-0.	1.
1.23	0.78	1.12	1.49	1483.	2.	2.	2.

F0	F1	F2	F3	F2	F2A	F2B	F3	F3A	F3B
118.64	116.64	116.88	116.96	118.65	118.97	118.97	118.98	118.98	118.95
0.32	0.24	0.08	0.02	0.24	0.05	0.05	0.02	0.02	0.01

R2	R2A	R2B	R2	R2A	R2B	A2	A2A	A2B	A2	A2A	A2B
0.749	0.697	0.762	0.916	0.898	0.889	0.153	0.000	0.001	0.000	0.000	0.001
0.111	0.105	0.075	0.042	0.057	0.040	0.118	0.018	0.009	0.016	0.003	0.008

TP2A	TP2B	TP3A	TP3B	N22A	N22B	N23A	N23B	SNR2A	SNR2B	SNR3A	SNR3B
143.	-379.	137.	-385.	5.	4.	4.	4.	-12.2	-12.2	-9.3	-9.3
82.	01.	55.	55.	1.	1.	1.	1.	0.7	0.7	0.5	0.5

INP2A	INP2B	INP3A	INP3B	ES	LIN(1065.)	LIN(228.)	NDBV(75.)
13.1	13.6	13.3	13.3	-3.1	0.73	2.28	-3.6
0.7	0.7	0.6	0.7	0.0	0.15	0.15	0.3

WIND : 21.5 (0.033 KTS) OFFSET : 1.467294 (0.001059) Hz

*** [REDACTED] ***

■ The bootstrap demodulation does have one option not previously described as part of the initial demodulation. In the initial modulation, the received signal is cross-correlated with the transmitted probe waveform. In the spectral domain, this corresponds to the multiplication of the conjugate of the probe spectrum, $\hat{A}(w)$ times the received signal spectrum $X(w)$. Let $X(w)$ be defined as

$$X(w) = A(w)C(w) + N(w) \quad (33)$$

where $C(w)$ is the channel spectrum $N(w)$ is the noise spectrum. Thus, the correlator output $Y(w)$ is

$$Y(w) = |A(w)|^2 C(w) + A^*(w)N(w) \quad (34)$$

of which the first term is the signal contribution. For the random probe sequences considered $|A(w)|^2$ is a constant in expectation, but in any particular instance has some ripple. Consequently $Y(w)$ does not equal $C(w)$ even in the absence of the noise term.

■ As a low cost feature, the current receiver includes the option of using the inverse filter $1/A(w)$ rather than the conjugate filter $A^*(w)$ in deriving the channel impulse measurement. This feature is in effect only if INVFLG in the RFILE header is 1, and then only for the bootstrap demodulation. With inverse filtering $Y(w)$ becomes

$$\begin{aligned} Y(w) &= \frac{1}{A(w)} [A(w)C(w) + N(w)] \\ &= C(w) + N(w)/A(w) \end{aligned} \quad (35)$$

so that $Y(w)$ is exactly the channel impulse response in the absence of noise. This feature has been used very little and is not considered likely to improve system error performance.

4.4 Other Receiver Outputs

4.4.1 General:

The preceding discussion of the receiver outputs has been centered on the block summary which can be generated either periodically (typically every 4 hours) or at the operator's discretion. In order to allow close monitoring of receiver performance, a number of other outputs are available which are produced more frequently. These are the line and page summaries, the message printout, the oscilloscope display and the digital magnetic tape.

4.4.2 Line Summaries

Figure 11 depicts a typical page summary, which is produced at approximately 1/2 hour intervals. The first page summary of a computer run contains the RFILE/VFILE/Data Header information found in the block summary in addition to the data shown in this figure. A page summary is composed of several line summaries, plus a block of statistical data corresponding to the bursts received during that page. In Figure 11, a typical line summary is encircled with a solid line. Another type of output line, known as an input level summary, is encircled with a dotted line and will be discussed later.

A line summary is produced for each burst received. The caption line above the line summaries in Figure 11 is helpful in interpreting the contents of the line summary. The first data in the line summary is the time of arrival for the burst in DAY:HOURL:MIN:SEC-SAM format, where SAM is the complex sample number (within a 1 second interval). Thus the start

*** [REDACTED] ***

RECVR : 04 JUN 79B - RECEIVER

PAGE 16

DAY	HR	MIN	SEC	SAM	DT	F	L1	R	SNR	NZR	INF	E	DBV
53	5	27	5-	38	9204	119.005	6.921	1.000	-10.5	1	12.0	0	-3.5
53	5	31	59-	37	14847	118.987	7.096	1.000	-10.8	1	12.0	0	-3.4
53	5	36	8-	0									-3.7
53	5	36	19-	46	13321	119.011	8.646	0.970	-10.6	1	11.7	0	-3.5
53	5	41	9-	49	14851	119.006	8.021	0.964	-11.3	1	12.2	0	-3.5
53	5	44	19-	44	9723	118.966	6.571	0.973	-11.1	1	12.6	0	-3.6
53	5	47	59-	49	11269	119.010	7.172	0.918	-10.4	1	12.6	0	-3.5
53	5	51	9-	50	9729	118.950	6.604	0.896	-10.9	1	13.1	0	-3.5
53	5	54	49-	50	11264	118.955	5.994	0.949	-11.0	1	12.8	0	-3.6
53	5	59	29-	43	14329	118.942	7.349	0.960	-11.1	1	12.0	0	-3.4
53	6	2	49-	36	10233	118.996	6.769	0.968	-10.2	1	11.8	0	-3.4
53	6	6	10-	0									-3.7
53	6	7	9-	48	13324	119.008	6.792	0.964	-10.6	1	12.4	0	-3.5
53	6	10	59-	50	11778	119.032	9.167	0.975	-10.1	1	12.7	0	-3.5
53	6	14	39-	49	11263	119.037	7.448	0.919	-10.3	1	12.8	0	-3.4
53	6	17	29-	45	8700	119.022	8.354	1.000	-11.0	1	12.3	0	-3.5

L0	L1	L2	L3	TS0	TS1	TS2	TS3
5.06	7.35	12.98	24.26	1236.	-0.	1.	1.
1.17	0.86	1.12	1.56	572.	4.	5.	3.

FS0	FS1	FS2	FS3	F2	F2A	F2B	F3	F3A	F3B
119.14	118.91	119.00	119.01	118.91	118.98	118.98	118.93	118.99	119.00
0.40	0.29	0.10	0.09	0.27	0.05	0.04	0.05	0.03	0.03

R2	R2A	R2B	R3	R3A	R3B	A2	A2A	A2B	A3	A3A	A3B
0.973	0.854	0.969	1.000	0.927	0.995	0.035	0.001	0.001	0.008	0.000	0.000
0.040	0.121	0.048	0.000	0.064	0.016	0.141	0.003	0.004	0.028	0.003	0.003

TP2A	TP2B	TP3A	TP3B	NZ2A	NZ2B	NZ3A	NZ3B	SNR2A	SNR2B	SNR3A	SNR3B
121.	-380.	154.	-369.	1.	1.	1.	1.	-13.4	-13.3	-10.6	-10.6
95.	99.	85.	91.	0.	0.	0.	0.	0.9	0.9	0.3	0.5

INF2A	INF2B	INF3A	INF3B	SS	L0N(26.)	L1N(0.)	NDBV(2.)
12.2	12.5	12.2	12.5	-3.5	2.76	0.00	-3.7
0.6	0.5	0.6	0.5	0.0	0.16	0.00	0.0

PAGE SUMMARY : 14 BURSTS 140 SYMS 0 SYM ERRS 21.5 KTS
 BLOCK SUMMARY : 329. BURSTS 3290. SYMS 7. SYM ERRS 21.5 KTS

*** [REDACTED] ***

Figure 11: Page and Line Summaries [REDACTED]

(This figure classified [REDACTED])



of a given burst can be located to a specific complex sample in the data. DT is the number of complex samples between the burst and its predecessor, F is the frequency of the incoming signal in spectral line spacings and with the inverted sign mentioned earlier ($F = F_3$). L1 is the output of the secondary search. R is the magnitude of the normalized correlation coefficient as found in the bootstrap zero-shifting operation ($R = R_3$). SNR is the estimated input signal to noise ratio in dB, and is obtained by averaging, SNR3A and SNR3B. SNR is valid only for input S/N's below 0 dB. NZR is the number of non-zero points in the channel impulse response obtained by averaging NZ3A and NZ3B. Similarly INF is the average of INF3A and INF3B and indicates the S/N in dB of the symbol decision making process. E represents the number of character errors relative to the test message. DBV is the signal energy in dBV as found in the bootstrap stage ($DBV = S_3$). Note that all of the quantities except L1 are obtained in either the bootstrapping stage or final demodulation step of the receiver.

Since line summaries are printed only when a burst is received, no measurements of this type are printed under noise alone conditions. Because operation with noise alone is an important part of performance evaluation, (for false alarms), a periodic output line, called the input level summary, for such a situation is provided. As indicated within the dotted circle of Figure 11, this line consists of simply the time and input level in dBV ($DBV = NDBV$ in this line).

4.4.3 Page Summaries

The page summary as indicated in Figure 11 consists of a short title, page number, and caption followed by a series of line and input level

summaries. At the conclusion of these lines, a data block completely analogous to that of the block summary is printed. The data block gives statistical data for the bursts on this page only, hence it is normally the quickest statistical result available. The page summary concludes with a tally of the number of bursts, the number of characters and character errors (bootstrap demodulation) and the average speed in knots (based on F3) for the bursts on the page. Immediately below this line are the same results for the overall data block currently in progress.

4.4.4 Teleprinter Output ■

■ During the operation of the receiver, the block and page summaries are printed on a line printer whose output is delayed for viewing by several inches due to its construction. To allow the operator to be nearly instantaneously informed of system operation, the control teleprinter provides a single line of output for each burst. This line consists of the time of arrival of the burst in the same format as the line summary, plus the message in both hexadecimal and radix 40 notation. Figure 12 depicts a typical teleprinter output. To alert the operator that a message will soon be printed, the teleprinter rings a bell when the demodulation process is initiated. It rings the bell again after the message is printed. Thus, the operator can sense the proper operation of the receiver when signal is present by simply listening.

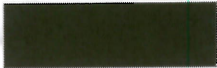
4.4.5 Oscilloscope Display ■

■ A oscilloscope display of the magnitude of either the channel impulse response or the channel transfer function is also available. The choice of time or frequency domain display is made according to the

DAY	HR	MIN	SEC	SAM	DT	F	L1	R	SNR	NZR	INF	E	DBV
53:	5:	27:	9-	38		943E	4487	BFEC	2D00		NSUA-NUSC780		
53:	5:	27:	9-	38	9204	119.005	6.921	1.000	-10.5	1	12.0	0	-3.
53:	5:	31:	59-	37		943E	4487	BFEC	2D00		NSUA-NUSC780		
53:	5:	31:	59-	37	14847	118.987	7.096	1.000	-10.8	1	12.0	0	-3.
53:	5:	36:	0-	0									-3.7
53:	5:	36:	19-	46		943E	4487	BFEC	2D00		NSUA-NUSC780		
53:	5:	36:	19-	46	13321	119.011	8.646	0.970	-10.6	1	11.7	0	-3.
53:	5:	41:	9-	49		943E	4487	BFEC	2D00		NSUA-NUSC780		
53:	5:	41:	9-	49	14851	119.006	8.021	0.964	-11.3	1	12.2	0	-3.
53:	5:	44:	19-	44		943E	4487	BFEC	2D00		NSUA-NUSC780		
53:	5:	44:	19-	44	9723	118.966	6.571	0.973	-11.1	1	12.6	0	-3.
53:	5:	47:	59-	49		943E	4487	BFEC	2D00		NSUA-NUSC780		
53:	5:	47:	59-	49	11269	119.010	7.172	0.918	-10.4	1	12.6	0	-3.
53:	5:	51:	9-	50		943E	4487	BFEC	2D00		NSUA-NUSC780		
53:	5:	51:	9-	50	9729	118.950	6.604	0.896	-10.9	1	13.1	0	-3.
53:	5:	54:	49-	50		943E	4487	BFEC	2D00		NSUA-NUSC780		
53:	5:	54:	49-	50	11264	118.955	5.994	0.949	-11.0	1	12.8	0	-3.
53:	5:	59:	29-	43		943E	4487	BFEC	2D00		NSUA-NUSC780		
53:	5:	59:	29-	43	14329	118.942	7.349	0.960	-11.1	1	12.0	0	-3.
53:	6:	2:	49-	36		943E	4487	BFEC	2D00		NSUA-NUSC780		
53:	6:	2:	49-	36	10233	118.996	6.769	0.968	-10.2	1	11.8	0	-3.
53:	6:	6:	40-	0									-3.7
53:	6:	7:	9-	48		943E	4487	BFEC	2D00		NSUA-NUSC780		
53:	6:	7:	9-	48	13324	119.008	6.792	0.964	-10.6	1	12.4	0	-3.
53:	6:	10:	59-	50		943E	4487	BFEC	2D00		NSUA-NUSC780		
53:	6:	10:	59-	50	11778	119.032	9.167	0.975	-10.1	1	12.7	0	-3.
53:	6:	14:	39-	49		943E	4487	BFEC	2D00		NSUA-NUSC780		
53:	6:	14:	39-	49	11263	119.037	7.448	0.919	-10.3	1	12.8	0	-3.
53:	6:	17:	29-	45		943E	4487	BFEC	2D00		NSUA-NUSC780		
53:	6:	17:	29-	45	8700	119.022	8.354	1.000	-11.0	1	12.3	0	-3.

Figure 12: Teleprinter Output

(This figure classified [REDACTED])



position of SENSE SWITCH 3 on the front of the computer. Either display consists of N_{HI} time or frequency points as obtained by the most recent channel measurement operation, the time display is given prior to the thresholding on magnitude squared, the frequency display is given after thresholding. When the demodulation process is entered, four channel measurements are made (A, B initial demodulation; A, B bootstrap demodulation) and displayed. This leaves the result of the B pass of the final demodulation on the screen for the longest period of time. The display inserts a zero line at about a 5% duty cycle so as to provide a reference in looking at the magnitudes. No absolute levels are available in the display as the output points are adjusted to provide a maximum resolution display. Further, no hard copy of the display is available so that it serves primarily as a qualitative aid for the operator.

4.4.6 Magnetic Tape

When the input to the receiver is analog, a 1/2" digital magnetic tape is produced containing the data header information and the unprocessed complex pairs. This tape is written at 800 bits per inch in an industry compatible (IBM-style) format on up to 10-1/2" reels. The structure of the tape is very simple and will be explained below. A "word" here consists of 16 bits with the most significant byte of each word being the first byte on tape (PDP-11 users beware).

The tape consists of a 256-word header record followed by consecutive data records of 1,024 words each. No end of file marks are automatically placed on the tape. They may be placed at the end of the tape by the operator, however, the normal procedure is to write the tape until an EOT (end of tape) indication is received.

The first record consists of 256 words, of which the first 128 words are an alphanumeric header, as printed in the RFILE header. The characters are in ASCII format with the parity on (Mark parity), packed two characters per word in the usual manner. Table 1 below is helpful in understanding the contents of the header. Here WORD (1)...WORD (256) are the (FORTRAN index) symbols for the 16 bit words on the header. Numbers are to be interpreted in conventional two's complement form.

Table 1. Constants in header record

(Table

WORD(1)...WORD(128)	}	ASCII Title
WORD(129)	DAY	} STARTING TIME OF DATA
WORD(130)	HOUR	
WORD(131)	MIN	
WORD(132)	SEC	
WORD(133)	KHZ	} CLOCK FREQUENCY ($4f_R$) IN KHZ, HZ, MHZ $f_R = 1/4 [1000. * KHZ + HZ + .001 * MHZ]$
WORD(134)	HZ	
WORD (135)	MHZ	
WORD(136)	N_Q	} # of carrier cycles/complex pair
WORD(137)...WORD(256)	}	Not used, may be trash

The remaining records consist of 1024 words of consecutive input data or equivalently 512 complex integer pairs. The first complex pair on the record corresponds to the oldest complex pair received, the last corresponds to the most recent. Thus, the time order on tape is conventional.

APPENDIX A

Relation between 1978 and 1979 Nomenclature

<u>1978</u>	<u>1979</u>	<u>1978</u>	<u>1979</u>
FLØ	LØ	No equivalent	R2
FL1	L1	R1A	R2A
No equivalent	L2	R1B	R2B
FL2	L3	R2	R3
		R2A	R3A
		R2B	R3B
TLOCØ	TSØ		
TLOC1	TS1		
No equivalent	TS2	No equivalent	A2
TLDC2	TS3	T1A	A2A
		T1B	A2B
FLOCØ	FSØ	T2	A3
FLOC1	FS1	T2A	A3A
No equivalent	FS2	T2B	A3B
FLOC2	FS3		
No equivalent	F2	DT1	No equivalent
		DT2	DT (line summary only)
F1A	F2A		
F1B	F2B	FS1A	TP2A
F2	F3	FS1B	TP2B
F2A	F3A	FS2A	TP3A
F2B	F3B	FS2B	TP3B
NZ1A	NZ2A	FLØN()	LØN()
NZ1B	NZ2B	FLIN()	LIN()
NZ2A	NZ3A		
NZ2B	NZ3B	NDBV	NDBV
SNR1A	SNR2A		
SNR1B	SNR2B	Parameters new to 1979 version:	
SNR2A	SNR3A	ZSHLIM - limit on final ZSHIFT	
SNR2B	SNR3B	frequency shift	
INF1A	INF2A		
INF1B	INF2B		
INF2A	INF3A		
INF2B	INF3B		
S1A	No equivalent		
S1B	No equivalent		
S2	S3		
S2A	No equivalent		
S2B	No equivalent		

PART 3

PERFORMANCE OF THE M7 SYSTEM SIMULATION ■

26 JULY 1979

CONTENTS ■

	<u>Page</u>
List of Figures	ii
List of Tables	iii
1. Introduction ■	1
2. Simulation Technique ■	1
2.1 Synthetic Data Tapes ■	2
2.2 M7BX3A Version ■	3
2.3 CELTHRA ■	7
3. Simulation Results ■	9
3.1 Data Description ■	9
3.2 Synchronization Performance ■	10
3.3 Information Demodulation Performance ■	12
3.4 Other Receiver Outputs ■	19
4. Conclusions and Future Studies ■	41
Appendix A: Detailed Specification of M7BX3A ■	
Appendix B: Summary Sheets from M7BX3A Simulation ■	
References	

LIST OF FIGURES ■

<u>Figure</u>	<u>Title</u>	<u>Page</u>
2.1	CELTHRA Impulse Response ■	8
3.1	P_{MISS} vs S/N (U)	13
3.2	$P_{\text{E}}(\text{SYM})$ vs S/N for CIDEAL ■	15
3.3	$P_{\text{E}}(\text{SYM})$ vs S/N for CELTHRA ■	16
3.4	$P_{\text{E}}(\text{SYM})$ after bootstrapping for CIDEAL and CELTHRA ■	18
3.5	Means of $L\phi$, $L1$, $L2$ and $L3$ vs S/N for CIDEAL ■	20
3.6	Means of $L\phi$, $L1$, $L2$ and $L3$ vs S/N for CELTHRA ■	22
3.7	ξ_0 and ξ_1 vs S/N	23
3.8	Mean and standard deviation of $FS\phi$ vs S/N ■	25
3.9	Mean and standard deviation of $FS1$ vs S/N ■	25
3.10	Mean and standard deviation of $FS2$ vs S/N ■	27
3.11	Mean and standard deviation of $F2A/B$ vs S/N ■	28
3.12	Mean and standard deviation of $F3$ vs S/N ■	28
3.13	Mean and standard deviation of $R2$ vs S/N ■	30
3.14	Mean and standard deviation of $R3$ vs S/N ■	30
3.15	Mean and standard deviation of $A2$ vs S/N ■	31
3.16	Mean and standard deviation of $A3$ vs S/N ■	31
3.17	Means of $NZ2A/B$ and $NZ3A/B$ vs S/N ■	33
3.18	Measured S/N vs actual S/N ■	35
3.19	S/N measurement error ξ vs S/N ■	37
3.20	Standard deviation of $SNR2A/B$ and $SNR3A/B$ vs S/N ■	38
3.21	INF vs S/N ■	39

LIST OF TABLES

<u>Table</u>	<u>Title</u>	<u>Page</u>
2.1	Characteristics of the M7BX3A Version	5
3.1	Fixed Parameters in Simulation	9
3.2	Data Summary	11
3.3	Search Outputs under Noise	40

[REDACTED]

Performance of the M7 System Simulation [REDACTED]

1. Introduction [REDACTED]

[REDACTED] The results of extensive performance evaluation of the M7 communication system by means of simulated data are presented. These results include the effects of noise, channel multipath, Doppler and time of arrival uncertainty, and are presented over a range of input signal to noise ratios. All of the results are for the M7BX3 version of the system described below, however, the accompanying discussion applies to other versions also. The results indicate that the system is successful in acquiring and demodulating signals well below a 0dB input signal to noise ratio.

[REDACTED] This paper assumes a familiarity with the nomenclature and techniques of the M7 system. The information contained in Reference 1, "A Guide to the Parameters and Outputs of the M7 Communication System" provides the recommended background.

2. Simulation Technique [REDACTED]

[REDACTED] The M7 receiver is capable of accepting either analog or magnetic tape inputs. In order to simulate the effects of a typical acoustic channel and to exactly control the input signal to noise ratio, magnetic tapes containing synthetic data were generated and provided as input to the receiver. Because a large number of bursts is required to evaluate communication performance, a single input tape contains signal and noise under constant conditions and represents of the order

[REDACTED]

[REDACTED]

of 24 hours of real time operation. Each data tape is designated by DDD:HH where DDD is the day of the year and HH is the hour the tape was generated.

2.1 Synthetic Data Tapes [REDACTED]

[REDACTED] Construction of a synthetic data tape begins with the specification of a particular signal file, or SFILE. The signal in the SFILE can be generated according to any version of the M7 system and the particular message in the information component is specifiable. The random bit stream, known as the KFILE, is also specified at this point. After constructing the signal, an arbitrary Doppler offset can be applied, where this offset includes the time dilation effects of Doppler.

[REDACTED] A second file, called the CFILE is constructed to represent the impulse response of an acoustic channel. Examples of the two CFILES on which the results are based will be presented later.

[REDACTED] The synthetic data tape is constructed from an SFILE and a CFILE at a specified signal to noise ratio. First the signal is passed through the channel by a lagged correlation technique so that it is extended in time as required by the channel. Note that the signal has Doppler imposed on it prior to the channel. The energy content of the signal is measured. A noise vector is obtained by analog to digital conversion of the unfiltered output of a Hewlett-Packard 1381 random noise generator (set for no internal clipping) and the energy of the noise vector is measured. Then the filtered signal vector is added to the noise vector in a ratio to yield the desired signal to noise ratio.

[REDACTED]

█ To ensure that time of arrival uncertainty can be properly evaluated, the spacing between bursts is set by a random selector based on the noise source. A pair of signals is separated by $4096 + 512x$ complex samples where x is an integer uniformly distributed on $0 \leq x \leq 15$. The fixed offset of 4096 complex samples is provided to eliminate misses due to post-detection blanking. The starting time of each burst on the data tape is printed for later analysis.

█ In summary, each synthetic data tape contains of the order of 24 hours of data (~350 M7B bursts) having the following conditions held constant:

1. Signal version
2. KFILE random bit stream
3. Information on signal
4. Doppler offset
5. Channel multipath response
6. Signal to noise ratio

Signals appear at the quasi-random delays indicated, with both the noise and the arrival delays being independent from one tape to the next.

2.2 M7BX3A Version █

█ The particular version of the M7 on which the simulation was based is designated M7BX3A and represents the most advanced version currently available. The designator 'B' indicates the burst time bandwidth (TW) product is 4096, the designator '3' indicates the burst contains 10 symbol positions filled from a 64-ary signalling alphabet. The final



descriptor 'A' refers to the particular detection thresholds in use which will be described later.

The parameters indicated below were selected to allow evaluation of a significant version of the M7 system at sea over ranges of several hundred miles. As such the system is on the boundary between a tactical and a strategic communication system. Similarly, the Doppler range was selected so as to yield real time operation on existing equipment yet have some realism for tactical communications.

Table 2.1 gives the characteristics of the M7BX3A version. The indicated center frequency was selected to be compatible with the ONR-sponsored Eleuthera sound projector. With care, the results given here can be scaled to any frequency below 400 Hz. A detailed specification of the M7BX3A parameters appears in Appendix A.

As indicated above, the transmission contains 10 symbols taken from a 64-ary signalling alphabet. This yields the equivalent of 60 information bits per burst, or a bit rate of .75 bits/sec. Note that no error correcting codes have been used in the system. The 8 second symbol duration is sufficient to counter channel multipaths arising from ranges of several hundred miles.

The synchronization process of the M7BX3A receiver uses a 50% overlap factor in both the time and frequency domains ($NE = 2048$, $NT\phi = 2$). The Doppler search is conducted over 15 time dilation bins, each having a width of 16 spectral lines ($ND = 15$, $NW = 16$). This yields a Doppler range of ± 21.8 Kts as indicated in Table 2.1. Secondary synchronization



*** [REDACTED] ***

SYSTEM CHARACTERISTICS

M7BX3A - SPECIAL HIGH RATE VERSION FOR '78 NSUA
NHQ = 16 , INFO = NSUA-NUSC780

30 OCT 78 AT 1109 HR (RETYPED 05 JAN 78 AT 0757 HR)

CENTER FREQUENCY (HZ)	204.800
BANDWIDTH (4 DB ; HZ)	51.200
BURST DURATION (SEC)	80.000
BURST T-W PRODUCT	4096
MODULATION TYPE	64-ARY BIORTHOGONAL
SYMBOL DURATION (SEC)	8.000
SYMBOL T-W PRODUCT	409
BIT RATE (BITS/SEC)	0.750
BITS / BURST	60
DOPPLER RANGE (+-KT)	21.842

*** [REDACTED] ***

Table 2.1 M7BX3A Characteristics [REDACTED]
(Table Classified [REDACTED])

[REDACTED]

is performed over a ± 1 spectral line interval with a spacing of 1/5 spectral lines between searches. (DF1 = 1., NT1 = 5).

Based on previous synchronization studies, a low pass filter integration time of 16 samples was selected. (NH ϕ = 16). Given this choice, the primary and secondary thresholds were set at 2 and 4 standard deviations above the mean of their respective noise distributions. This was done to prevent false alarms from contaminating the various signal measurements. As will be shown later, the choice of thresholds was excellent.

The time dilation effects of Doppler were compensated for by a 32nd order interpolation using a $\sin x/x$ interpolation function with a 512 point quantization between zeros on its abscissa. (NO = 32, NI = 512). Fine grain Doppler removal by ZSHIFT process was limited to $\pm .2$ spectral lines (ZSHLIM = .2).

The channel response measurement was constrained to a 256 complex point (5 second) width, with a 10dB threshold on magnitude squared (NH1 = 256, R2RAT1 = .1). Impulse response and spectral displays during receiver operation showed these choices to be satisfactory.

Parameters for the bootstrap operation were taken to be identical with those of the first pass. (DF2 = DF1, R2RAT2 = R2RAT1).

A single random bit stream (KFILE) designated as K12013 was used throughout the simulation. It was obtained by undersampling a noise source by a factor of 4 and observing the polarity of the result. In terms of

balance (number of ones versus number of zeros) of the sequence is .09 binomial standard deviations away from equality. Although certain earlier KFILES were modified to be compatible with the Naval Ocean Systems Center Channel Adaptive Receiver and used the same symbol alphabet in each symbol position, K12013 was not modified and therefore has different alphabets for each symbol position. Thus the KFILE on which the simulation results are based has no known structure beyond that of a random bit stream.

2.3 CELTHRA

Two linear channels were studied in the simulation. The first is the ideal, single impulse channel, designated CIDEAL, which serves as a point of reference. The second channel was taken from a measured channel as described below.

For realism, a simulated channel was constructed from data provided by K. Metger of the University of Michigan and J. Speisberger of Scripps Institute of Oceanography. These data were obtained by periodic pseudo random sequences transmission between the ONR Eleuthera source and the 'MS' hydrophone, a distance of 350 nm. Conversion from the analog data plot to digital form was performed by choosing paths within 13 dB of the largest path. This yielded a ten point complex impulse response over 1.75 seconds, as shown in Figure 2.1, designated CELTHRA. Although CELTHRA is not intended to be a typical

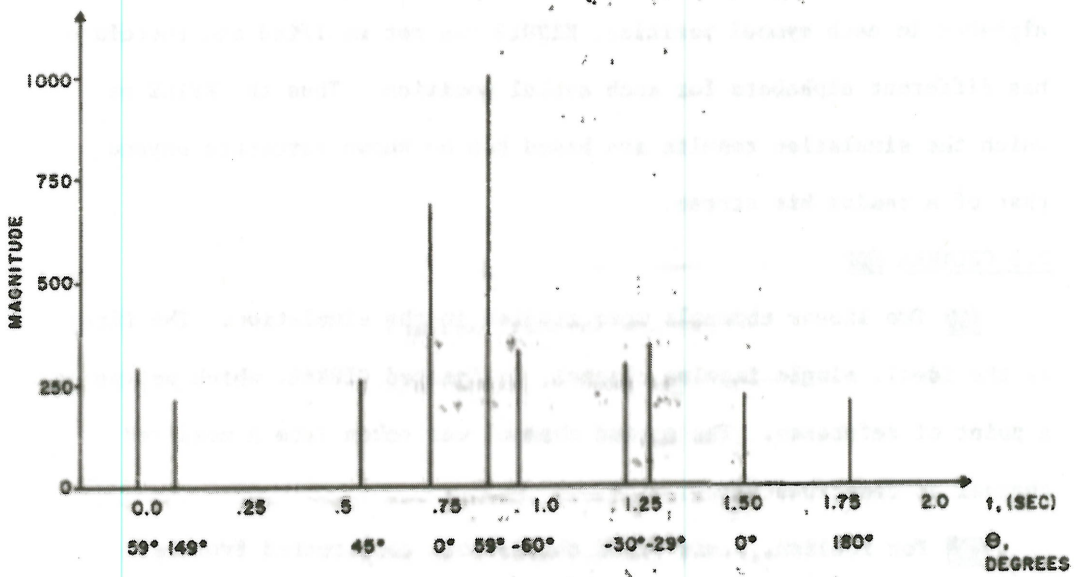
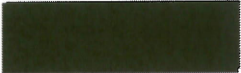


Figure 2.1: CELTHRA Impulse Response

(This figure



or canonical channel for all communication environments, it does provide an interesting test of the M7 system performance.

3. Simulation Results

This section highlights the more interesting results from the simulation. After defining the data set, the synchronization and information demodulation performance of the M7BX3A system are studied as a function of input signal to noise ratio. Several of the more interesting collateral receiver outputs are also considered. A complete summary of the data is given in Appendix B.

3.1 Data Description:

Approximately 588 hours of data, containing 9027 bursts were studied by simulation. All of the data kept the items in Table 3.1 constant. The differences between data tapes were then the channel and signal-to-noise ratio. The message was selected for a demonstration at the Naval Symposium on Underwater Acoustics at the Naval Undersea Systems Center during 1978. The selected Doppler locates the signal at the extreme edge of the most remote time dilation bin so as to severely test both the synchronization and zero frequency shifting algorithms.

Table 3.1 Fixed Parameters in Simulation
(Table classified)

- System: M7BX3A
- KFILE: K12013
- MESSAGE: MSUA-MUSC78 (Radix 40)/943E 4487 DFEC (Hex)
- DOPPLER: 21.5 Kc opening



Table 3.2 gives an index of the data tapes on which the simulation is based. The data consist of evaluations over different input signal to noise ratios for both the ideal (CIDEAL) and measured (CELTHRA) channel. The tapes with signal to noise ratios over -7dB were intended to provide calibration data and contain no misses or symbol errors. In general, each tape contains about 24 hours of data or, equivalently, 368 bursts and 3680 symbol decisions.

3.2 Synchronization Performance

Operation of the M7 communication system can be considered in terms of two consecutive processes: synchronization and information demodulation. The synchronization process determines if a signal is present, and if it is present, it determines the signal's starting time and Doppler offset. The performance of the information demodulation process will be described in Section 3.3.

The classical measure of detection performance is the Receiver Operating Characteristic (ROC) curve which is immediately applicable in the two alternative forced choice problem. A continuously operating system, such as the M7 receiver, is not readily described by an ROC curve since the probability of false alarm, $P(\text{FA})$, is difficult to define. The approach taken here was to fix the two decision thresholds and then examine the probability of miss and the false alarm rate at these thresholds.

Table 3.2: Data Summary

(Table classified)

<u>S/N (dB)</u>	<u>CIDEAL</u>			<u>CELTHRA</u>		
	<u>ID</u>	<u>Duration</u>	<u>Bursts</u>	<u>ID</u>	<u>Duration</u>	<u>Bursts</u>
+10	108:07	22:41	349	106:10	7:43	118
+5	124:10	25:10	389	123:10	25:09	385
0	109:09	11:08	166	107:07	25:09	385
-5	28:13	26:30	410	110:09	15:51	238
-7	53:10	37:37	578	64:10	21:10	324
-8	50:08	37:45	583			
-8.5	19:16	25:16	388			
-9	18:09	36:37	565	64:07	23:59	368
-10	11:09	33:46	512	52:08	25:08	386
-11	15:07	15:50	246	58:13	25:01	385
-12	22:09	21:41	332	57:08	25:10	382
-13	113:07	25:09	387	60:10	24:52	387
-14	149:07	25:01	382	61:12	24:59	382
		<u>344:11</u>	<u>5287</u>		<u>244:11</u>	<u>3740</u>

9027 Bursts

588:22 Hours

Figure 3.1 shows the probability of miss as a function of input signal to noise ratio for the two channels with the receiver operating with the 2,4 standard deviation thresholds, M7BX3A. The probability of miss decreases rapidly with signal to noise rates, and is about a factor of 10 higher for CELTHRA than CIDEAL. No misses in 385 bursts were measured at -11dB for CIDEAL, for CELTHRA no misses were measured in 512 bursts at -10dB. Using these same thresholds no false alarms were obtained in 588 hours (~24 1/2 days) of real time operation.

The low false alarm rate indicated above, suggests a reduction in thresholds to improve detection performance at the expense of false alarm rate. To examine this possibility, another version of M7BX3 was based on thresholds located at the 1,2 standard deviation points of the noise alone distribution. This version was designated M7BX3B and experienced 16 false alarms in 11 hours and 57 minutes, for a false alarm rate of about 1 1/3 false alarms per hour. With CIDEAL at a signal to noise ratio of -14dB, these thresholds lowered the probability of miss from .40 to .21, or about a factor of two. Similarly, these thresholds lowered the probability of miss for CELTHRA at -14dB from .83 to .59. This improvement in probability of miss does not appear to be worth the corresponding drastic increase in false alarm rate.

3.3 Information Demodulation Performance

When the SFILE is constructed for a simulated data tape, a message is specified. Each version of the receiver includes a message

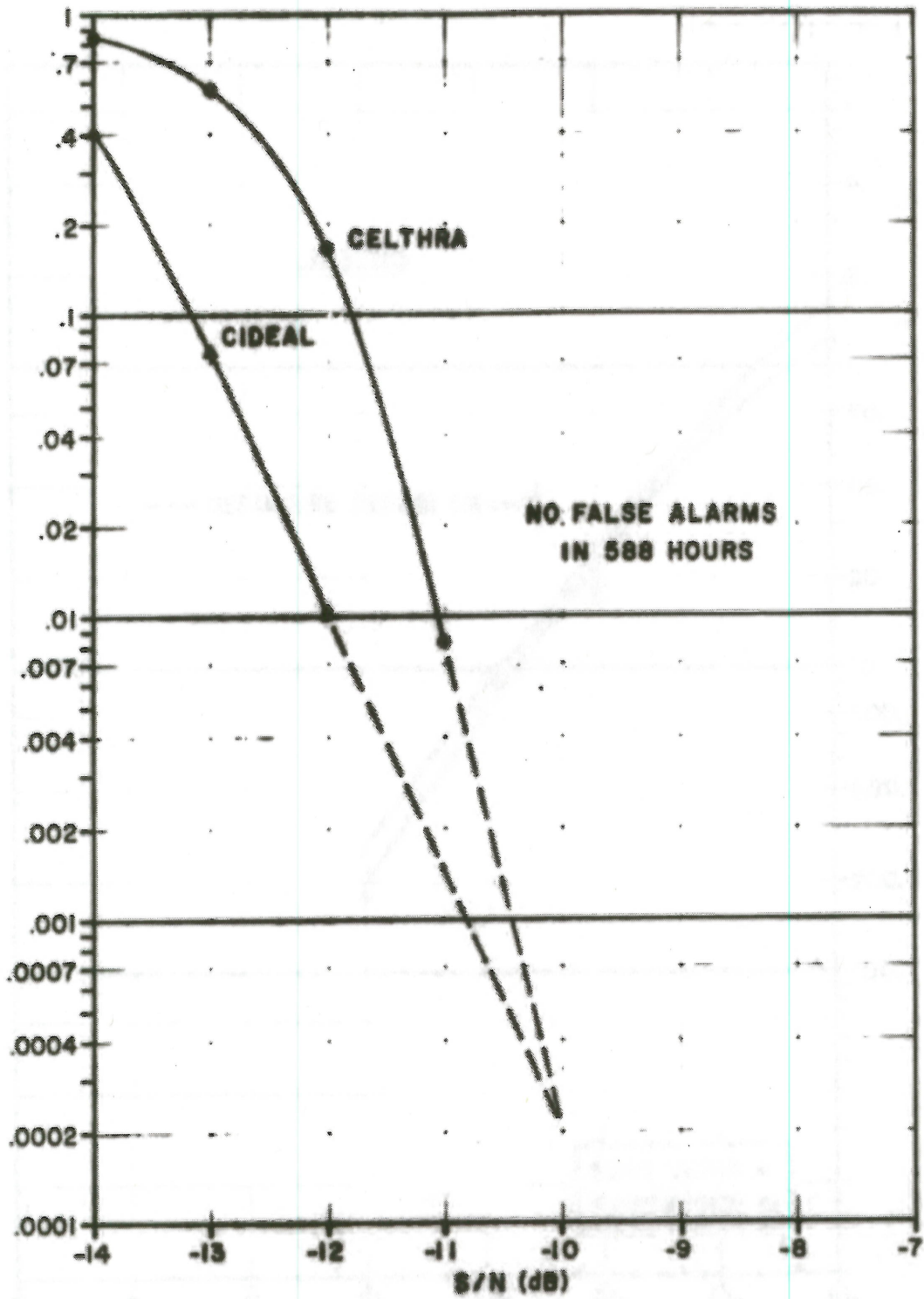


Figure 3.1: P_{MISS} vs S/N

(This figure classified)

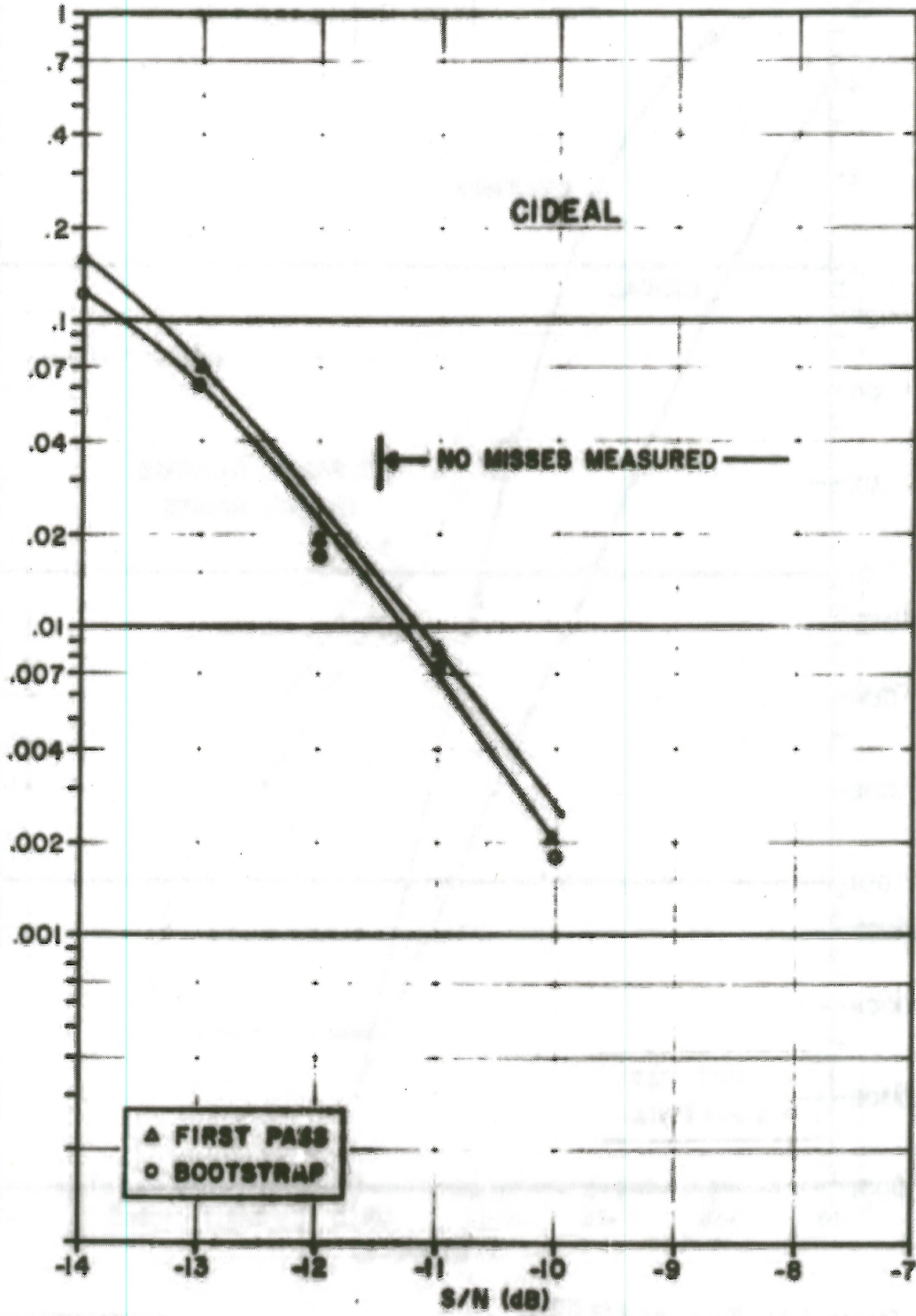


Figure 3.2: $P_E(SYN)$ vs S/N for CIDEAL

(This figure classified

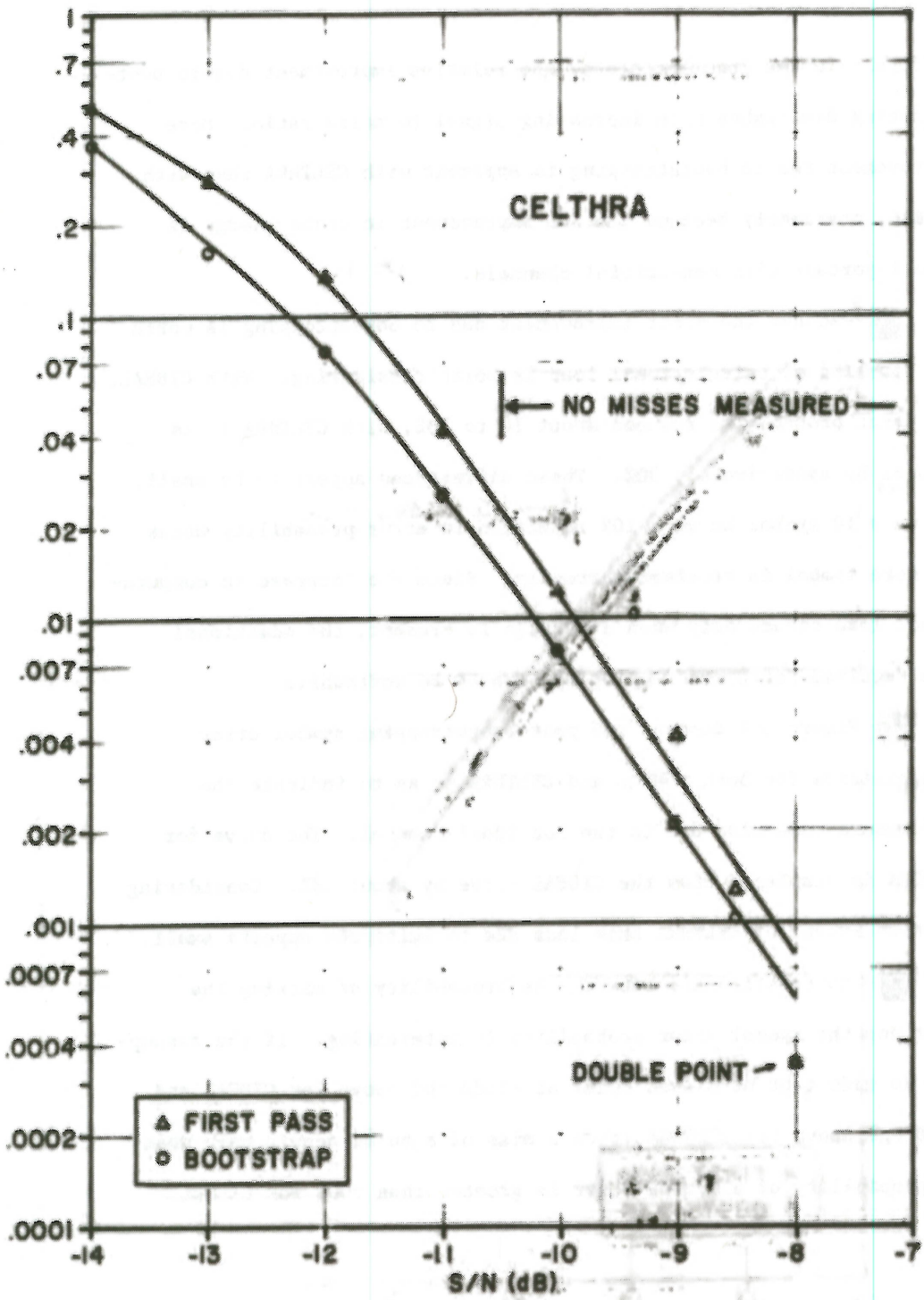


Figure 3.3: $P_E(SYM)$ vs S/N for CELTHRA

(This figure classified

difficult to see from the plots, the relative improvement due to bootstrapping diminishes with increasing signal to noise ratio. More improvement due to bootstrapping is apparent with CELTHRA than with CIDEAL, presumably because the 3dB improvement in probe energy is more important with non-trivial channels.

Whether the error improvement due to bootstrapping is worth the doubling of calculational load is worth considering. With CIDEAL, the error probably is reduced about 10 to 20%, with CELTHRA it is reduced by approximately 30%. These differences appear to be small, but in a 10 symbol burst a 10% reduction in error probability means one more symbol is received correctly. Since the increase in computational load occurs only when a message is present, the additional time required for bootstrapping appears to be worthwhile.

Figure 3.4 depicts the post-bootstrapping symbol error probabilities for both CIDEAL and CELTHRA so as to indicate the performance reduction due to the non ideal channel. The curve for CELTHRA is displaced from the CIDEAL curve by about 1dB. Considering the time extent of CELTHRA this loss due to multipath appears small.

The relationship between the probability of missing the burst and the symbol error probability is interesting. If the assumption is made that no misses occur at -11dB and above for CIDEAL and - 9dB and above for CELTHRA, then a miss of a burst occurs only when the probability of a symbol error is greater than .007 for CIDEAL

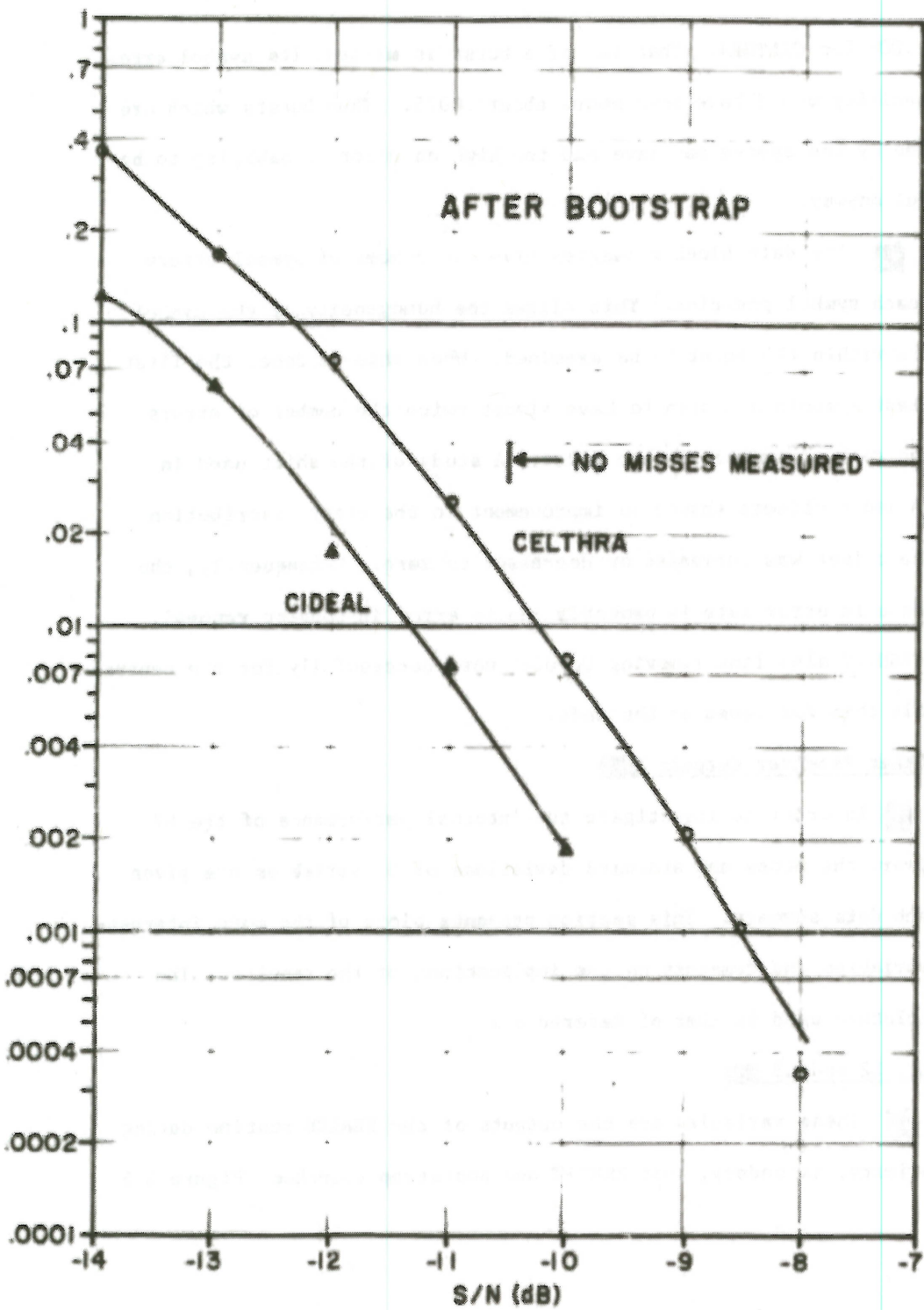


Figure 3.4: $P_E(\text{SYM})$ after bootstrapping for CIDEAL and CELTHRA

(This figure classified

and .008 for CELTHRA. That is, if a burst is missed, its symbol error probability would have been above about .0075. Thus bursts which are missed by the system may have had too high an error probability to be useful anyway.

The data block summaries give the number of symbol errors for each symbol position. This allows the homogeneity of the symbol errors within the burst to be examined. When this is done, the first and last symbols are seen to have almost twice the number of errors of the central symbols in the burst. A study of the shift used in the A and B offsets showed no improvement in the error distribution as the offset was increased or decreased to zero. Consequently, the increase in error rate is probably due to error in Doppler removal, with ZSHIFT algorithm removing Doppler more successfully for the central symbols than for those at the ends.

3.4 Other Receiver Outputs

In order to investigate the internal performance of the M7 receiver, the means and standard deviations of 50 variables are given in each data summary. This section presents plots of the more interesting variables and comments on the implications of the results. The nomenclature used is that of Reference 1.

L₀, L1, L2 and L3

These variables are the outputs of the SEARCH routine during the primary, secondary, post ZSHIFT and bootstrap searches. Figure 3.5

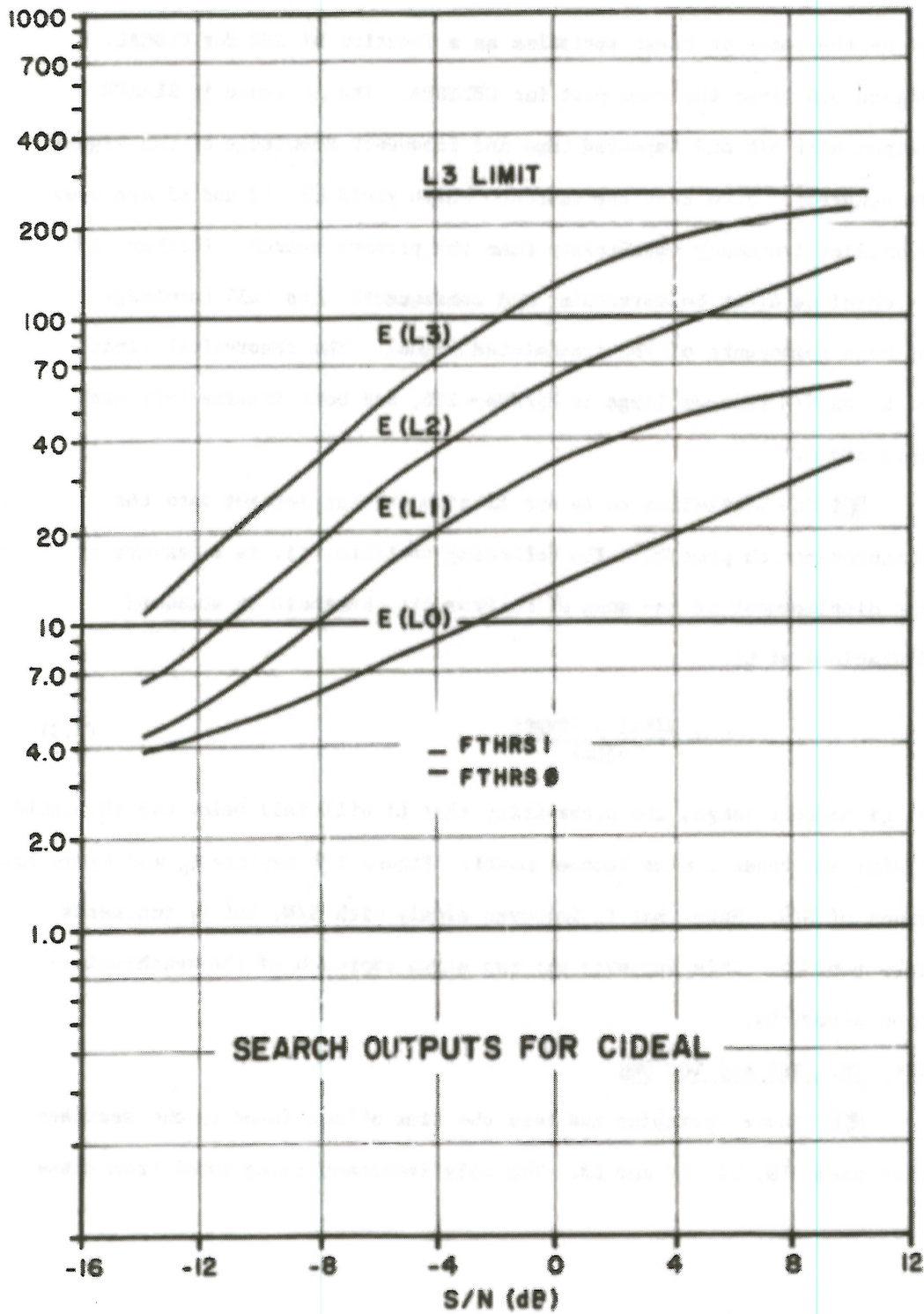


Figure 3.5: Means of $L\phi$, $L1$, $L2$ and $L3$ vs S/N for CIDEAL

(This figure

gives the means of these variables as a function of SNR for CIDEAL. Figure 3.6 gives the same plot for CELTHRA. The increase in SEARCH output with S/N and improved time and frequency knowledge of the signal is apparent. Note that the searches which yield L1, L2 and L3 are over a smaller frequency uncertainty than the primary search. Further, L3 is obtained after bootstrapping and consequently has full knowledge of both components of the transmitted signal. The theoretical limit of L3 as S/N becomes large is $N_B/NH\phi = 256$, and both figures indicate this trend.

■ The statistics on L_0 and L_1 also provide insight into the synchronization process. The following variable, ξ_1 , is a measure of the displacement of the mean of L_1 from the threshold in standard deviations of L_1 .

$$\xi_1 = \frac{E(L_1) - FTHRS_1}{\sigma(L_1)} \quad (3.2)$$

As ξ_1 becomes large, the probability that L_1 will fall below the threshold $FTHRS_1$ and cause a miss becomes small. Figure 3.7 depicts ξ_0 and ξ_1 as functions of S/N. Note that ξ_0 improves slowly with S/N, but ξ_1 increases more rapidly. This supports the two stage approach of the synchronization algorithm.

TS₀, TS₁, TS₂ and TS₃ ■

■ These variables indicate the time offset found by the searches that yield L_0 , L_1 , L_2 and L_3 . The only important thing noted from these

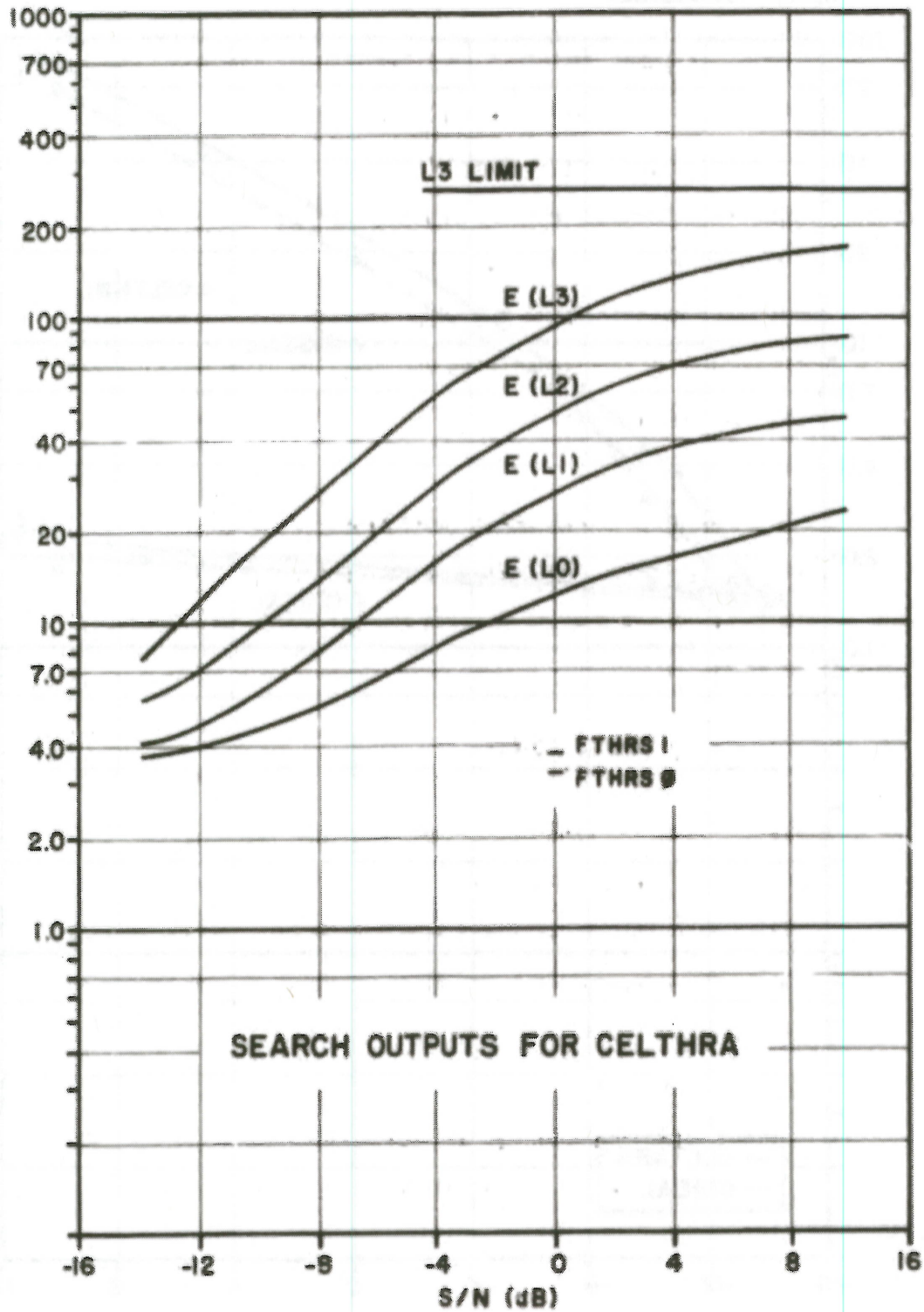


Figure 3.6: Means of L ϕ , L1, L2 and L3 vs S/N for CELTHRA

(This figure

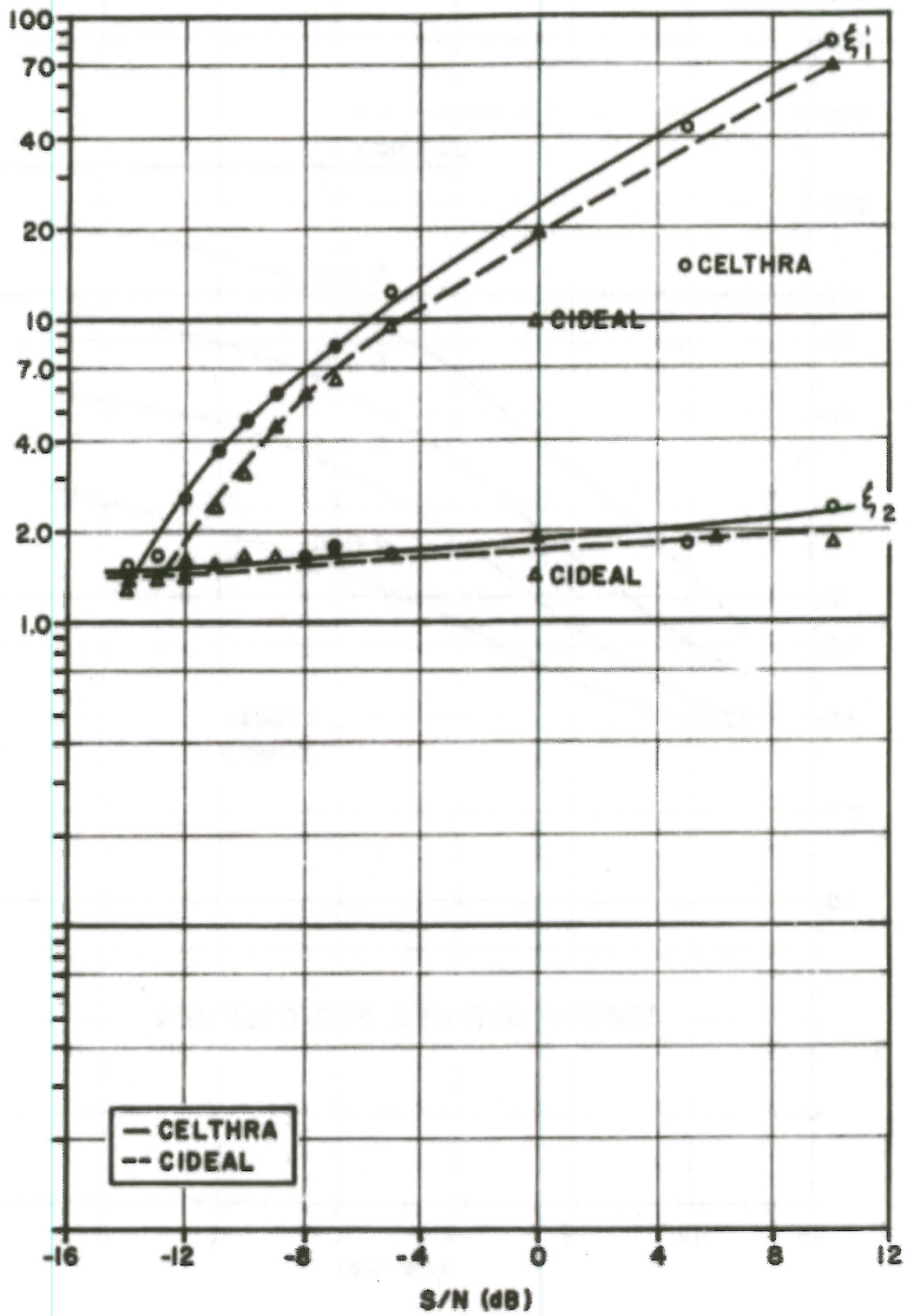


Figure 3.7: ϵ_0 and ϵ_1 vs S/N

(This figure

variables is that TS1, TS2 and TS3 are small and have small variances. This indicates that the primary search is very successful in determining the time origin of the signal, as given by TS0.

FS0, FS1, FS2 and FS3

These variables give the frequency location of the signal as found by the searches that yield L0, L1, L2 and L3. Figures 3.8, 3.9 and 3.10 give the means and standard deviations for FS0, FS1 and FS2. The ordinate in these plots has units of spectral lines, so that an ordinate value of .1 corresponds to $.1/T_B = 1.25$ MHz. The transmitted signal was at an offset of 119 lines and hence the plots indicate the error relative to the actual Doppler

The primary search which gives FS0 is performed on widths of 1/2 line spacing ($NT0 = 2$) and hence the standard deviation shown in Figure 3.8 could be attributed to fluctuation of plus or minus one search interval. These fluctuations must be nearly symmetric to yield the mean values.

The secondary search which gives FS1 is on 1/5 line spacing ($NT1 = 5$) and consequently has a finer resolution than the primary search. Unfortunately, the mean value of FS1 in Figure 3.9 indicates a distinct bias toward a lower frequency, 118.8 for CIDEAL and 118.6 for CELTHRA. This bias is believed to be caused by the fact that the secondary search is conducted relative to a vector centered in the time dilation bin, with the signal located at the extreme edge of that bin. This apparent bias was the reason for inserting the post-ZSHIFT search. Note that the particular channel has negligible effect on the standard deviation of either FS0 or FS1.

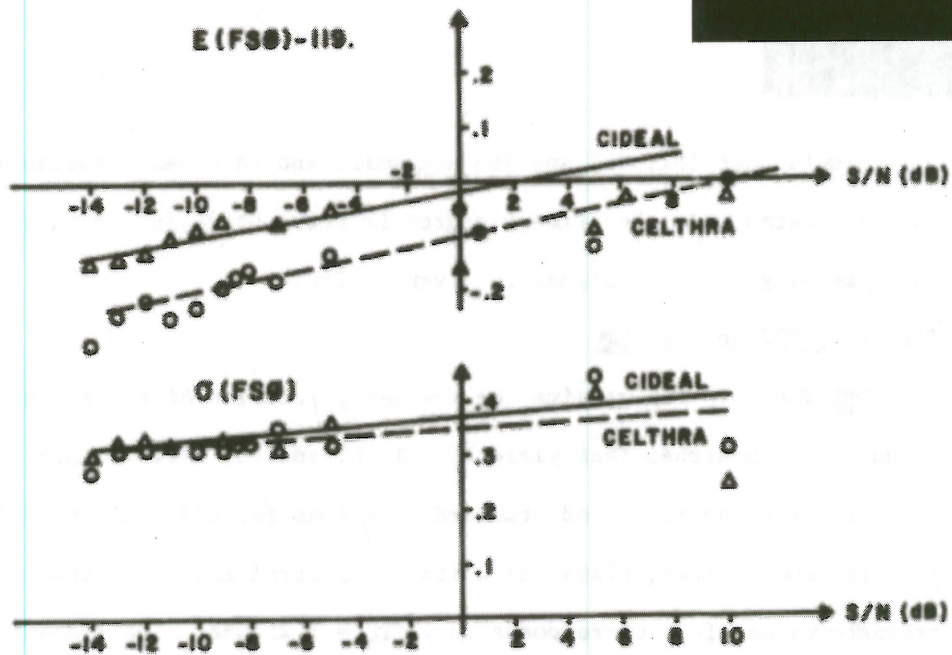


FIGURE 3.8: Mean and standard deviation of $FS\phi$ vs S/N

(This figure)

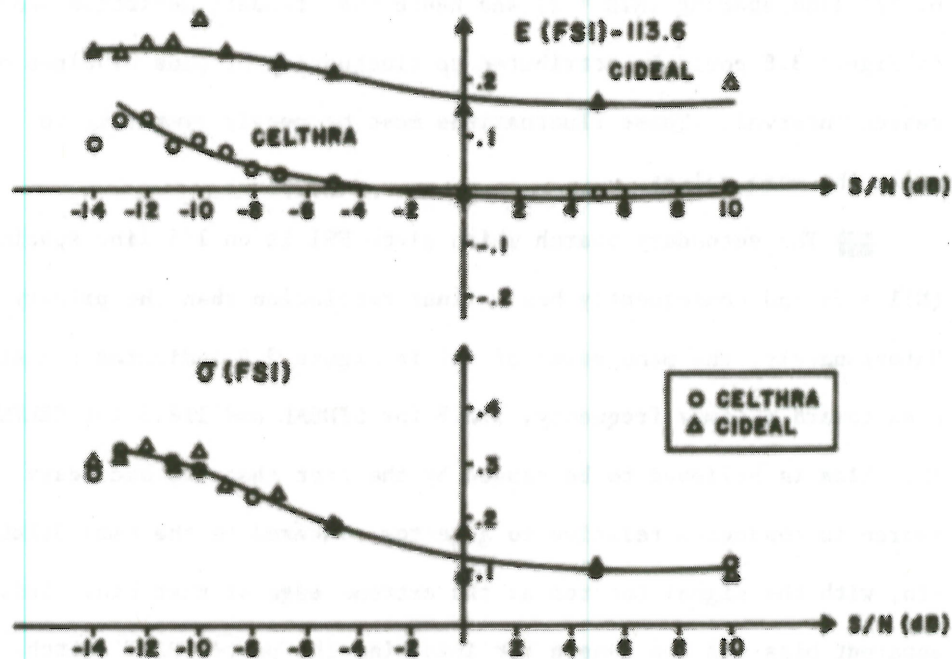


Figure 3.9: Mean and standard deviation of $FS1$ vs S/N

(This figure)

Figure 3.10 gives the mean and standard deviation of FS2 as a function of S/N. This variable is the frequency location found by the post ZSHIFT search and is not biased as FS1 was. For low S/N (<7dB) the error in FS2 is less than .05 lines or .063 mHz for both channels. As S/N increases the error for CELTHRA remains near zero but that for CIDEAL increases to 12 lines or .25 mHz. The reason for this increase is not known. The standard deviation of FS2 for both channels is less than .1 lines or .125 mHz.

F2, F2A, F2B, F3, F3A, F3B

These variables are the frequency locations found by the ZSHIFT routine. F2 is calculated between the secondary search and the post-ZSHIFT search and is nearly identical to FS1 described above. F2A and F2B are the frequency locations found by the ZSHIFT routine after the post-ZSHIFT search which yields FS2. The suffixes A, B represent the two time shifts applied to demodulate the first and last halves of the burst. For compactness, the following equation will be used to compress any pair of A, B shift variables to a single variable:

$$X_{NA/B} = \frac{X_{NA} + X_{NB}}{2} \quad (3.3)$$

That is, the A/B notation indicates the average of the two shifts.

Figure 3.11 gives the mean and standard deviation of F2A/B versus S/N. Here both channels have the same error, approximately .03 lines, .038 mHz, which is amazingly independent of S/N. The standard deviation of F2A/B is also the same for both channels and is less than .05 lines, .063 mHz, for S/N > -8dB.

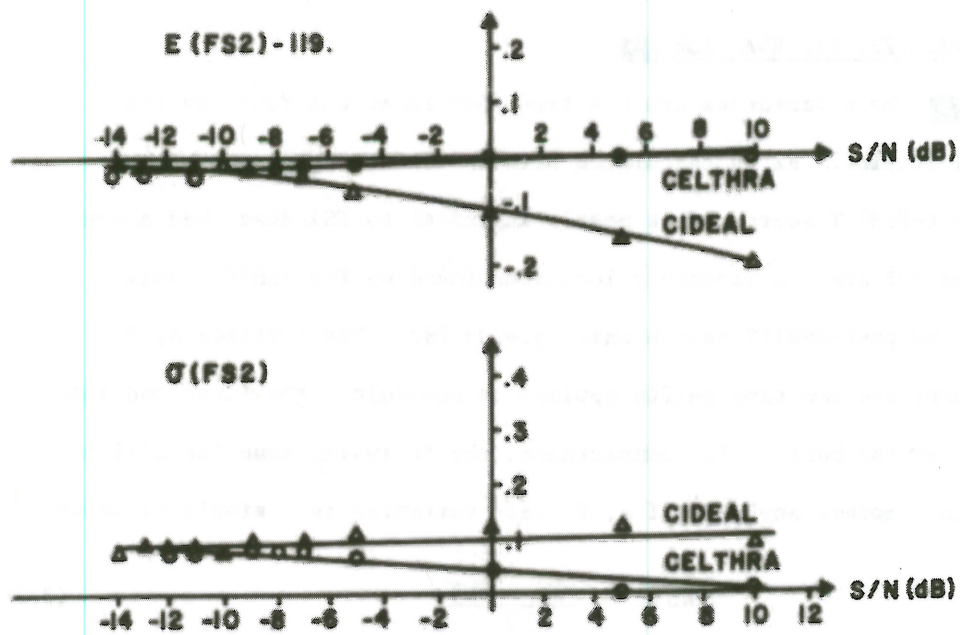


Figure 3.10: Mean and standard deviation of FS2 vs S/N

(This figure)

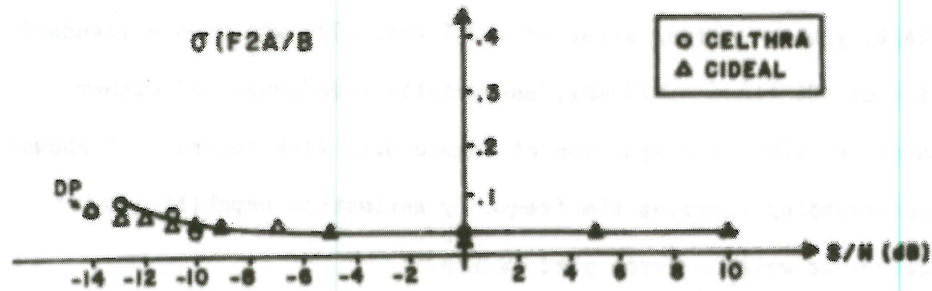
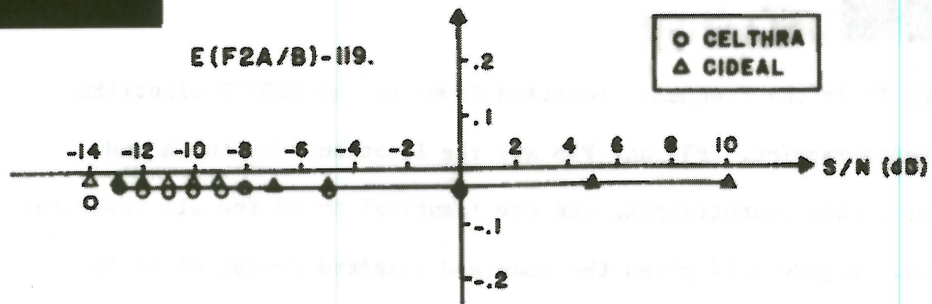
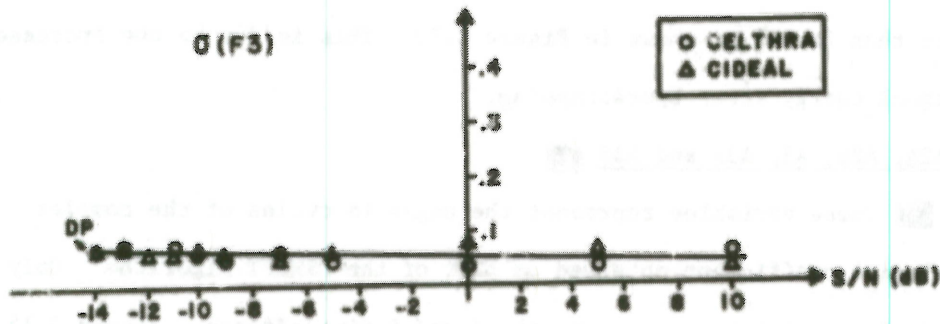
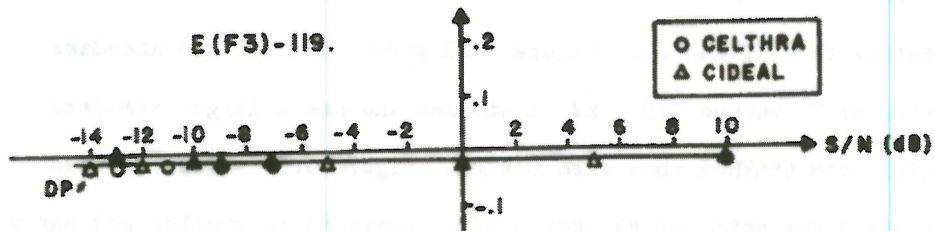


Figure 3.11: Mean and standard deviation of F2A/B vs S/N

(This figure)



DP DOUBLE POINT

Figure 3.12: Mean and standard deviation of F3 vs S/N

(This figure)

■ F3 is the frequency location found by the ZSHIFT algorithm after bootstrapping. F3A and F3B are the locations for the A and B passes during bootstrapping and are identical to F3 for all practical purposes. Figure 3.12 gives the mean and standard deviation of F3 on a function of S/N. The error and standard deviation of F3 is less than F2A/B, giving a final error of .02 lines, .025 mHz with a standard deviation of .06 lines, .075 mHz, essentially independent of either the channel of S/N. A comparison of Figure 3.12 with Figure 3.11 shows that bootstrapping improves the frequency estimation capabilities of the receiver as well as error performance.

R2, R2A, R2B, R3, R3A and R3B ■

■ These values are the magnitudes of the normalized correlation coefficient obtained as part of the ZSHIFT algorithm. Because of the time offset at the A and B shifts, R2A, R2B and R3A, R3B are less interesting than R2 and R3. Figure 3.13 gives the mean and standard deviation of R2 versus S/N. R2 is smaller and has a larger standard deviation with CELTHRA than with CIDEAL. Figure 3.14 gives the mean and standard deviation of R3 versus S/N. Again R3 is smaller and has a larger standard deviation through CELTHRA than CIDEAL, but both values are better than for R2 as shown in Figure 3.13. This is due to the increase in signal energy after bootstrapping.

A2, A2A, A2B, A3, A3A and A3B ■

■ These variables represent the angle in cycles of the complex correlation coefficient obtained as part of the ZSHIFT algorithm. Only A2 and A3 are of interest due to the A and B time offsets. Figure 3.15 gives the mean and standard deviation of A2 as a function of S/N. For

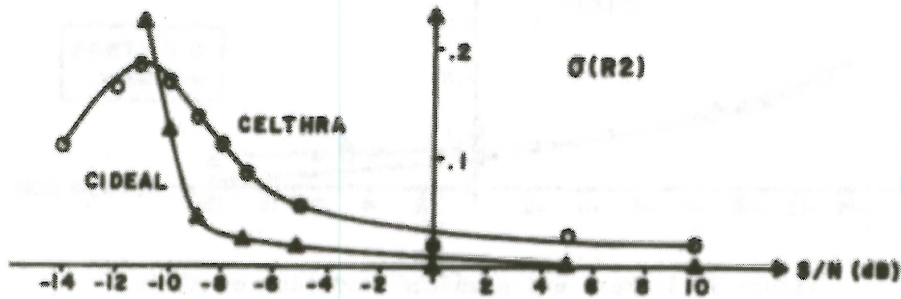
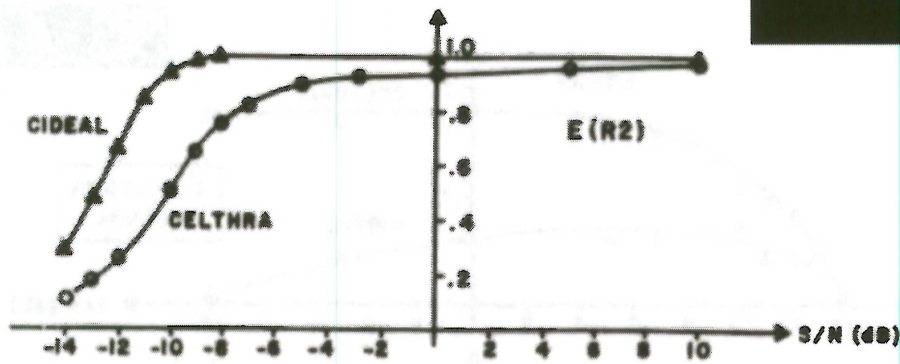


Figure 3.13: Mean and standard deviation of R_2 vs S/N

(This figure [redacted])

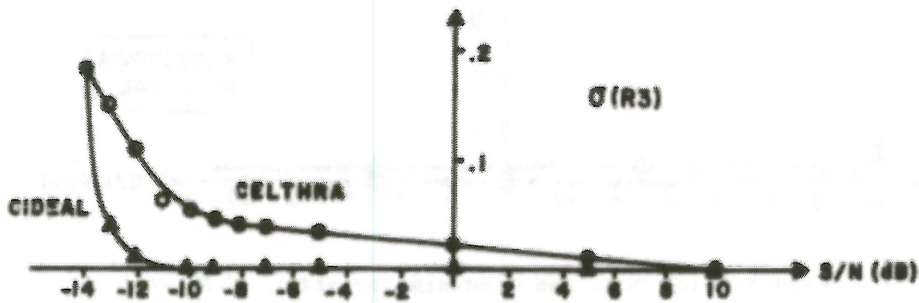
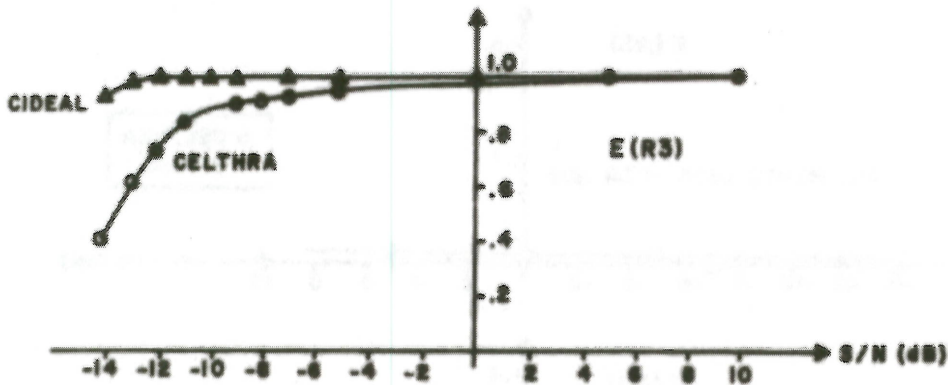


Figure 3.14: Mean and standard deviation of R_3 vs S/N

(This figure [redacted])

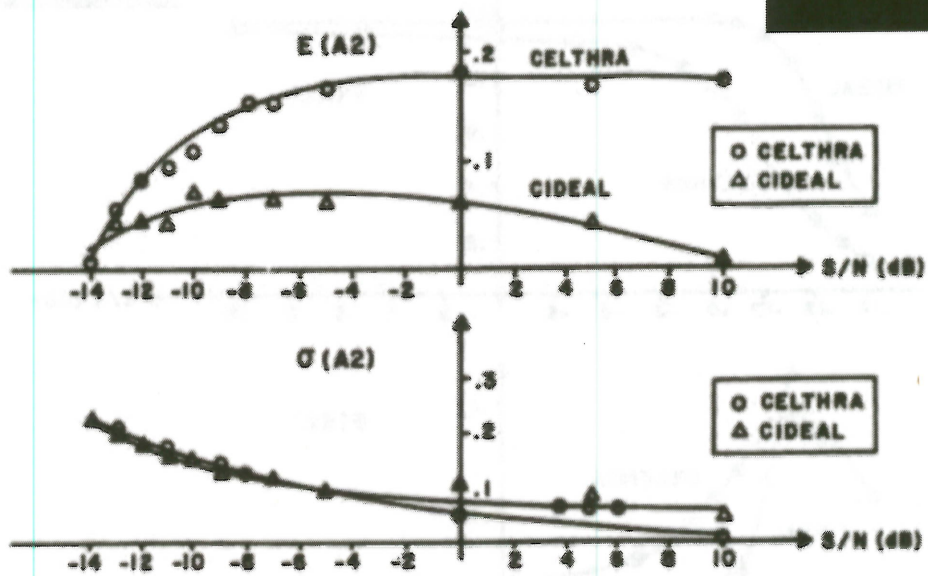


Figure 3.15: Mean and standard deviation of A2 vs S/N

(This figure

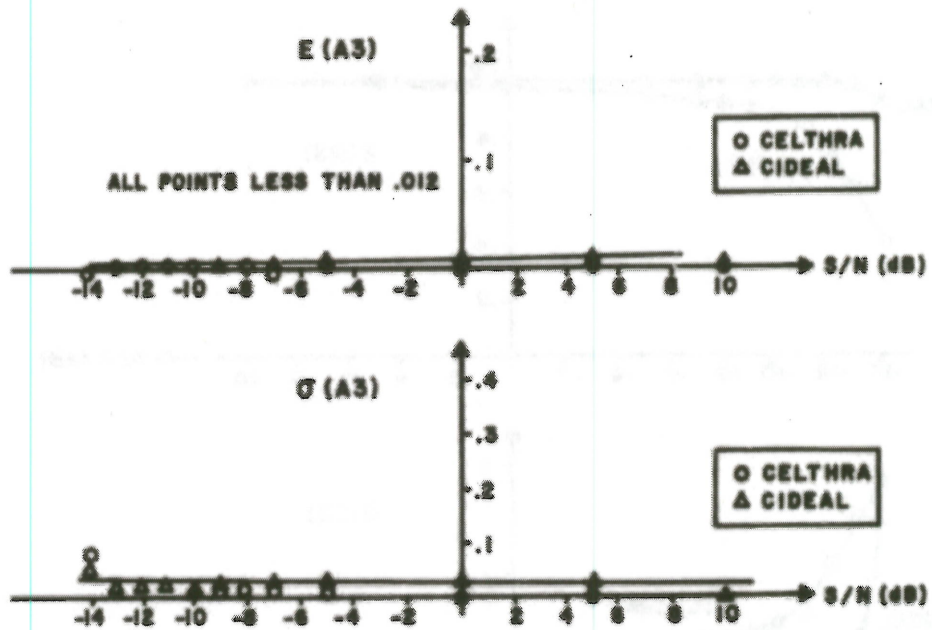


Figure 3.16: Mean and standard deviation of A3 vs S/N

(This figure

CELTHRA the mean offset angle actually increases with S/N. This is associated with the bias observed in FS1. Once the bootstrapping process is performed, the angle A3 becomes very small, as indicated in Figure 3.16. Here the angle is less than .012 cycles (4.32°) with a standard deviation of less than .04 cycles (14.4°). This is for both channels and all S/Ns measured.

TP2A, TP2B, TP3A, TP3B

These measurements give the time displacement of the NH1 long window of the probe measurement relative to the start of the NB long vector. Of interest here is that the "A" values are positive due to the pre-shift and the "B" values are negative due to the post-shift. The difference TPNA-TPNB is of the order of $2NH_1$ as expected.

NZ2A, NZ2B, NZ3A, NZ3B

These measurements give the number of non-zero points in the probe measurement after thresholding by R2CUT1 or R2CUT2. Figure 3.17 depicts the mean values of NZ2A/B and NZ3A/B as function of S/N. The standard deviations of these variables are of little interest. For $S/N > -7\text{dB}$ both averages have constant values, indicating the number of non zero points is controlled by the threshold and the channel. Smaller values of S/N introduce more noise and consequently more non-zero points in the impulse response. The number of such points is reduced after bootstrapping as indicated by comparison of the NZ2A/B plot with the NZ3A/B plot. Note that although the probe window allows for 256 points ($NH1 = 256$), only a very small number, -5 are actually non-zero

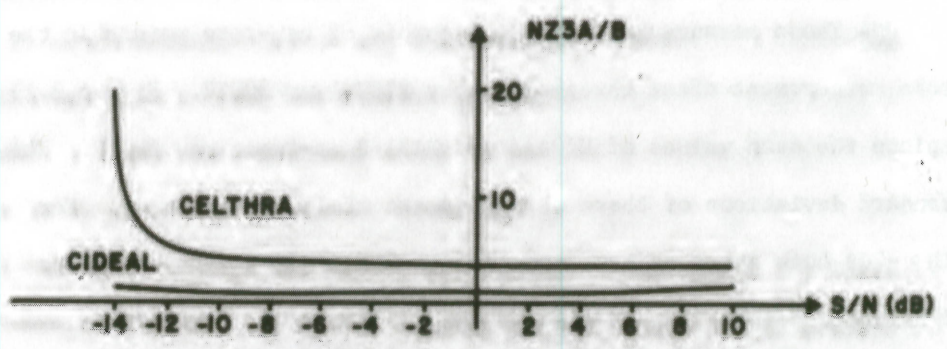
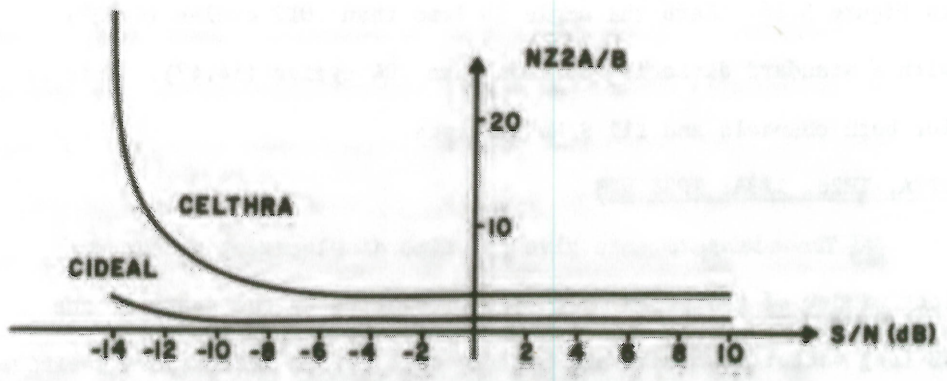


Figure 3.17: Means fo NZ2A/B and NZ3A/B vs S/N

(This figure

██████████

SNR2A, SNR2B, SNR3A, SNR3B, S3, NDBV ██████████

■ An important problem in the evaluation of communication systems is the determination of the signal to noise ratio under which the system is operating. The synthetic data on which the present study is based has a precisely controlled signal to noise ratio due to its construction. In a sea experiment, however, measurement of signal to noise ratio requires care. The simulation data does allow evaluation of signal to noise ratio estimation techniques which could then be used in a sea test.

■ $SNR2A/B$ and $SNR3A/B$ are measures of the signal to noise ratio based on the energy in the measured probe response relative to that in a displaced interval of equal length. The scale factor in determining these quantities has been set up so that $SNR2X$ is 3dB less than $SNR3X$ and $SNR3X$ is intended to approximate the actual received signal to noise ratio. Figure 3.18 depicts $SNR2A/B$ and $SNR3A/B$ as a function of S/N. The standard deviations of these quantities are small (-.5dB). Also shown is the equality line which represents the behavior of an ideal S/N measurement. $SNR3A/B$ approaches the equality line for low S/N but is not useful for S/N greater than 0 db. $SNR3A/B$ is remarkably independent of the particular channel, however.

■ Alternatively, the signal to noise ratio could be calculated by measuring the signal energy in an equal signal-free interval. The signal energy during a burst is measured as S3 after bootstrapping. The signal-free energy is measured as NDBV, where both quantities are

██████████

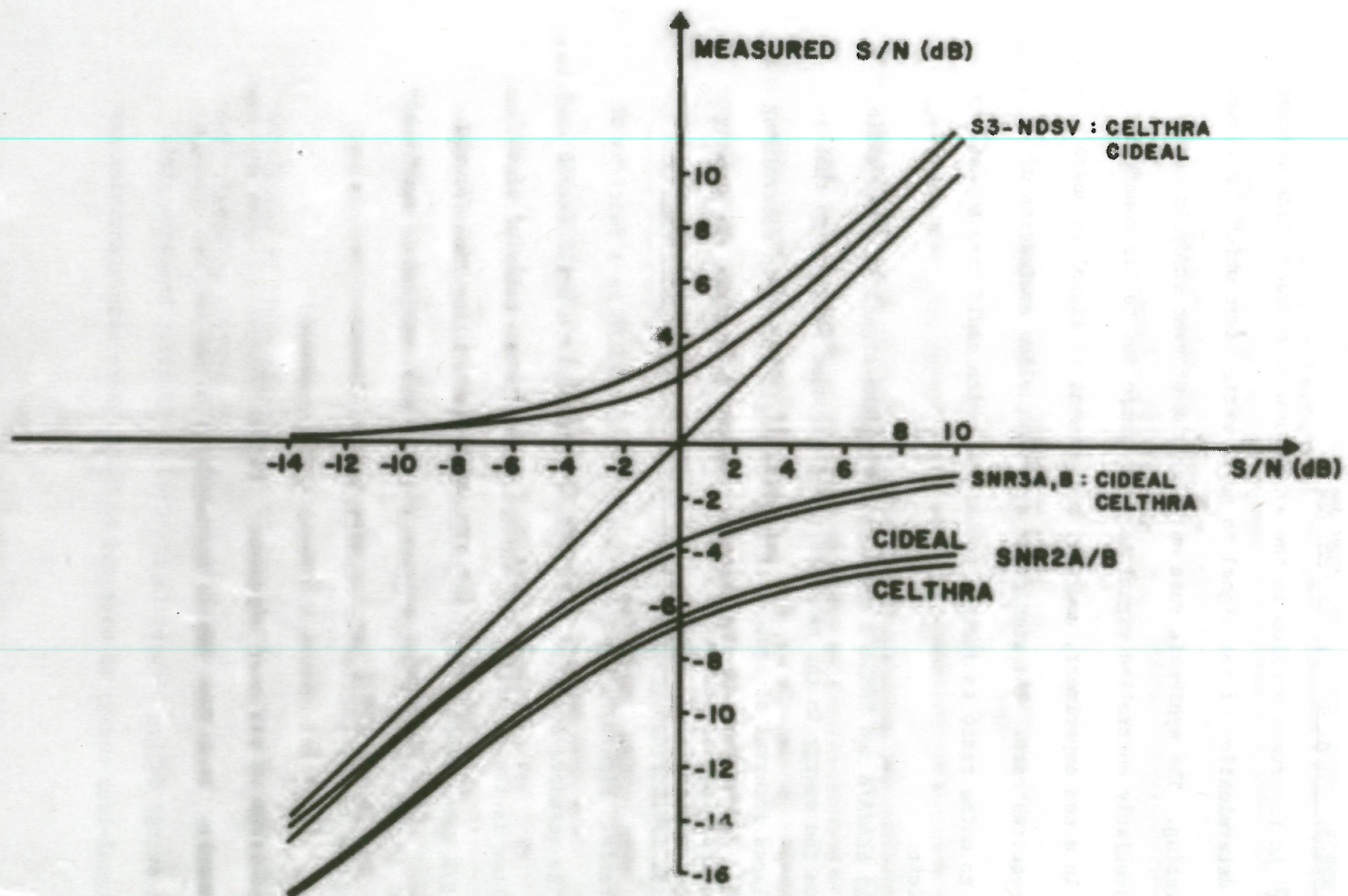


Figure 3.18: Measured S/N vs actual S/N

(This figure

in decibels and use the same reference point, Figure 3.18 gives $S3-NDBV$ for both channels. Here the approximation is best for $S/N > 0$ dB and again the particular channel in use has little effect.

Combining the two measurement approaches yields a technique applicable over a wide range of S/N s. Define

$$\frac{S}{N} \text{ estimated, dB} = \frac{SNR3A + SNR3B}{2} + (S3 - NDBV) \quad (3.4)$$

as the sum of the two signal to noise ratio estimates. The error, ϵ , in dB between the applied S/N and $(S/N)_{\text{estimated}}$ is shown in Figure 3.19. Note the ordinate scale is expanded relative to Figure 3.18. For S/N between +10 and -14 dB, $S/N_{\text{estimated}}$ is within .75 dB of actual and is nearly independent of the channel. Figure 3.20 gives the standard deviation of $SNR2A/B$ and $SNR3A/B$.

INF2A, INF2B, INF3A, INF3B

These measurements indicate the signal to noise ratio in decibels at the symbol filter outputs, measured as an energy ratio of the filter having the largest output to the average energy of the other filters. Amazingly little difference between INF2A, INF2B and INF3A, INF3B was noted, even though INF3X has the advantage of bootstrapping. Define

$$INF = 1/4 (INF2A + INF2B + INF3A + INF3B) \quad (3.5)$$

as the average of all four variables. Figure 3.21 depicts INF for the two channels. Note that INF is proportional to S/N only for low S/N .

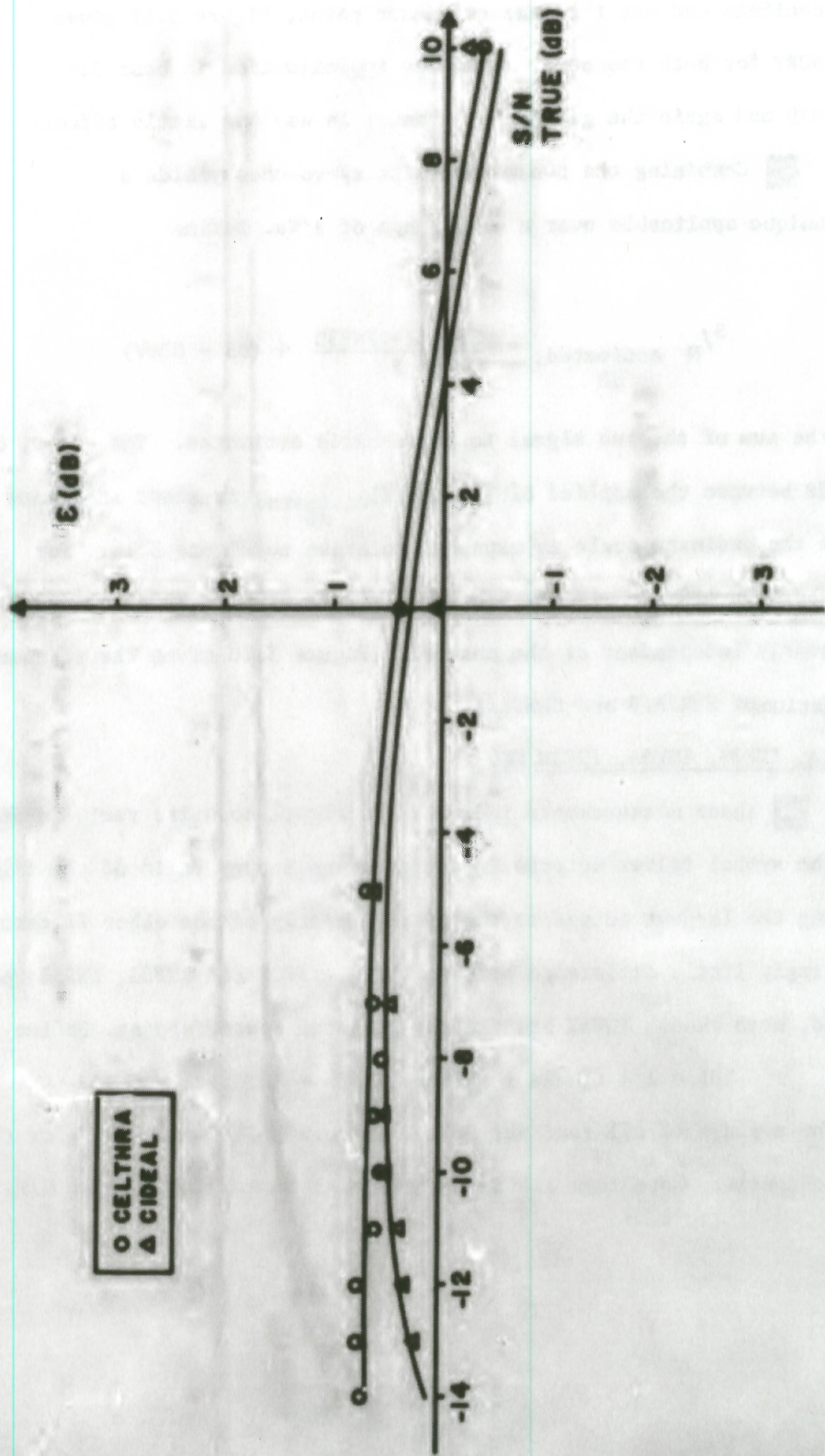


Figure 3.19: S/N measurement error ϵ vs S/N

(This figure

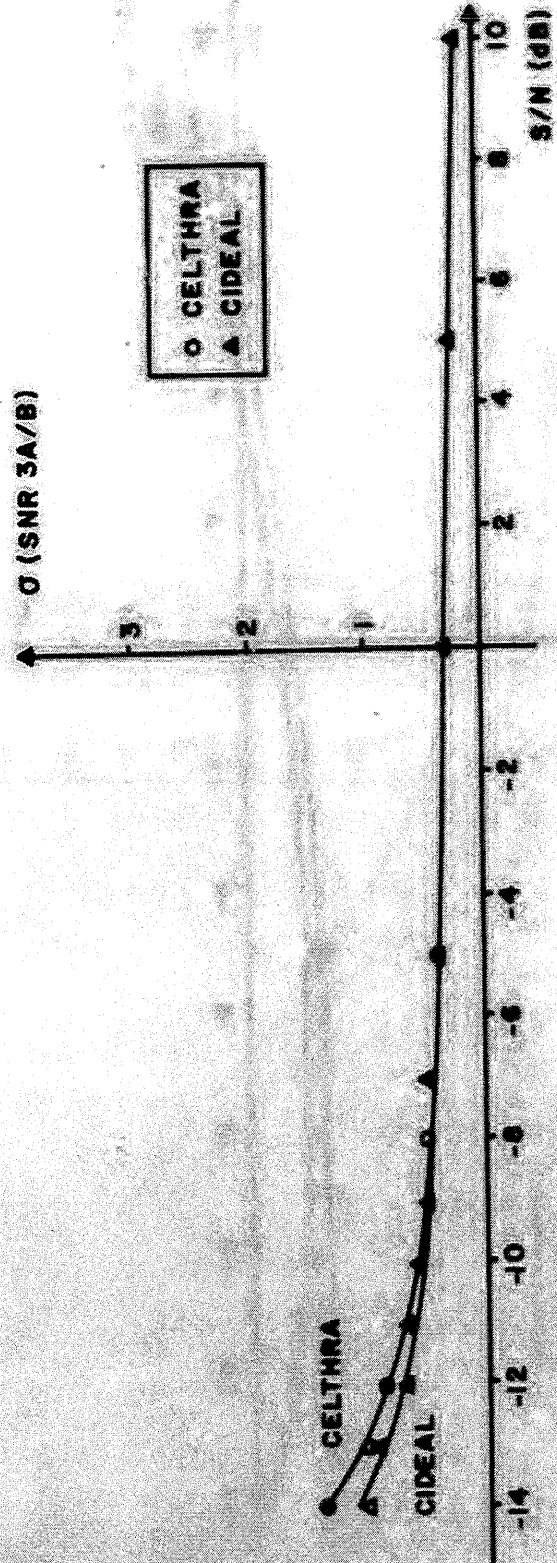


Figure 3.20: Standard deviation of SN2A/B and SNR3A/B vs S/N

(This figure [redacted])



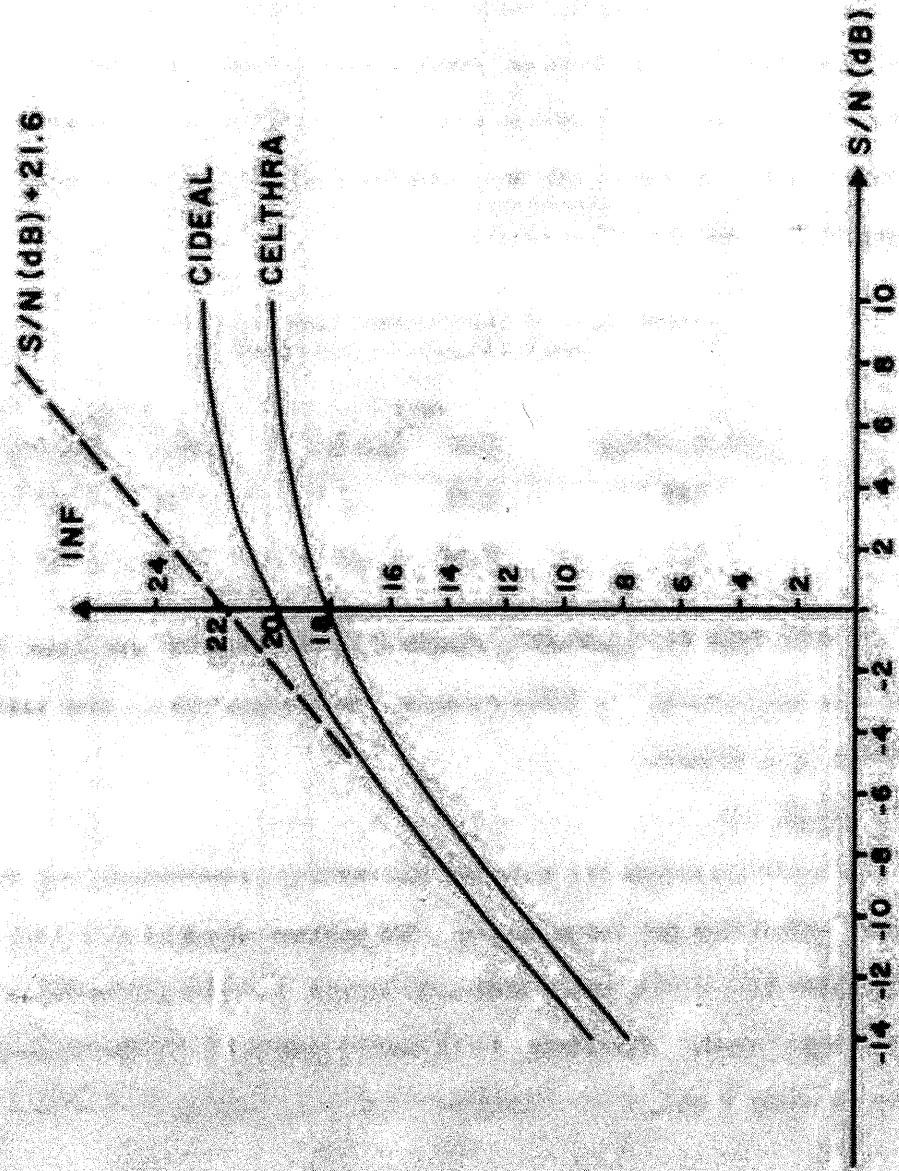


Figure 3.21: INF vs S/N

(This figure

LON, LIN

These measurements give the mean and standard deviation of the primary and secondary search algorithms under noise alone. For both channels, the statistics are nearly constant as long as the receiver makes no misses. If the receiver makes misses, some signal energy enters into the statistic and the means of the variables increase. Table 3.3 gives the statistics and compares them with those obtained independently with the RTHRS Program.

Table 3.3 Search Outputs under Noise
(Table classified)

<u>Search Output</u>	<u>RECVR</u>		<u>RTHRS</u>	
	<u>Mean</u>	<u>Std Dev</u>	<u>Mean</u>	<u>Std Dev</u>
LON	2.71	.12	2.94	.15
LIN	2.26	.17	2.59	.29

Note that the statistics obtained by the receiver are lower than those obtained through the RTHRS program. No explanation of this result is currently available.

SPEED, OFFSET

These variables are provided for operator convenience, but their standard deviations are worth noting. The maximum standard deviation in vessel speed is .02 Kts, which indicates rather accurate determination of the vessel speed. Similarly, the standard deviation of the frequency offset is about 1 mHz, which coincidentally is the smallest step size on

[REDACTED]

the frequency synthesizer available to the project. When considered in conjunction with the time synchronization capability of the system, the performance of the system in resolving the time and frequency uncertainty of the signal is excellent.

4. Conclusions and Future Studies [REDACTED]

[REDACTED] The performance of the M7BX3 version of the M7 communication system has been evaluated with simulated data corresponding to an ideal channel, CIDEAL, and a measured 350 min channel, CELTHRA. Examination of results at different S/Ns indicate that the system yields symbol error probabilities better than .0001 for S/Ns greater than -7dB, with no misses and essentially zero false alarms. Performance with CIDEAL is approximately 1 1/2 dB better than with CELTHRA. Examination of the statistics of various interval variables indicate accurate time of arrival, Doppler effort and S/N measurements can be made. Further, the algorithms within the receiver are performing consistently and as expected.

[REDACTED] An at-sea evaluation of the system under controlled conditions and adequate duration is the only logical next step. Further system improvements and simulations should only be attempted with the benefit of actual sea results. The hardware and software have been ready for a year prior to this writing, consequently a sea evaluation could be quickly and economically performed.

[REDACTED]

APPENDIX A

Detailed Specification of M7EX3A ■

SYSTEM PARAMETERS

BTBX3B - SPECIAL HIGH RATE VERSION FOR '78 NSUA
LARGE ZSHLIM FOR HIGH SNR OPERATION
NH0 = 16, INFO = NSUA-NUSC730
05 FEB 79 AT 0834 HR

ALPHABET SIZE, NA	64
BLOCK LENGTH, NB	4096
NO. OF DILATION BINS, ND	15
OVERLAP COUNT, NE	2048
FAST-DETECTION BLANKING, NE1	4096
NO. OF SYMBOLS, NG	10
SYNCH LP FILTER LENGTH, NH0	16
PROBE LP FILTER LENGTH, NH1	756
INTERPOLATION TABLE INTER-ZERO SIZE, NI	512
NUMBER OF BITS / CHARACTER, NL	6
TOTAL NUMBER OF LINES SEARCHED, NM	240
ORDER OF INTERPOLATION, NO	32
SYSTEM Q, NQ	4
SYMBOL LENGTH, NS	409
LAST SYMBOL LENGTH, NSLAST	415
PRIMARY FRACTIONAL LINE SHIFTS, NT0	2
SECONDARY FRACTIONAL LINE SHIFTS, NT1	5
NO. OF INTEGER FREQUENCY LINES / DILATION BIN, NH	16
VERSE FLAG (1 = INVERSE IS USED), INVELG	0
NO. OF SIGNAL LINES / PAGE, NSLPP	24
NUMBER OF PRIMARY SEARCHES / NOISE PRINT, NSINT	22
CENTER FREQUENCY, F0 (KHZ,HZ,MHZ;16) :	0 204 800

PRIMARY THRESHOLD, FTHRS0	[REDACTED]	3.235
SECONDARY THRESHOLD, FTHRS1		3.730
SYNCH R2 CUT LEVEL, R2RAT0		0.100
PROBE R2 CUT LEVEL, R2RAT1		0.100
BOOT R2 CUT LEVEL, R2RAT2		0.100
SECONDARY SEARCH WIDTH, DF1		1.00
BOOTSTRAP SEARCH WIDTH, DF2		1.00
ZSHIFT LIMIT, ZSHLIM		0.500

CORRECT MESSAGE (RADIX 40) : NSUA-NUSC780

CORRECT MESSAGE (HEX) : 943E 4467 BFEC 2D00

*** [REDACTED] ***

[REDACTED]

APPENDIX B

SUMMARY SHEETS FROM
M7BX3A SIMULATION ■

*** [REDACTED] ***

RECVR : 11 FEB 79A - BLOCK SUMMARY : 106: 10: 15 TO 106: 17: 58 (7: 43)

M7BX3A - SPECIAL HIGH RATE VERSION FOR '78 NSUA
NH0 = 16 , INFO = NSUA-NUSC780

30 OCT 78 AT 1109 HR (RETYPED 05 JAN 78 AT 0757 HR)

NA NB ND NE NG NH0 NH1 NI NL NM NO NS NSL NT0 NT1 NH
64 4096 15 2048 10 16 256 512 6 240 32 4 409 415 2 5 16

ZSHLIM FTHRS0 FTHRS1 R2CUT0 R2CUT1 R2CUT2 DF1 DF2 NE1 INVFLG
0.200 3.235 3.730 0.100 0.100 0.100 1.000 1.000 4096 0

K12013

K STREAM FOR M7BX5

12 OCT 78 AT 1330 HR

NK : 4 NIV : 512 NOV : 32

M7BX3 THROUGH CIDEAL AT +10. DB SNR
TWIST = 118. (21.5 KT) ; INFO = NSUA-NUSC78

16 APR 79 AT 1015 HR

STARTING TIME : 106 : 10 : 15 : 0 NO = 4
CENTER FREQUENCY : 204.800 CLOCK FREQUENCY : 0 819. 200

118. BURSTS 1180. SYMBOLS 7080. BITS

0./ 0. SYMBOL ERRORS 0.000000/ 0.000000 PE(SYM)

MBOL ERRORS BY LOCATION :

0. 0. 0. 0. 0. 0. 0. 0.
0. 0. 0. 0. 0. 0. 0. 0.
0. 0. 0. 0. 0. 0. 0. 0.
0. 0.

L0 L1 L2 L3 TS0 TS1 TS2 TS3
33.35 60.42 115.31 227.02 -184. 0. 2. 0.
12.69 0.70 0.93 0.35 1461. 4. 2. 2.

FS0 FS1 FS2 FS3 F2 F2A F2B F3 F3A F3B
118.97 118.79 118.81 118.81 118.96 118.96 118.97 118.99 118.98 118.99
0.24 0.09 0.09 0.09 0.09 0.05 0.03 0.03 0.04 0.05

R2 R2A R2B R3 R3A R3B A2 A2A A2B A3 A3A A3B
1.000 0.902 1.000 1.000 0.900 1.000 0.010 0.005 0.006 0.001 0.006 0.006
0.000 0.010 0.000 0.000 0.008 0.000 0.041 0.001 0.001 0.000 0.001 0.001

TP2A TP2B TP3A TP3B NZ2A NZ2B NZ3A NZ3B SNR2A SNR2B SNR3A SNR3B
167. -334. 107. -403. 2. 1. 2. 1. -3.9 -4.1 -1.1 -0.9
79. 43. 73. 69. 0. 0. 0. 0. 0.2 0.2 0.1 0.1

INF2A INF2B INF3A INF3B S3 LON(225.) L1N(86.) NDRV(15.)
22.4 22.9 22.4 22.9 14.1 2.71 2.29 2.9
0.2 0.2 0.1 0.2 0.0 0.12 0.16 4.4

...EED : 21.5 (0.02) KTS OFFSET : 1.485126 (0.001114) HZ

*** [REDACTED] ***

*** [REDACTED] ***

RECVR : 11 FEB 79A - BLOCK SUMMARY : 123: 10: 47 TO 124: 11: 56 (25: 9)

M7BX3A - SPECIAL HIGH RATE VERSION FOR '78 NSUA
NH0 = 16 , INFO = NSUA-NUSC780

30 OCT 78 AT 1109 HR (RETYPED 05 JAN 78 AT 0757 HR)

NA NB ND NE NG NH0 NH1 NI NL NM NO NQ NS NSL NT0 NT1 NH
64 4096 15 2048 10 16 256 512 6 240 32 4 409 415 2 5 16

ZSHLIM FTHRS0 FTHRS1 R2CUT0 R2CUT1 R2CUT2 DF1 DF2 NE1 INVFLG
0.200 3.235 3.730 0.100 0.100 0.100 1.000 1.000 4096 0

K12013

K STREAM FOR M7BX5

12 OCT 78 AT 1330 HR

NK : 4 NIV : 512 NOV : 32

M7BX3 THROUGH CIDEAL AT +5.0 DB SNR
TWIST = 119. (21.5 KT) ; INFO = NSUA-NUSC78

03 MAY 79 AT 1047 HR

STARTING TIME : 123 : 10 : 47 : 0

NQ = 4

CENTER FREQUENCY : 204.800

CLOCK FREQUENCY : 0 819. 200

385. BURSTS

3850. SYMBOLS

23100. BITS

0./ 0. SYMBOL ERRORS 0.000000/ 0.000000 PE(SYM)

SYMBOL ERRORS BY LOCATION :

0. 0. 0. 0. 0. 0. 0. 0.
0. 0. 0. 0. 0. 0. 0. 0.
0. 0. 0. 0. 0. 0. 0. 0.
0. 0. 0. 0. 0. 0. 0. 0.

L0 L1 L2 L3 TS0 TS1 TS2 TS3
23.24 50.77 96.54 190.44 -160. -1. 2. 0.
11.06 1.11 1.51 0.94 1411. 4. 3. 3.

FS0 FS1 FS2 FS3 F2 F2A F2B F3 F3A F3B
118.91 118.76 118.85 118.87 118.90 118.97 118.98 118.98 118.98 118.99
0.41 0.11 0.12 0.12 0.15 0.05 0.02 0.07 0.05 0.06

R2 R2A R2B R3 R3A R3B A2 A2A A2B A3 A3A A3B
1.000 0.912 1.000 1.000 0.909 1.000 0.044 0.004 0.004 0.008 0.004 0.004
0.003 0.018 0.000 0.000 0.015 0.000 0.080 0.003 0.003 0.026 0.003 0.003

TP2A TP2B TP3A TP3B NZ2A NZ2B NZ3A NZ3B SNR2A SNR2B SNR3A SNR3B
150. -343. 119. -396. 2. 1. 2. 1. -4.7 -4.8 -1.8 -1.7
84. 60. 75. 73. 0. 0. 0. 0. 0.3 0.2 0.2 0.2

INF2A INF2B INF3A INF3B S3 LON(726.) L1N(281.) NDBV(50.)
21.5 22.1 21.5 22.1 6.2 2.70 2.28 -0.9
0.3 0.3 0.3 0.3 0.0 0.12 0.16 2.4

SPEED : 21.5 (0.02) KTS

OFFSET : 1.485681 (0.001503) HZ

*** [REDACTED] ***

*** [REDACTED] ***

RECVR : 11 FEB 79A - BLOCK SUMMARY : 107: 7: 52 TO 108: 9: 1 (25: 9)

7BX3A - SPECIAL HIGH RATE VERSION FOR '78 NSUA
NH0 = 16 , INFO = NSUA-NUSC780

30 OCT 78 AT 1109 HR (RETYPED 05 JAN 78 AT 0757 HR)

NA NB ND NE NG NH0 NH1 NI NL NM NO NQ NS NSL NT0 NT1 NW
24 4056 15 2048 10 16 256 512 6 240 32 4 409 415 2 5 16

ZSHLIN FTHRS0 FTHRS1 R2CUT0 R2CUT1 R2CUT2 DF1 DF2 NE1 INVFLG
0.200 3.235 3.730 0.100 0.100 0.100 1.000 1.000 4056 0

K12013

K STREAM FOR M7BX5

12 OCT 78 AT 1330 HR

NK : 4 NIV : 512 NOV : 32

M7BX3 THROUGH CIDEAL AT 0.0 DB SNR

THIST = 119. (21.5 KT) ; INFO = NSUA-NUSC78

17 APR 79 AT 0752 HR

STARTING TIME : 107 : 7 : 52 : 0

NQ = 4

CENTER FREQUENCY : 204.800

CLOCK FREQUENCY : 0 819. 200

385. BURSTS

3850. SYMBOLS

23100. BITS

0. / 0. SYMBOL ERRORS 0.000000/ 0.000000 PE(SYM)

SYMBOL ERRORS BY LOCATION :

0. 0. 0. 0. 0. 0. 0. 0.
0. 0. 0. 0. 0. 0. 0. 0.
0. 0. 0. 0. 0. 0. 0. 0.
0. 0. 0. 0. 0. 0. 0. 0.

L0 L1 L2 L3 TS0 TS1 TS2 TS3
12.25 33.65 63.87 126.10 -222. -0. 1. 0.
6.45 3.05 1.70 1.73 1381. 5. 4. 4.

FS0 FS1 FS2 FS3 F2 F2A F2B F3 F3A F3B
118.84 118.74 118.90 118.92 118.83 118.97 118.98 118.98 118.98 118.99
0.58 0.17 0.12 0.12 0.21 0.01 0.04 0.08 0.04 0.06

R2 R2A R2B R3 R3A R3B A2 A2A A2B A3 A3A A3B
0.996 0.922 1.000 1.000 0.920 1.000 0.063 0.002 0.003 0.011 0.002 0.003
0.019 0.025 0.000 0.000 0.021 0.000 0.108 0.003 0.003 0.031 0.003 0.003

TP2A TP2B TP3A TP3B NZ2A NZ2B NZ3A NZ3B SNR2A SNR2B SNR3A SNR3B
44. -351. 127. -384. 1. 1. 1. 1. -6.5 -6.6 -3.6 -3.5
84. 75. 79. 79. 0. 0. 0. 0. 0.3 0.3 0.2 0.3

INFOA INFOB INFO3A INFO3B S3 LINC(727.) LINC(283.) NDBV(50.)
19.8 20.2 19.8 20.2 0.7 2.71 2.28 -2.9
0.3 0.4 0.3 0.4 0.0 0.12 0.15 1.0

SPEED : 21.5 (0.02) KTS

OFFSET : 1.486259 (0.001552) HZ

*** [REDACTED] ***

*** [REDACTED] ***

RECVR : 11 FEB 79A - BLOCK SUMMARY : 110: 9: 4 TO 111: 0: 55 (15: 51)

*BX3A - SPECIAL HIGH RATE VERSION FOR '78 NSUA
NH0 = 16 , INFO = NSUA-NUSC780

30 OCT 78 AT 1109 HR (RETYPED 05 JAN 78 AT 0757 HR)
NA NB ND NE NG NH0 NH1 N1 NL NM NO NQ NS NSL NT0 NT1 NW
34 4036 15 2048 10 16 256 512 6 240 32 4 409 415 2 5 16
ZSHLIM FTHRS0 FTHRS1 R2CUT0 R2CUT1 R2CUT2 DF1 DF2 NE1 INVFLG
0.200 3.235 3.730 0.100 0.100 0.100 1.000 1.000 4036 0

K12013
K STREAM FOR M7BX5

12 OCT 78 AT 1330 HR
NK : 4 NIV : 512 NOV : 32

M7BX3 THROUGH CIDEAL AT -5.0 DB SNR
TWIST = 119. (21.5 KT) ; INFO = NSUA-NUSC78

20 APR 79 AT 0904 HR
STARTING TIME : 110 : 9 : 4 : 0 NQ = 4
CENTER FREQUENCY : 204.800 CLOCK FREQUENCY : 0 819. 200

238. BURSTS 2320. SYMBOLS 14280. BITS
0./ 0. SYMBOL ERRORS 0.000000/ 0.000000 PE(SYM)

SYMBOL ERRORS BY LOCATION :

0. 0. 0. 0. 0. 0. 0. 0.
0. 0. 0. 0. 0. 0. 0. 0.
0. 0. 0. 0. 0. 0. 0. 0.
0. 0. 0. 0. 0. 0. 0. 0.
L0 L1 L2 L3 TS0 TS1 TS2 TS3
7.84 17.08 31.38 61.46 480. 1. 0. 0.
2.77 1.08 1.58 1.76 1520. 5. 5. 4.

FS0 FS1 FS2 FS3 F2 F2A F2B F3 F3A F3B
118.95 118.81 118.94 118.96 118.86 118.97 118.98 118.98 118.99 119.00
0.36 0.19 0.11 0.10 0.19 0.04 0.05 0.06 0.05 0.03

R2 R2A R2B R3 R3A R3B A2 A2A A2B A3 A3A A3B
0.994 0.931 1.000 1.000 0.929 1.000 0.051 0.001 0.001 0.009 0.001 0.001
0.019 0.037 0.004 0.000 0.030 0.000 0.097 0.004 0.004 0.029 0.003 0.003

TP2A TP2B TP3A TP3B NZ2A NZ2B NZ3A NZ3B SNR2A SNR2B SNR3A SNR3B
134. -371. 131. -383. 1. 1. 1. 1. -9.7 -9.7 -6.7 -6.7
85. 83. 85. 87. 0. 0. 0. 0. 0.5 0.5 0.3 0.4

INF2A INF2B INF3A INF3B S3 LON(475.) LIN(107.) NDBV(32.)
15.6 16.9 16.6 16.8 -2.3 2.71 2.28 -3.4
0.5 0.5 0.5 0.5 0.0 0.13 0.20 0.4

SPEED : 21.5 (0.02) KTS OFFSET : 1.466806 (0.001921) HZ

*** [REDACTED] ***

*** [REDACTED] ***

RECVR : 11 FEB 79A - BLOCK SUMMARY : 64: 10: 56 TO 65: 8: 6 (21: 10)

M7BX3A - SPECIAL HIGH RATE VERSION FOR '78 NSUA
NH0 = 16 , INFO = NSUA-NUSC780

30 OCT 78 AT 1109 HR (RETYPED 05 JAN 78 AT 0757 HR)

NA NB ND NE NG NH0 NH1 NI NL NM NO NQ NS NSL NT0 NT1 NW
S4 4096 15 2048 10 16 256 512 6 240 32 4 409 415 2 5 16

ZSHLIM FTHRS0 FTHRS1 R2CUT0 R2CUT1 R2CUT2 DF1 DF2 NE1 INVFLG
0.200 3.235 3.730 0.100 0.100 0.100 1.000 1.000 4096 0

K12013

K STREAM FOR M7BX5

12 OCT 78 AT 1330 HR

NK : 4 NIV : 512 NOV : 32

M7BX3 THROUGH CIDEAL AT -7.0 DB SNR
TWIST = 119. (21.5 KT) ; INFO = NSUA-NUSC780

05 MAR 79 AT 1056 HR

STARTING TIME : 64 : 10 : 56 : 0 NO = 4
CENTER FREQUENCY : 204.800 CLOCK FREQUENCY : 0 819. 200

324. BURSTS 3240. SYMBOLS 19440. BITS

0./ 0. SYMBOL ERRORS 0.000000/ 0.000000 PE(SYM)

SYMBOL ERRORS BY LOCATION :

0. 0. 0. 0. 0. 0. 0. 0.
0. 0. 0. 0. 0. 0. 0. 0.
0. 0. 0. 0. 0. 0. 0. 0.
0. 0.

L0 L1 L2 L3 TS0 TS1 TS2 TS3
6.61 12.43 22.34 42.94 617. 0. -0. 1.
2.03 1.08 1.49 2.03 1464. 5. 5. 5.

FS0 FS1 FS2 FS3 F2 F2A F2B F3 F3A F3B
118.92 118.83 118.97 118.98 118.85 118.97 118.98 118.99 118.99 119.00
0.31 0.24 0.10 0.10 0.23 0.07 0.05 0.05 0.05 0.01

R2 R2A R2B R3 R3A R3B A2 A2A A2B A3 A3A A3B
0.991 0.331 0.998 1.000 0.931 1.000 0.064-0.001 0.000 0.005 0.000 0.001
0.025 0.042 0.010 0.003 0.037 0.003 0.117 0.011 0.004 0.026 0.006 0.006

TF2A TF2B TP3A TP3B NZ2A NZ2B NZ3A NZ3B SNR2A SNR2B SNR3A SNR3B
147. -356. 100. -381. 1. 1. 1. 1. -11.2 -11.2 -8.3 -8.2
32. 36. 34. 26. 0. 0. 0. 0. 0.6 0.5 0.5 0.5

INF2A INF2B INF3A INF3B S3 LON(612.) L1N(108.) NDBV(42.)
15.9 15.2 15.0 15.2 -2.5 2.72 2.27 -3.7
0.6 0.5 0.6 0.5 0.0 0.14 0.13 0.3

SPEED : 21.5 (0.02) KTS OFFSET : 1.487075 (0.001311) HZ

*** [REDACTED] ***

*** [REDACTED] ***

RECYR : 11 FEB 79A - BLOCK SUMMARY : 64: 7: 56 TO 65: 7: 55 (23: 59)

M7BX3A - SPECIAL HIGH RATE VERSION FOR '78 NSUA
NH0 = 16 , INFO = NSUA-NUSC780

30 OCT 78 AT 1109 HR (RETYPED 05 JAN 78 AT 0757 HR)

NA NB ND NE NG NH0 NH1 NI NL NM NO NS NSL NT0 NT1 NW
64 4095 15 2048 10 16 256 512 6 240 32 4 409 415 2 5 16

ZSHLIM FTHRS0 FTHRS1 R2CUT0 R2CUT1 R2CUT2 DF1 DF2 NE1 INVFLG
0.200 3.235 3.730 0.100 0.100 0.100 1.000 1.000 4056 0

K12013

K STREAM FOR M7BX5

12 OCT 78 AT 1330 HR

NK : 4 NIV : 512 NOV : 32

M7BX3 THROUGH CIDEAL AT -9.0 DB SNR
TWIST = 119. (21.5 KT) ; INFO = NSUA-NUSC78

05 MAR 79 AT 0756 HR

STARTING TIME : 64 : 7 : 56 : 0 NO = 4
CENTER FREQUENCY : 204.800 CLOCK FREQUENCY : 0 819. 200

368. BURSTS

3680. SYMBOLS

22080. BITS

0./ 0. SYMBOL ERRORS 0.000000/ 0.000000 PE(SYM)

SYMBOL ERRORS BY LOCATION :

0. 0. 0. 0. 0. 0. 0. 0.
0. 0. 0. 0. 0. 0. 0. 0.
0. 0. 0. 0. 0. 0. 0. 0.
0. 0. 0. 0. 0. 0. 0. 0.

L0 L1 L2 L3 TS0 TS1 TS2 TS3
5.39 8.72 15.22 29.24 914. 0. -0. 0.
1.33 0.87 1.34 1.70 1226. 5. 5. 5.

FS0 FS1 FS2 FS3 F2 F2A F2B F3 F3A F3B
118.90 118.85 118.98 118.99 118.86 118.98 118.99 118.99 118.99 119.00
0.33 0.26 0.10 0.09 0.25 0.07 0.05 0.06 0.04 0.03

R2 R2A R2B R3 R3A R3B A2 A2A A2B A3 A3A A3B
0.982 0.897 0.979 1.000 0.937 0.999 0.063 0.000 0.001 0.003 0.000 0.001
0.041 0.106 0.094 0.003 0.043 0.008 0.124 0.021 0.031 0.025 0.011 0.006

TP2A TP2B TP3A TP3B NZ2A NZ2B NZ3A NZ3B SNR2A SNR2B SNR3A SNR3B
131. -372. 130. -375. 1. 1. 1. 1. -12.9 -12.9 -10.3 -10.0
88. 83. 86. 87. 0. 0. 0. 0. 0.8 0.8 0.5 0.5

INF2A INF2B INF3A INF3B S3 LONG(690.) LINC(66.) NDBV(48.)
13.4 13.6 13.4 13.6 -3.3 2.72 2.29 -3.8
0.7 0.7 0.7 0.7 0.0 0.14 0.1E 0.2

SPEED : 21.5 (0.02) KTS

OFFSET : 1.487269 (0.001283) HZ

*** [REDACTED] ***

*** [REDACTED] ***

RECVR : 11 FEB 79A - BLOCK SUMMARY : 52: 8: 50 TO 53: 9: 58 (25: 8)

M7BX3A - SPECIAL HIGH RATE VERSION FOR '78 NSUA
NH0 = 16 , INFO = NSUA-NUSC780

30 OCT 78 AT 1109 HR (RETYPED 05 JAN 78 AT 0757 HR)

NA NB ND NE NG NH0 NH1 NI NL NM NO NS NSL NT0 NT1 NW
64 4096 15 2048 10 16 256 512 6 240 32 4 409 415 2 5 16

ZSHLIM FTHRS0 FTHRS1 R2CUT0 R2CUT1 R2CUT2 DF1 DF2 NE1 INVFLG
0.200 3.235 3.730 0.100 0.100 0.100 1.000 1.000 4096 0

K12013

K STREAM FOR M7BX5

12 OCT 78 AT 1330 HR

NK : 4 NIV : 512 NOV : 32

M7BX3 THROUGH IDEAL CHANNEL AT -10. DB SNR
TWIST = 119. (21.5 KT) ; INFO = NSUA-NUSC78

21 FEB 79 AT 0850 HR

STARTING TIME : 52 : 8 : 50 : 0 NO = 4
CENTER FREQUENCY : 204.800 CLOCK FREQUENCY : 0 819. 200

386. BURSTS 3660. SYMBOLS 23160. BITS

8./ 7. SYMBOL ERRORS 0.002073/ 0.001813 PE(SYM)

SYMBOL ERRORS BY LOCATION :

1. 0. 1. 0. 4. 0. 0. 1.
0. 1. 1. 0. 3. 0. 0 1.
1. 0. 1. 0. 3. 0. 0 1.
0. 1. 1. 0. 3. 0. 0 1.

L0 L1 L2 L3 TS0 TS1 TS2 TS3
5.20 7.36 12.64 24.12 1056. 1. -0. -0.
1.19 0.78 1.16 1.49 881. 5. 5. 5.

F50 F51 FS2 FS3 F2 F2A F2B F3 F3A F3B
118.91 118.82 118.99 118.99 118.83 118.98 118.99 118.99 118.99 119.00
0.32 0.30 0.08 0.07 0.30 0.05 0.07 0.07 0.04 0.02

R2 R2A R2B R3 R3A R3B A2 A2A A2B A3 A3A A3B
0.940 0.821 0.941 1.000 0.933 0.997 0.072 0.006 0.001 0.001 0.000 0.001
0.129 0.176 0.141 0.004 0.047 0.012 0.150 0.063 0.042 0.019 0.009 0.011

TP2A TP2B TP3A TP3B NZ2A NZ2B NZ3A NZ3B SNR2A SNR2B SNR3A SNR3B
137. -373. 137. -374. 1. 1. 1. 1. -13.7 -13.7 -10.8 -10.8
90. 90. 84. 88. 0. 0. 0. 0. 0.8 0.8 0.6 0.6

INF2A INF2B INF3A INF3B S3 L0NC 726.) L1NC 26.) NDBV(50.)
12.5 12.7 12.5 12.7 -3.5 2.74 2.25 -3.8
0.7 0.7 0.7 0.7 0.0 0.15 0.15 0.2

SPEED : 21.5 (0.01) KTS OFFSET : 1.487364 (0.000993) HZ

*** [REDACTED] ***

*** [REDACTED] ***

RECVR : 11 FEB 79A - BLOCK SUMMARY : 58: 13: 19 TO 59: 14: 20 (25: 1)

'BX3A - SPECIAL HIGH RATE VERSION FOR '78 NSUA
NH0 = 16 , INFO = NSUA-NUSC780

30 OCT 78 AT 1109 HR (RETYPED 05 JAN 78 AT 0757 HR)

NA NB ND NE NG NH0 NH1 NI NL NM NO NO NS NSL NT0 NT1 NW
64 4096 15 2048 10 16 256 512 6 240 32 4 409 415 2 5 16

ZSHLIM FTHRS0 FTHRS1 R2CUT0 R2CUT1 R2CUT2 DF1 DF2 NE1 INVFLG
0.200 3.235 3.730 0.100 0.100 0.100 1.000 1.000 4096 0

K12013

K STREAM FOR M7BX5

12 OCT 78 AT 1330 HR

NK : 4 NIV : 512 NOV : 32

M7BX3 THROUGH CIDEAL AT -11.0 DB SNR

TWIST = 119. (21.5 KT) ; INFO = NSUA-NUSC78

27 FEB 79 AT 1319 HR

STARTING TIME : 58 : 13 : 19 : 0 NO = 4

CENTER FREQUENCY : 204.800 CLOCK FREQUENCY : 0 819. 200

385. BURSTS /385

3850. SYMBOLS

23100. BITS

32./ 29. SYMBOL ERRORS 0.008312/ 0.007532 PE(SYM)

SYMBOL ERRORS BY LOCATION :

6. 2. 3. 3. 5. 0. 0. 4.
3. 6.
3. 1. 2. 3. 7. 0. 0. 4.
3. 6.

L0 L1 L2 L3 TS0 TS1 TS2 TS3
4.73 6.31 10.49 19.62 986. 1. -1. 0.
0.94 0.69 0.98 1.36 836. 5. 5. 5.

FS0 FS1 FS2 FS3 F2 F2A F2B F3 F3A F3B
118.90 118.87 118.99 118.99 118.88 118.98 118.99 118.99 118.99 119.00
0.32 0.29 0.09 0.08 0.28 0.06 0.06 0.06 0.05 0.05

R2 R2A R2B R3 R3A R3B A2 A2A A2B A3 A3A A3B
0.859 0.653 0.835 1.000 0.925 0.996 0.041 0.002-0.006 0.002-0.001 0.000
0.226 0.280 0.242 0.004 0.068 0.016 0.151 0.106 0.084 0.024 0.019 0.006

TP2A TP2B TP3A TP3B NZ2A NZ2B NZ3A NZ3B SNR2A SNR2B SNR3A SNR3B
123. -376. 125. -384. 1. 1. 1. 1. -14.6 -14.6 -11.8 -11.7
86. 88. 84. 84. 0. 0. 0. 0. 1.1 1.0 0.7 0.7

INF2A INF2B INF3A INF3B S3 LON(718.) L1N(18.) NDBV(51.)
11.5 11.7 11.5 11.7 -3.6 2.73 2.29 -4.0
0.8 0.8 0.8 0.8 0.0 0.15 0.12 0.1

SPEED : 21.5 (0.02) KTS

OFFSET : 1.487337 (0.001159) HZ

*** [REDACTED] ***

*** [REDACTED] ***

RECVR : 11 FEB 79A - BLOCK SUMMARY : 57: 8: 22 TO 58: 9: 32 (25: 10)

M7BX3A - SPECIAL HIGH RATE VERSION FOR '78 NSUA
NH0 = 16 , INFO = NSUA-NUSC780

30 OCT 78 AT 1109 HR (RETYPED 05 JAN 78 AT 0757 HR)

NA NB ND NE NG NH0 NH1 NI NL NM NO NQ NS NSL NT0 NT1 NW
64 4096 15 2048 10 16 256 512 6 240 32 4 409 415 2 5 16

ZSHLIM FTHRS0 FTHRS1 R2CUT0 R2CUT1 R2CUT2 DF1 DF2 NE1 INVFLG
0.200 3.235 3.730 0.100 0.100 0.100 1.000 1.000 4096 0

K12013

K STREAM FOR M7BX5

12 OCT 78 AT 1330 HR

NK : 4 NIV : 512 NOV : 32

$p_{miss} = .010471$

M7BX3 THROUGH IDEAL CHANNEL AT -12.0 DB SNR
TWIST = 119. (21.5 KT) ; INFO = NSUA-NUSC78

26 FEB 79 AT 0822 HR

STARTING TIME : 57 : 2 : 22 : 0
CENTER FREQUENCY : 204.800

N0 = 4
CLOCK FREQUENCY : 0 819. 200

378. BURSTS / 382

3780. SYMBOLS

22680. BITS

73. / 67. SYMBOL ERRORS

0.019312 / 0.017725 PE(SYM)

SYMBOL ERRORS BY LOCATION :

5. 6. 9. 14. 6. 4. 7. 5.
4. 13.
5. 6. 7. 12. 7. 4. 7. 5.
2. 12.

L0 L1 L2 L3 TS0 TS1 TS2 TS3
4.39 5.39 8.73 16.13 773. 0. -0. -0.
0.74 0.66 0.95 1.34 763. 4. 5. 5.

F50 F51 F52 F53 F2 F2A F2B F3 F3A F3B
118.87 118.86 118.99 118.99 118.86 118.98 118.99 118.99 118.99 119.00
0.33 0.31 0.09 0.08 0.31 0.07 0.08 0.06 0.06 0.04

R2 R2A R2B R3 R3A R3B A2 A2A A2B A3 A3A A3B
0.873 0.483 0.613 0.998 0.914 0.984 0.045-0.004 0.006 0.002-0.001-0.000
0.315 0.290 0.324 0.011 0.066 0.058 0.178 0.137 0.137 0.022 0.010 0.022

TP2A TP2B TP3A TP3B NZ2A NZ2B NZ3A NZ3B SNR2A SNR2B SNR3A SNR3B
135. -371. 138. -370. 2. 1. 1. 1. -15.3 -15.3 -12.5 -12.5
89. 87. 87. 88. 1. 0. 0. 0. 1.3 1.2 0.7 0.7

INF2A INF2B INF3A INF3B S3 L0N(844.) L1N(8.) NDBV(55.)
10.6 10.8 10.7 10.2 -3.7 2.74 2.62 -3.9
0.8 0.8 0.8 0.8 0.0 0.16 0.53 0.2

SPEED : 21.5 (0.02) KTS

OFFSET : 1.487334 (0.001159) HZ

*** [REDACTED] ***

*** [REDACTED] ***

RECVR : 11 FEB 79A - BLOCK SUMMARY : 60: 10: 19 TO 61: 11: 11 (24: 52)

M7BX3A - SPECIAL HIGH RATE VERSION FOR '78 NSUA
NH0 = 16 , INFO = NSUA-NUSC780

30 OCT 78 AT 1109 HR (RETYPED 05 JAN 78 AT 0757 HR)
NA NB ND NE NG NH0 NH1 NI NL NM NO NS NSL NT0 NT1 NW
64 4096 15 2048 10 16 256 512 6 240 32 4 409 415 2 5 16
ZSHLIM FTHRS0 FTHRS1 R2CUT0 R2CUT1 R2CUT2 DF1 DF2 NE1 INVFLG
0.200 3.235 3.730 0.100 0.100 0.100 1.000 1.000 4096 0

K12013
K STREAM FOR M7BX5

12 OCT 78 AT 1330 HR
NK : 4 NIV : 512 NOV : 32

Pror = .075

M7BX3 THROUGH CIDEAL AT -13.0 DB SNR
TWIST = 119. (21.5 KT) ; INFO = NSUA-NUSC78

01 MAR 79 AT 1019 HR
STARTING TIME : 60 : 10 : 19 : 0 NO = 4
CENTER FREQUENCY : 204.800 CLOCK FREQUENCY : 0 819. 200

358. BURSTS /387 3580. SYMBOLS 21450. BITS
245./ 224. SYMBOL ERRORS 0.068436/ 0.062570 PE(SYM)

SYMBOL ERRORS BY LOCATION :

22. 27. 22. 25. 36. 12. 19. 16.
28. 38. 19. 26. 18. 19. 28. 13. 19. 15.
27. 40.

L0 L1 L2 L3 TS0 TS1 TS2 TS3
4.00 4.67 7.38 13.22 441. 0. -0. -0.
0.53 0.56 0.85 1.36 777. 5. 5. 6.

FS0 FS1 FS2 FS3 F2 F2A F2B F3 F3A F3B
118.86 118.85 118.99 119.00 118.85 118.98 118.99 119.00 118.99 119.00
0.33 0.31 0.09 0.08 0.30 0.08 0.08 0.07 0.05 0.04

R2 R2A R2B R3 R3A R3B A2 A2A A2B A3 A3A A3B
0.486 0.307 0.390 0.985 0.849 0.947 0.042 0.007-0.001 0.000-0.002-0.001
0.327 0.260 0.321 0.076 0.158 0.125 0.196 0.178 0.139 0.026 0.037 0.037

TP2A TP2B TP3A TP3B NZ2A NZ2B NZ3A NZ3B SNR2A SNR2B SNR3A SNR3B
121. -374. 129. -365. 2. 2. 2. 1. -16.0 -16.1 -13.4 -13.4
59. 131. 98. 130. 6. 8. 8. 7. 1.4 1.3 1.0 0.9

INF2A INF2B INF3A INF3B S3 L0N(944.) L1N(24.) NDBV(59.)
9.7 9.9 9.9 9.8 -3.8 2.74 2.87 -4.0
0.9 0.9 0.8 0.9 0.0 0.16 0.64 0.1

SPEED : 21.5 (0.02) KTS OFFSET : 1.487409 (0.001083) HZ

*** [REDACTED] ***

*** [REDACTED] ***

RECVR : 11 FEB 79A - BLOCK SUMMARY : 61: 12: 26 TO 62: 13: 25 (24: 59)

M7BX3A - SPECIAL HIGH RATE VERSION FOR '78 NSUA
NH0 = 16 , INFO = NSUA-NUSC780

30 OCT 78 AT 1109 HR (RETYPED 05 JAN 78 AT 0757 HR)

NA	NB	ND	NE	NG	NH0	NH1	NI	NL	NM	NO	NO	NS	NSL	NT0	NT1	NW
64	4096	15	2048	10	16	256	512	6	240	32	4	409	415	2	5	16

ZSHLIM	FTHRS0	FTHRS1	R2CUT0	R2CUT1	R2CUT2	DF1	DF2	NE1	INVFLG
0.200	3.235	3.730	0.100	0.100	0.100	1.000	1.000	4096	0

K12013

K STREAM FOR M7BX5

12 OCT 78 AT 1330 HR

NK : 4 NIV : 512 NOV : 32

$p_{mus} = .40838$

M7BX3 THROUGH CIDEAL AT -14.0 DB SNR
TWIST = 119. (21.5 KT) ; INFO = NSUA-NUSC78

02 MAR 79 AT 1228 HR

STARTING TIME : 61 : 12 : 26 : 0

NO = 4

CENTER FREQUENCY : 204.800

CLOCK FREQUENCY : 0 819. 200

226 BURSTS / 382

2260. SYMBOLS

13560. BITS

374.7

284. SYMBOL ERRORS

0.165487 / 0.125664 PE(SYM)

SYMBOL ERRORS BY LOCATION :

44.	43.	40.	42.	53.	26.	28.	27.
26.	45.						
32.	24.	24.	36.	38.	21.	27	23.
25.	41.						

L0	L1	L2	L3	TS0	TS1	TS2	TS3
3.84	4.30	6.47	10.81	190.	0.	-0.	-0.
0.40	0.42	0.67	1.40	715.	4.	5.	6.

FS0	FS1	FS2	FS3	F2	F2A	F2B	F3	F3A	F3B
118.85	118.85	118.99	118.99	118.86	118.99	118.99	118.99	118.99	118.00
0.30	0.30	0.08	0.08	0.30	0.10	0.09	0.07	0.06	0.07

R2	R2A	R2B	R3	R3A	R3B	A2	A2A	A2B	A3	A3A	A3B
0.293	0.203	0.241	0.926	0.723	0.810	0.018	0.014	0.001	0.003	0.003	0.001
0.282	0.206	0.256	0.181	0.242	0.279	0.223	0.186	0.202	0.058	0.082	0.082

TP2A	TP2B	TP3A	TP3B	NZ2A	NZ2B	NZ3A	NZ3B	SNR2A	SNR2B	SNR3A	SNR3B
136.	-380.	126.	-381.	4.	2.	2.	1.	-16.6	-16.7	-14.3	-14.3
157.	124.	117.	131.	13.	10.	10.	7.	1.4	1.5	1.0	1.1

INF2A	INF2B	INF3A	INF3B	S3	L0N(1399.)	L1N(111.)	NDEV(76.)
8.6	9.0	9.0	9.1	-3.8		2.75		3.01		-4.0
1.0	0.9	0.9	0.9	0.0		0.16		0.60		0.1

SPEED : 21.5 (0.02) KTS

OFFSET : 1.487345 (0.001060) HZ

*** [REDACTED] ***

*** [REDACTED] ***

RECVR : 11 FEB 79A - BLOCK SUMMARY : 108: 7: 49 TO 109: 6: 30 (22: 41)

'BX3A - SPECIAL HIGH RATE VERSION FOR '78 NSUA
NA0 = 16 , INFO = NSUA-NUSC780

30 OCT 78 AT 1109 HR (RETYPED 05 JAN 78 AT 0757 HR)

NA NB ND NE NG NH0 NH1 NI NL NM NO NO NS NSL NT0 NT1 NW
64 4096 15 2048 10 16 256 512 6 240 32 4 409 415 2 5 16

ZSHLIM FTHRS0 FTHRS1 R2CUT0 R2CUT1 R2CUT2 DF1 DF2 NE1 INVFLG
0.200 3.235 3.730 0.100 0.100 0.100 1.000 1.000 4096 0

K11013

K STREAM FOR M7BX5

12 OCT 78 AT 1330 HR

NK : 4 NIV : 512 NOV : 32

M7BX3 THROUGH CELTHRA CHANNEL AT +10. DB SNR
TWIST = 119. (21.5 KT) ; INFO = NSUA-NUSC78

18 APR 79 AT 0749HR

STARTING TIME : 108 : 7 : 49 : 0 NG = 4
CENTER FREQUENCY : 204.600

CLOCK FREQUENCY : 0 619. 200

349. BURSTS

3490. SYMBOLS

20940. BITS

0./ 0. SYMBOL ERRORS 0.000000/ 0.000000 PE(SYM)

SYMBOL ERRORS BY LOCATION :

0. 0. 0. 0. 0. 0. 0. 0.
0. 0. 0. 0. 0. 0. 0. 0.
0. 0. 0. 0. 0. 0. 0. 0.

L0 L1 L2 L3 T50 T51 T52 T53
21.78 46.57 84.77 167.98 -1193. 0. -1. 1.
10.23 0.62 0.75 0.73 586. 1. 1. 1.

F50 F51 F52 F53 FZ FZA F2B F3 F3A F3B
118.00 118.60 119.00 119.00 118.60 118.97 118.97 118.98 118.98 118.99
0.31 0.11 0.01 0.01 0.11 0.04 0.04 0.06 0.00 0.01

R2 R2A R2B R3 R3A R3B A2 A2A A2B A3 A3A A3B
0.979 0.978 0.933 0.998 0.954 0.937 0.173 0.002 0.001 0.000 0.001 0.000
0.021 0.017 0.020 0.004 0.012 0.027 0.002 0.000 0.000 0.000 0.000 0.000

TP2A TP2B TP3A TP3B NZ2A NZ2B NZ3A NZ3B SNR2A SNR2B SNR3A SNR3B
170. -320. 166. -346. 4. 3. 4. 3. -4.3 -4.3 -1.4 -1.2
40. 23. 41. 53. 0. 0. 0. 0. 0.2 0.1 0.1 0.2

INF2A INF2B INF3A INF3B S3 LON(649.) L1N(354.) NDEV(45.)
20.2 20.2 20.2 20.2 14.1 2.71 2.26 2.5
0.1 0.2 0.1 0.1 0.0 0.12 0.17 5.2

SPEED : 21.5 (0.00) KTS

OFFSET : 1.487500 (0.000167) HZ

*** [REDACTED] ***

*** [REDACTED] ***

RECVR : 11 FEB 79A - BLOCK SUMMARY : 124: 10: 50 TO 125: 12: 0 (25: 10)

M7BX3A - SPECIAL HIGH RATE VERSION FOR '78 NSUA
NH0 = 16 , INFO = NSUA-NJSC780

30 OCT 78 AT 1105 HR (RETYPED 05 JAN 78 AT 0757 HR)

NA NB ND NE NG NH0 NH1 NI NL NM NO NS NSL NT0 NT1 NW
64 4096 15 2048 10 16 256 512 6 240 32 4 409 415 2 5 16

ZSHLIM FTHRS0 FTHRS1 R2CUT0 R2CUT1 R2CUT2 DF1 DF2 NE1 INVFLG
0.200 3.235 3.730 0.100 0.100 0.100 1.000 1.000 4096 0

K12013

K STREAM FOR M7BX5

12 OCT 78 AT 1330 HR

NK : 4 NIV : 512 NOV : 32

M7BX3 THROUGH CELTHRA AT +5.0 DB SNR
TWIST = 119. (21.5 KT) ; INFO = NSUA-NUSC78

04 MAY 79 AT 1050 HR

STARTING TIME : 124 : 10 : 50 : 0

NQ = 4

CENTER FREQUENCY : 204.800

CLOCK FREQUENCY : 0 819. 200

389. BURSTS

3890. SYMBOLS

23340. BITS

0./ 0. SYMBOL ERRORS 0.000000/ 0.000000 PE(SYM)

SYMBOL ERRORS BY LOCATION :

0. 0. 0. 0. 0. 0. 0. 0.
0. 0. 0. 0. 0. 0. 0. 0.
0. 0. 0. 0. 0. 0. 0. 0.
0. 0. 0. 0. 0. 0. 0. 0.

L0 L1 L2 L3 TS0 TS1 TS2 TS3
18.03 38.96 71.22 140.84 -1203. 1. -1. 1.
8.28 2.43 1.19 1.13 569. 2. 1. 1.

FS0 FS1 FS2 FS3 F2 F2A F2B F3 F3A F3B
118.88 118.59 119.00 119.00 118.59 118.97 118.97 118.98 118.98 118.99
0.44 0.10 0.00 0.00 0.10 0.03 0.05 0.03 0.04 0.04

R2 R2A R2B R3 R3A R3B A2 A2A A2B A3 A3A A3B
0.969 0.972 0.921 0.992 0.950 0.937 0.169 0.002 0.001 0.000 0.001 0.000
0.029 0.025 0.030 0.016 0.014 0.030 0.056 0.000 0.000 0.000 0.000 0.000

TP2A TP2B TP3A TP3B NZ2A NZ2B NZ3A NZ3B SNR2A SNR2B SNR3A SNR3B
156. -327. 152. -357. 4. 3. 4. 3. -5.0 -5.0 -2.1 -2.0
53. 57. 53. 58. 0. 0. 0. 0. 0.2 0.2 0.2 0.2

INF2A INF2B INF3A INF3B SS LONC 712.) LINK 390.) NDBVC 50.)
13.7 13.5 13.6 13.6 6.2 2.70 2.27 -1.3
0.2 0.3 0.2 0.3 0.0 0.12 0.14 2.5

SPEED : 21.5 (0.00) KTS

OFFSET : 1.467500 (0.000000) HZ

*** [REDACTED] ***

*** [REDACTED] ***

RECVR : 11 FEB 79A - BLOCK SUMMARY : 109: 9: 17 TO 109: 20: 25 (11: 8)

'BX3A - SPECIAL HIGH RATE VERSION FOR '78 NSUA
NH0 = 16 , INFO = NSUA-NUSC780

30 OCT 78 AT 1109 HR (RETYPED 05 JAN 78 AT 0757 HR)

NH NB ND NE NG NH0 NH1 NI NL NM NO NQ NS NSL NT0 NT1 NW
34 4096 15 2048 10 16 256 512 6 240 32 4 409 415 2 5 16

ZSHLIM FTHRS0 FTHRS1 R2CUT0 R2CUT1 R2CUTZ DF1 DF2 NE1 INVFLG
0.200 3.235 3.730 0.100 0.100 0.100 1.000 1.000 4056 0

K12013

K STREAM FOR M7BX5

12 OCT 78 AT 1330 HR

NK : 4 NIV : 512 NOV : 32

M7BX5 THROUGH CELTHRA CHANNEL AT 0.0 DB SNR
TWIST = 119. (21.5 KT) ; INFO = NSUA-NUSC78

19 APR 79 AT 0917 HR

STARTING TIME : 109 : 9 : 17 : 0

NQ = 4

CENTER FREQUENCY : 204.800

CLOCK FREQUENCY : 0 819. 200

166. BURSTS

1660. SYMBOLS

3960. BITS

0./ 0. SYMBOL ERRORS 0.000000/ 0.000000 PE(SYM)

SYMBOL ERRORS BY LOCATION :

0. 0. 0. 0. 0. 0. 0. 0.
0. 0. 0. 0. 0. 0. 0. 0.
0. 0. 0. 0. 0. 0. 0. 0.
0. 0. 0. 0. 0. 0. 0. 0.

L0 L1 L2 L3 TS0 TS1 TS2 TS3
12.61 26.19 47.49 95.39 -880. 1. -1. 1.
5.02 1.18 1.47 1.55 1295. 2. 1. 1.

FS0 FS1 FS2 FS3 F2 F2A F2B F3 F3A F3B
118.95 118.58 119.00 119.00 118.58 118.96 118.97 118.98 118.98 118.99
0.32 0.09 0.04 0.04 0.10 0.04 0.03 0.04 0.03 0.04

R2 R2A R2B R3 R3A R3B A2 A2A A2B A3 A3A A3B
0.954 0.944 0.907 0.874 0.938 0.934 0.182-0.002-0.001-0.000-0.000-0.000
0.036 0.038 0.034 0.026 0.024 0.031 0.049 0.002 0.001 0.000 0.001 0.001

TF2A TF2B TF3A TF3B NZ2A NZ2B NZ3A NZ3B SNR2A SNR2B SNR3A SNR3B
144. -348. 138. -372. 4. 3. 4. 3. -6.7 -6.7 -3.8 -3.8
60. 54. 58. 58. 0. 1. 0. 1. 0.4 0.4 0.3 0.3

INF2A INF2B INF3A INF3B S3 LON(340.) LIN(133.) NDBV(23.)
10.2 18.0 18.2 18.1 0.7 2.71 2.29 -2.7
0.3 0.4 0.3 0.4 0.0 0.12 0.15 1.3

SPEED : 21.5 (0.00) KTS

OFFSET : 1.487439 (0.000454) HZ

*** [REDACTED] ***

*** [REDACTED] ***

RECVR : 11 FEB 79A - BLOCK SUMMARY : 28: 13: 35 TO 29: 16: 5 (26: 30)

'EX3A - SPECIAL HIGH RATE VERSION FOR '78 NSUA
NH0 = 16 , INFO = NSUA-NUSC780

30 OCT 78 AT 1109 HR (RETYPED 05 JAN 78 AT 0757 HR)

NA	NB	ND	NE	NG	NH0	NH1	NI	NL	NM	NO	NQ	NS	NSL	NT0	NT1	NW
84	4096	15	2048	10	16	256	512	6	240	32	4	409	415	2	5	16

ZSHLIM	FTHRS0	FTHRS1	R2CUT0	R2CUT1	R2CUT2	DF1	DF2	NE1	INVFLG
0.200	3.235	3.730	0.100	0.100	0.100	1.000	1.000	4096	0

K12013

K STREAM FOR M7BX5

12 OCT 78 AT 1330 HR

NK : 4 NIV : 512 NGV : 32

M7BX3 THROUGH CELTHRA CHANNEL AT -5.0 DB SNR
TWIST = 119. (21.5 KT) , INFO = NSUA-NUSC78

28 JAN 78 AT 1335 HR

STARTING TIME : 28 : 13 : 35 : 0

NQ = 4

CENTER FREQUENCY : 204.800

CLOCK FREQUENCY : 0 819. 200

410. BURSTS

4100. SYMBOLS

24690. BITS

0./

0. SYMBOL ERRORS

0.000000/

0.000000 PE(SYM)

SYMBOL ERRORS BY LOCATION :

0.	0.	0.	0.	0.	0.	0.	0.
0.	0.	0.	0.	0.	0.	0.	0.
0.	0.	0.	0.	0.	0.	0.	0.
0.	0.	0.	0.	0.	0.	0.	0.

L0	L1	L2	L3	TS0	TS1	TS2	TS3
7.15	13.11	23.30	45.32	-373.	1.	-1.	1.
2.35	1.03	1.33	1.76	1516.	2.	2.	2.

FS0	FS1	FS2	FS3	F2	F2A	F2B	F3	F3A	F3B
118.87	118.61	118.99	118.99	118.62	118.97	118.97	118.98	118.98	118.99
0.32	0.18	0.07	0.07	0.13	0.06	0.04	0.05	0.05	0.06

R2	R2A	R2B	R3	R3A	R3B	A2	A2A	A2B	A3	A3A	A3B
0.887	0.857	0.875	0.947	0.901	0.911	0.167	0.001	0.001	0.001	0.000	0.000
0.055	0.058	0.049	0.037	0.044	0.040	0.097	0.003	0.006	0.011	0.002	0.002

TP2A	TP2B	TP3A	TP3B	NZ2A	NZ2B	NZ3A	NZ3B	SNR2A	SNR2B	SNR3A	SNR3B
139.	-359.	134.	-371.	4.	4.	4.	4.	-9.9	-9.9	-6.9	-6.9
59.	56.	57.	56.	1.	1.	0.	1.	0.5	0.5	0.4	0.4

INF2A	INF2B	INF3A	INF3B	S3	LON(750.)	LIN(237.)	NDEV(52.)
15.4	15.2	15.6	15.4	-2.3	2.73	2.27	-3.5
0.5	0.5	0.5	0.5	0.0	0.14	0.16	0.5

SPEED : 21.5 (0.01) KTS

OFFSET : 1.487329 (0.000887) HZ

*** [REDACTED] ***

*** [REDACTED] ***

RECVR : 11 FEB 79A - BLOCK SUMMARY : 53: 10: 51 TO 55: 0: 28 (37: 37)

M7BX3A - SPECIAL HIGH RATE VERSION FOR '78 NSUA
NH0 = 16 , INFO = NSUA-NUSC760

30 OCT 78 AT 1109 HR (RETYPED 05 JAN 78 AT 0757 HR)

NA NE ND NE NG NH0 NH1 NI NL NM NO NQ NS NSL NT0 NT1 NW
64 4096 15 2048 10 16 256 512 6 240 32 4 409 415 2 5 16

ZSHLIM FTHRS0 FTHRS1 R2CUT0 R2CUT1 R2CUT2 DF1 DF2 NE1 INVLG
0.200 3.235 3.730 0.100 0.100 0.100 1.000 1.000 4096 0

K12013

K STREAM FOR M7BX5

12 OCT 78 AT 1330 HR

NK : 4 NIV : 512 NOV : 32

M7BX3 THROUGH CELTHRA CHANNEL AT -7.0 DB SNR

TWIST = 119. (21.5 KT) , INFO = NSUA-NUSC78

(REWRITTEN VERSION OF POSSIBLY DEFECTIVE 023:08 TAPE)

22 FEB 78 AT 1051 HR

STARTING TIME : 53 : 10 : 51 : 0 NQ = 4

CENTER FREQUENCY : 204.800 CLOCK FREQUENCY : 0 819. 200

578. BURSTS

5780. SYMBOLS

34680. BITS

1./ 1. SYMBOL ERRORS 0.000173/ 0.000173 PE(SYM)

SYMBOL ERRORS BY LOCATION :

0. 0. 0. 0. 1. 0. 0. 0.
0. 0. 0. 0. 1. 0. 0. 0.
0. 0.

L0 L1 L2 L3 TS0 TS1 TS2 TS3
5.86 0.63 16.66 31.95 -151. 0. -1. 1.
1.52 0.94 1.25 1.57 1544. 2. 2. 2.

FS0 FS1 FS2 FS3 F2 F2A F2B F3 F3A F3B
118.82 118.63 118.98 118.98 118.65 118.97 118.97 118.98 118.98 118.99
0.35 0.23 0.08 0.05 0.23 0.07 0.05 0.05 0.03 0.05

R2 R2A R2B R3 R3A R3B A2 A2A A2B A3 A3A A3B
0.819 0.778 0.827 0.926 0.872 0.897 0.153-0.001-0.001 0.001 0.000 0.000
0.025 0.087 0.062 0.041 0.050 0.045 0.115 0.018 0.003 0.012 0.007 0.003

TP2A TP2B TP3A TP3B N22A N22B N23A N23B SNR2A SNR2B SNR3A SNR3B
136. -359. 136. -379. 5. 4. 4. 4. -11.4 -11.3 -8.4 -8.4
62. 60. 57. 58. 1. 1. 1. 1. 0.6 0.6 0.4 0.5

INF2A INF2B INF3A INF3B S3 LON(1077.) LIN(268.) NDBV(75.)
13.9 13.8 14.1 13.8 -3.3 2.72 2.30 -3.7
0.6 0.6 0.6 0.6 0.0 0.14 0.16 0.3

SPEED : 21.5 (0.01) KTS

OFFSET : 1.487279 (0.001015) HZ

*** [REDACTED] ***

*** [REDACTED] ***

RECVR : 11 FEB 79A - BLOCK SUMMARY : 50: 8: 33 TO 51: 22: 18 (37: 45)

M7BX3A - SPECIAL HIGH RATE VERSION FOR '78 NSUA
NH0 = 16 , INFO = NSUA-NUSC780

30 OCT 78 AT 1109 HR (RETYPED 05 JAN 78 AT 0757 HR)

NA NB ND NE NG NH0 NH1 NI NL NM NO NQ NS NSL NT0 NT1 NH
64 4096 15 2048 10 16 256 512 6 240 32 4 409 415 2 5 16

ZSHLIM FTHRS0 FTHRS1 R2CUT0 R2CUT1 R2CUT2 DF1 DF2 NE1 INVFLG
0.200 3.235 3.730 0.100 0.100 0.100 1.000 1.000 4096 0

K12013

K STREAM FOR M7UX5

12 OCT 78 AT 1330 HR

NK : 4 NIV : 512 NOV : 32

M7BX3 THROUGH CELTHRA CHANNEL AT -8.0 DB
TWIST = 119. (21.5 KT) , INFO = NSUA-NUSC78

19 FEB 79 AT 0833 HR

STARTING TIME : 50 : 8 : 33 : 0 NQ = 4
CENTER FREQUENCY : 204.500 CLOCK FREQUENCY : 0 819. 200

583. BURSTS 5830. SYMBOLS 34980. BITS

2./ 2. SYMBOL ERRORS 0.000343/ 0.000343 PE(SYM)

MBOL ERRORS BY LOCATION :

1. 0. 0. 0. 0. 0. 0. 1.
0. 0. 0. 0. 0. 0. 0. 1.
1. 0. 0. 0. 0. 0. 0. 1.
0. 0. 0. 0. 0. 0. 0. 1.

L0 L1 L2 L3 TS0 TS1 TS2 TS3
5.38 8.13 13.85 26.43 -28. 0. -0. 1.
1.35 0.78 1.12 1.49 1483. 2. 2. 2.

FS0 FS1 FS2 FS3 F2 F2A F2B F3 F3A F3B
118.84 118.64 118.98 118.98 118.65 118.97 118.97 118.98 118.98 118.99
0.32 0.24 0.08 0.08 0.24 0.05 0.05 0.06 0.08 0.01

R2 R2A R2B R3 R3A R3B A2 A2A A2B A3 A3A A3B
0.748 0.697 0.762 0.918 0.858 0.889 0.153-0.000-0.001 0.000-0.000 0.001
0.111 0.105 0.075 0.042 0.057 0.046 0.118 0.018 0.009 0.016 0.003 0.008

TP2A TP2B TP3A TP3B NZ2A NZ2B NZ3A NZ3B SNR2A SNR2B SNR3A SNR3B
143. -359. 137. -368. 5. 4. 4. 4. -12.2 -12.2 -9.3 -9.2
22. 61. 58. 59. 1. 1. 1. 1. 0.7 0.7 0.5 0.5

INF2A INF2B INF3A INF3B S3 LON(1068.) LIN(228.) NDBV(75.)
13.1 13.0 13.3 13.2 -3.1 2.73 2.28 -3.8
0.7 0.7 0.6 0.7 0.0 0.15 0.15 0.3

EED : 21.5 (0.02) KTS OFFSET : 1.487294 (0.001059) HZ

*** [REDACTED] ***

*** [REDACTED] ***

RECVR : 06 FEB 79A - BLOCK SUMMARY : 19: 16: 1 TO 20: 17: 17 (25: 16)

M7BX3A - SPECIAL HIGH RATE VERSION FOR '78 NSUA
NH0 = 16 , INFO = NSUA-NUSC780

30 OCT 78 AT 1100 HR (RETYPED 05 JAN 78 AT 0757 HR)

NA	NB	ND	NE	NG	NH0	NH1	NI	NL	NM	NO	NQ	NS	NSL	NT0	NT1	NH
64	4096	15	2048	10	16	256	512	6	240	32	4	409	415	2	5	16

ZSHLIM	FTHRS0	FTHRS1	R2CUT0	R2CUT1	R2CUT2	DF1	DF2	NE1	INVFLG
0.200	3.235	3.730	0.100	0.100	0.100	1.000	1.000	4096	0

K12013

K STREAM FOR M7BX5

12 OCT 78 AT 1330 HR

NK : 4 NIV : 512 NOV : 32

M7BX3 THROUGH CELTHRA CHANNEL AT -8.5 DB
TWIST = 119. (21.5 KT) , INFO = NSUA-NUSC78

19 JAN 79 AT 1601 HR

STARTING TIME : 19 : 16 : 1 : 0 NQ = 4
CENTER FREQUENCY : 204.800 CLOCK FREQUENCY : 0 819. 200

388. BURSTS 3880. SYMBOLS 23280. BITS

5./ 4. SYMBOL ERRORS 0.001289/ 0.001031 PE(SYM)

SYMBOL ERRORS BY LOCATION :

0.	0.	0.	1.	2.	0.	1.	0.
0.	1.						
0.	0.	0.	0.	2.	0.	1.	0.
0.	1.						

L0	L1	L2	L3	TS0	TS1	TS2	TS3
5.08	7.39	12.54	23.87	51.	1.	-1.	1.
1.15	0.75	1.08	1.50	1461.	3.	2.	2.

F50	F51	F52	F53	F2	F2A	F2B	F3	F3A	F3B
118.83	118.67	118.98	118.99	118.67	118.97	118.97	118.98	118.98	118.99
0.32	0.26	0.08	0.07	0.26	0.05	0.07	0.06	0.04	0.05

R2	R2A	R2B	R3	R3A	R3B	A2	A2A	A2B	A3	A3A	A3B
0.699	0.641	0.716	0.913	0.841	0.878	0.139	-0.001	-0.001	0.002	-0.000	-0.000
0.132	0.114	0.092	0.045	0.061	0.047	0.126	0.031	0.015	0.015	0.003	0.003

TP2A	TP2B	TP3A	TP3B	NZ2A	NZ2B	NZ3A	NZ3B	SNR2A	SNR2B	SNR3A	SNR3B
141.	-363.	137.	-372.	5.	4.	5.	4.	-12.5	-12.6	-9.7	-9.6
59.	51.	58.	59.	2.	1.	1.	1.	0.8	0.8	0.5	0.5

INF2A	INF2B	INF3A	INF3B	S3	LONG (729.)	LINC (134.)	NDBV (50.)
12.6	13.6	12.9	12.8	-3.2	2.73	2.27	-3.8
0.7	0.7	0.7	0.7	0.0	0.14	0.14	0.3

VEED : 21.5 (0.01) KTS

OFFSET : 1.487300 (0.000939) HZ

*** [REDACTED] ***

*** [REDACTED] ***

RECVR : 11 FEB 79A - BLOCK SUMMARY : 18: 9: 35 TO 19: 22: 16 (36: 37)

'BX3A - SPECIAL HIGH RATE VERSION FOR '78 NSUA
NH0 = 16 , INFO = NSUA-NUSC780

30 OCT 78 AT 1109 HR (RETYPED 05 JAN 78 AT 0757 HR)

NA NB ND NE NG NH0 NH1 NI NL NM NO NS NSL NT0 NT1 NH
54 4056 15 2048 10 16 256 512 6 240 32 4 409 415 2 5 16

ZSHLIM FTHRS0 FTHRS1 R2CUT0 R2CUT1 R2CUT2 DF1 DF2 NE1 INVFLG
0.200 3.235 3.730 0.100 9.100 0.100 1.000 1.000 4096 0

K12013

K STEAM FOR M7BX5

12 OCT 78 AT 1330 HR

NK : 4 NIV : 512 NOV : 32

M7BX3 THROUGH CELTHRA CHANNEL AT -9.0 DB
TWIST = 119. (21.5 KT) , INFO = NSUA-NUSC78

18 JAN 79 AT 0939 HR (REPLACES BAD TAPE OF 010:13)

STARTING TIME : 18 : 9 : 39 : 0 NO = 4

CENTER FREQUENCY : 204.800

CLOCK FREQUENCY : 0 819. 200

555. BURSTS

5650. SYMBOLS

33900. BITS

24./

12. SYMBOL ERRORS

0.004248/ 0.002124 PE(SYM)

SYMBOL ERRORS BY LOCATION :

4. 0. 0. 0. 6. 1. 5. 1.
1. 6. 0. 0. 2. 1. 3. 1.
3. 0. 0. 0. 2. 1. 3. 1.
0. 2. 0. 0. 0. 0. 0. 0.

L0 L1 L2 L3 TS0 TS1 TS2 TS3
4.88 6.90 11.54 21.74 370. 1. -0. 0.
1.05 0.73 1.08 1.41 1324. 3. 2. 2.

FS0 FS1 FS2 FS3 F2 F2A F2B F3 F3A F3B
118.81 118.67 118.98 118.98 118.69 118.97 118.97 118.98 118.98 118.99
0.31 0.27 0.08 0.08 0.27 0.06 0.06 0.05 0.05 0.07

R2 R2A R2B R3 R3A R3B A2 A2A A2B A3 A3A A3B
0.651 0.586 0.664 0.504 0.829 0.873 0.134 0.000 0.002 0.000 0.000 0.000
0.135 0.124 0.098 0.046 0.066 0.054 0.132 0.032 0.018 0.015 0.005 0.007

TP2A TP2B TP3A TP3B NZ2A NZ2B NZ3A NZ3B SNR2A SNR2B SNR3A SNR3B
139. -354. 139. -371. 5. 4. 4. 4. -13.0 -13.0 -10.1 -10.1
62. 51. 57. 58. 2. 1. 1. 1. 0.6 0.6 0.5 0.5

INF2A INF2B INF3A INF3B S3 L0NC (1041.) L1NC (130.) NDBV (73.)
12.2 12.1 12.5 12.4 -3.3 2.74 2.29 -3.8
0.7 0.7 0.7 0.7 0.0 0.15 0.15 0.3

SPEED : 21.5 (0.02) KTS

OFFSET : 1.487283 (0.001044) HZ

*** [REDACTED] ***

*** [REDACTED] ***

RECVR : 06 FEB 79A - BLOCK SUMMARY : 11: 9: 27 TO 12: 18: 13 (33: 46)

M7BX3A - SPECIAL HIGH RATE VERSION FOR '78 NSUA
NH0 = 16 , INFO = NSUA-NUSC780

30 OCT 78 AT 1109 HR (RETYPED 05 JAN 78 AT 0757 HR)

NA NE ND NE NG NH0 NH1 NI NL NM NO NS NSL NT0 NT1 NW
64 4096 15 2048 10 16 256 512 6 240 32 4 409 415 2 5 16

ZSHLIM FTHRS0 FTHRS1 R2CUT0 R2CUT1 R2CUT2 DF1 DF2 NE1 INVFLG
0.200 3.235 3.730 0.100 0.100 0.100 1.000 1.000 4096 0

K12013

> STREAM FOR M7BX5

12 OCT 78 AT 1330 HR

NK : 4 NIV : 512 NOV : 32

M7BX3 THROUGH CELTHRA CHANNEL AT -10.0 DB
TWIST = 119. (21.5 KT) , INFO = NSUA-NUSC78

11 JAN 79 AT 0327 HR

STARTING TIME : 11 : 9 : 27 : 0 NO = 4
CENTER FREQUENCY : 204.800 CLOCK FREQUENCY : 0 819. 200

512. BURSTS 5120. SYMBOLS 30720. BITS

64. / 40. SYMBOL ERRORS 0.012500/ 0.007812 PE(SYM)

SYMBOL ERRORS BY LOCATION :

6. 7. 6. 1. 8. 4. 11. 6.
2. 13.
3. 2. 5. 2. 8. 2. 3. 3.
2. 10.

L0 L1 L2 L3 TS0 TS1 TS2 TS3
4.64 5.86 9.64 17.89 467. 0. -1. 1.
0.86 0.70 1.02 1.37 1092. 2. 3. 3.

FS0 FS1 FS2 FS3 F2 F2A F2B F3 F3A F3B
118.77 118.69 118.98 118.98 118.70 118.97 118.97 118.99 118.98 118.99
0.31 0.29 0.08 0.08 0.29 0.04 0.06 0.06 0.05 0.06

R2 R2A R2B R3 R3A R3B A2 A2A A2B A3 A3A A3B
0.520 0.456 0.537 0.832 0.782 0.839 0.118-0.000-0.002-0.000-0.000 0.001
0.167 0.148 0.130 0.052 0.087 0.062 0.152 0.068 0.041 0.015 0.012 0.009

TP2A TP2B TP3A TP3B NZ2A NZ2B NZ3A NZ3B SNR2A SNR2B SNR3A SNR3B
135. -367. 134. -372. 6. 5. 5. 4. -13.8 -13.8 -11.0 -10.3
63. 52. 59. 58. 2. 2. 1. 1. 0.9 0.9 0.6 0.6

INF2A INF2B INF3A INF3B S3 LON(1004.) LIN(71.) NDEV(69.)
11.2 11.2 11.7 11.6 -3.5 2.73 2.31 -3.9
0.8 0.8 0.8 0.8 0.0 0.15 0.20 0.2

VEED : 21.5 (0.01) KTS

OFFSET : 1.487275 (0.001005) HZ

*** [REDACTED] ***

*** [REDACTED] ***

RECVR : 11 FEB 79A - BLOCK SUMMARY : 15: 7: 52 TO 15: 23: 42 (15: 50)

M7BX3A - SPECIAL HIGH RATE VERSION FOR '78 NSUA
NH0 = 16 , INFO = NSUA-NUSC730

30 OCT 78 AT 1109 HR (RETYPED 05 JAN 78 AT 0757 HR)
NA NB ND NE NG NH0 NH1 NI NL NM NO NS NSL NT0 NT1 NW
64 4096 15 2048 10 16 256 512 6 240 32 4 409 415 2 5 16
ZSHLIM FTHRS0 FTHRS1 R2CUT0 R2CUT1 R2CUT2 DF1 DF2 NE1 INVFLG
0.200 3.235 3.730 0.100 0.100 0.100 1.000 1.000 4096 0

K12013
K STREAM FOR M7BX5

12 OCT 78 AT 1330 HR
NK : 4 NIV : 512 NOV : 32

M7BX3 THROUGH CELTHRA CHANNEL AT -11.0 DB
TWIST = 119. (21.5 KT) , INFO = NSUA-NUSC730

miss

15 JAN 79 AT 0752 HR
STARTING TIME : 15 : 7 : 52 : 0 NQ = 4
CENTER FREQUENCY : 204.800 CLOCK FREQUENCY : 0 819. 200

244. BURSTS *1246* 2440. SYMBOLS 14640. BITS
106. / 63. SYMBOL ERRORS 0.043443/ 0.025820 PE(SYM)

MBOL ERRORS BY LOCATION :

14. 8. 5. 9. 8. 13. 13. 12.
6. 18.
7. 6. 0. 5. 2. 7. 0. 6.
5. 16.

L0 L1 L2 L3 TS0 TS1 TS2 TS3
4.21 5.02 8.01 14.61 581. 0. -0. 0.
0.64 0.54 0.76 1.25 813. 2. 3. 2.

FS0 FS1 FS2 FS3 F2 F2A F2B F3 F3A F3B
118.75 118.68 118.97 118.98 118.69 118.96 118.97 118.98 118.98 118.98
0.32 0.30 0.08 0.07 0.30 0.08 0.08 0.07 0.05 0.05

R2 R2A R2B R3 R3A R3B A2 A2A A2B A3 A3A A3B
0.365 0.319 0.371 0.251 0.709 0.775 0.093 0.006 0.007 0.003 0.000 0.001
0.185 0.147 0.148 0.064 0.054 0.085 0.174 0.107 0.088 0.023 0.008 0.010

TP2A TP2B TP3A TP3B NZ2A NZ2B NZ3A NZ3B SNR2A SNR2B SNR3A SNR3B
137. -372. 133. -368. 7. 6. 5. 4. -14.8 -14.7 -11.9 -11.9
62. 69. 62. 61. 3. 3. 1. 1. 1.0 1.0 0.7 0.7

INF2A INF2B INF3A INF3B S3 L0N(477.) L1N(10.) NDBV(32.)
10.1 10.1 10.5 10.7 -3.6 2.75 2.45 -3.9
0.5 0.5 0.8 0.9 0.0 0.15 0.45 0.2

PEED : 21.5 (0.91) KTS OFFSET : 1.487141 (0.001030) HZ

*** [REDACTED] ***

*** [REDACTED] ***

RECVR : 11 FEB 79A - BLOCK SUMMARY : 22: 7: 59 TO 23: 5: 40 (21 : 41)

M7BX3A - SPECIAL HIGH RATE VERSION FOR '78 NSUA
NH0 = 16 , INFO = NSUA-NUSC780

30 OCT 78 AT 1109 HR (RETYPED 05 JAN 78 AT 0757 HR)
NA NB ND NE NG NH0 NH1 NI NL NM NO NQ NS NSL NT0 NT1 NW
64 4098 15 2048 10 16 256 512 6 240 32 4 409 415 2 5 16
ZSHLIM FTHRS0 FTHRS1 R2CUT0 R2CUT1 R2CUT2 DF1 DF2 NE1 INVFLG
0.200 3.235 3.730 0.100 0.100 0.100 1.000 1.000 4096 0

K12013
K STREAM FOR M7BX5

12 OCT 78 AT 1330 HR
NK : 4 NIV : \ 512 NOV : 32

M7BX3 THROUGH CELTHRA CHANNEL AT -12.0 DB
TWIST = 119. (21.5 KT) , INFO = NSUA-NUSC78

P_{max} = .166

22 JAN 79 AT 0759 HR
STARTING TIME : 22 : 7 : 59 : 0 NO = 4
CENTER FREQUENCY : 204.800 CLOCK FREQUENCY : 0 819. 200

277. BURSTS / 332 2770. SYMBOLS 16620. BITS
377./ 211. SYMBOL ERRORS 0.136101/ 0.076173 PE(SYM)

MEOL ERRORS BY LOCATION :

52.	42.	24.	36.	46.	29.	40.	35.
18.	54.						
30.	21.	15.	17.	30.	15.	21.	21.
7.	34.						

L0	L1	L2	L3	TS0	TS1	TS2	TS3
3.99	4.50	6.94	11.72	377.	0.	-0.	0.
0.54	0.50	0.72	1.43	739.	3.	3.	3.

FS0	FS1	FS2	FS3	F2	F2A	F2B	F3	F3A	F3B
118.78	118.78	118.98	118.98	118.74	118.97	118.97	118.99	118.98	118.99
0.32	0.33	0.08	0.07	0.34	0.08	0.07	0.06	0.05	0.05

R2	R2A	R2B	R3	R3A	R3B	A2	A2A	A2B	A3	A3A	A3B
0.276	0.207	0.259	0.763	0.594	0.662	0.083	0.006	0.003	0.001	0.000	0.000
0.165	0.140	0.150	0.112	0.133	0.125	0.188	0.160	0.139	0.021	0.020	0.005

TF2A	TF2B	TF3A	TF3B	NZ2A	NZ2B	NZ3A	NZ3B	SNR2A	SNR2B	SNR3A	SNR3B
144.	-270.	138.	-371.	3.	8.	5.	5.	-15.4	-15.3	-13.0	-12.9
66.	99.	63.	62.	5.	9.	2.	2.	1.1	1.1	0.9	0.3

INF2A	INF2B	INF3A	INF3B	S3	LNK(269.)	LNK(44.)	NDBV(53.)
9.9	9.1	9.9	9.9	-3.7	2.75	3.08	-3.9
1.0	1.0	0.9	0.9	0.0	0.15	0.62	0.1

WIND : 21.5 (0.01) KTS

OFFSET : 1.487211 (0.000948) HZ

*** [REDACTED] ***

*** [REDACTED] ***

RECVR : 11 FEB 79A - BLOCK SUMMARY : 113: 7: 54 TO 114: 9: 3 (25: 9)

7BX3A - SPECIAL HIGH RATE VERSION FOR 78 NSUA
NH0 = 16 , INFO = NSUA-NUSC780

30 OCT 78 AT 1109 HR (RETYPED 05 JAN 78 AT 0757 HR)

NA NB ND NE NG NH0 NH1 NI NL NM NO NQ NS NSL NT0 NT1 NW
E4 4096 15 2048 10 16 256 512 6 240 32 4 409 415 2 5 16

ZSHLIM FTHRS0 FTHRS1 R2CUT0 R2CUT1 R2CUT2 DF1 DF2 NE1 INVFLG
0.200 3.235 3.730 0.100 0.100 0.100 1.000 1.000 4096 0

K12013

K STREAM FOR M7BX5

12 OCT 78 AT 1330 HR

NK : 4 NIV : 512 NOV : 32

Pmiss = .56

M7BX3 THROUGH CELTHRA AT -13. DB SNR
TWIST = 119. (21.5 KT) ; INFO = NSUA-NUSC78

23 APR 79 AT 0754 HR

STARTING TIME : 113 : 7 : 54 : 0

NQ = 4

CENTER FREQUENCY : 204.800

CLOCK FREQUENCY : 0 819. 200

172. BURSTS /387

1720. SYMBOLS

10320. BITS

480./

289. SYMBOL ERRORS

0.279070/

0.168023 PE(SYM)

SYMBOL ERRORS BY LOCATION :

53. 44. 38. 41. 58. 45. 52. 50.
35. 59.
34. 22. 21. 25. 34. 25. 39. 31.
19. 39.

L0 L1 L2 L3 T50 T51 T52 T53
3.77 4.20 6.13 9.52 157. 0. -1. 0.
0.39 0.35 0.65 1.49 723. 2. 3. 3.

FS0 FS1 FS2 FS3 F2 F2A F2B F3 F3A F3B
118.76 118.73 118.98 118.99 118.72 118.98 118.98 118.98 118.98 118.99
0.31 0.32 0.09 0.08 0.32 0.10 0.08 0.08 0.09 0.07

R2 R2A R2B R3 R3A R3B A2 A2A A2B A3 A3A A3B
0.182 0.145 0.192 0.622 0.441 0.507 0.056 0.009-0.013 0.002-0.007-0.007
0.152 0.127 0.134 0.151 0.164 0.161 0.208 0.177 0.145 0.024 0.054 0.054

TP2A TP2B TP3A TP3B NZ2A NZ2B NZ3A NZ3B SNR2A SNR2B SNR3A SNR3B
137. -362. 139. -374. 13. 11. 7. 6. -15.9 -15.8 -13.9 -13.8
79. 68. 68. 55. 7. 6. 4. 3. 1.2 1.3 1.0 1.1

INF2A INF2B INF3A INF3B S3 L0NK (545.) L1NK (117.) NDBV(62.)
9.1 9.1 9.3 9.2 -3.8 2.75 3.18 -3.9
0.9 0.9 0.8 0.9 0.0 0.16 0.57 0.1

SPEED : 21.5 (0.02) KTS

OFFSET : 1.487311 (0.001118) HZ

*** [REDACTED] ***

*** [REDACTED] ***

RECVR : 11 FEB 79A - BLOCK SUMMARY : 149: 7: 49 TO 150: 8: 50 (25: 1)

BX3A - SPECIAL HIGH RATE VERSION FOR '78 NSUA
NH0 = 16 , INFO = NSUA-NUSC780

30 OCT 78 AT 1109 HR (RETYPED 05 JAN 78 AT 0757 HR)

NA NB ND NE NG NH0 NH1 NI NL NM NO NQ NS NSL NT0 NT1 NW
24 4096 15 2045 10 15 256 512 E 240 32 4 409 415 2 5 16

ZSHLIM FTHRS0 FTHRS1 R2CUT0 R2CUT1 R2CUT2 DF1 DF2 NE1 INVFLG
0.200 3.235 3.730 0.100 0.100 0.100 1.000 1.000 4096 2

K12012

X STREAM FOR H7BX5

12 OCT 78 AT 1330 HR

NK : 4 NIV : 512 NOV : 32 P_{MIS} = .832

H7B/3 THROUGH CELTHRA AT -14.0 DB SNR
TWIST = 119. (21.5 KT) ; INFO = NSUA-NUSC78

29 MAY 78 AT 0749 HR

STARTING TIME : 149 : 7 : 49 : 0 N3 = 4
CENTER FREQUENCY : 204.600 CLOCK FREQUENCY : 0 819. 290

64. BURSTS /342

640. SYMBOLS

3840. BITS

314.7 342. SYMBOL ERRORS

0.490625/ 0.378125 PE(SYM)

SYMBOL ERRORS BY LOCATION :

35. 25. 25. 36. 37. 32. 36. 33.
11. 42.
21. 18. 21. 22. 32. 18. 30. 23.
13. 32.

L0 L1 L2 L3 T50 T51 T52 T53
3.69 4.04 5.54 7.40 -92. -0. -0. -0.
0.23 3.24 0.62 1.34 683. 3. 3. 3.

F50 F51 F52 F53 F2 F2A F2B F3 F3A F3B
118.70 118.68 118.97 118.98 118.69 118.95 118.96 118.97 118.98 118.99
0.27 0.28 0.09 0.09 0.25 0.09 0.09 0.07 0.09 0.09

R2 R2A R2B R3 R3A R3B A2 A2A A2B A3 A3A A3B
0.109 0.290 0.112 0.411 0.231 0.335 0.034 0.025 0.007-0.013-0.034-0.008
0.110 0.105 0.110 0.177 0.160 0.158 0.227 0.229 0.215 0.080 0.102 0.090

TR2A TR2B TR3A TR3B NR2A NR2B NR3A NR3B SNR2A SNR2B SNR3A SNR3B
127. -353. 137. -260. 7. 13. 11. 3. -16.7 -15.7 -14.0 -14.9
71. 70. 66. 50. 10. 7. 11. 7. 1.5 1.7 1.2 1.5

INFO INFOB INFOA INFOE SS LINC -973.1 LINC 75.1 NDEV(SS.)
7.1 7.1 6.7 3.5 -3.5 3.74 3.25 -4.0
0.7 0.5 0.6 0.8 0.0 0.15 0.49 0.1

SPEED : 21.5 (0.02) KTS

OFFSET : 1.467070 (0.001070) HZ

*** [REDACTED] ***


PART 4

COMPUTER REQUIREMENTS FOR THE M7
COMMUNICATION SYSTEM ■

2 MARCH 1979


Contents 

	<u>Page</u>
1. Introduction	1
2. Hardware Requirements	4
2.1 Speed Requirements	4
2.1.1 Synchronization Speed Requirements	5
2.1.2 Information Decoding Speed Requirements	8
2.2 Memory Requirements	10
2.2.1 KFILE storage	11
2.2.2 Input Buffer	12
2.2.3 Synchronization Files	12
2.2.4 Working Areas	13
2.2.5 Program Storage	15
2.2.6 Summary of Memory Requirements	
3. Software Development Requirements	19
3.1 Size and complexity of the present M7 implementation	21
3.2 Software development software	23
3.2.1 Operating system	23
3.2.2 High level language	24
3.2.3 Program development system	25
3.3 Software evaluation	26



[REDACTED]

List of Tables [REDACTED]

<u>Table</u>	<u>Title</u> [REDACTED]	<u>Pages</u>
1	Relevant M7 Parameters [REDACTED]	1
2	M7BX3 and M7BX4 Characteristics [REDACTED]	3
3	Hardware configurations of ACS computers [REDACTED]	4a
4	Software storage requirements [REDACTED]	17
5	Memory requirements summary [REDACTED]	18
6	Existing M7 software composition [REDACTED]	22

[REDACTED]

[REDACTED]

1. Introduction [REDACTED]

[REDACTED] In order to implement the M7 communications system, the computer selected for the task must meet requirements of speed of execution, memory size and software development capability. With the exception of the latter of these requirements, the specific requirements depend strongly on the parameters of the version being implemented. This paper discusses, with examples, these three major requirements.

[REDACTED] To understand the material presented, familiarity with the M7 system and its associated nomenclature will be required. An adequate summary for this purpose is contained in Reference 1, which should be available to the reader. Of the many parameters defined in Reference 1, those shown in Table 1 below will be relevant here:

Table 1: Relevant M7 Parameters [REDACTED]
(Table [REDACTED])

<u>Parameter</u>	<u>Definition</u>
N_A	No. of symbols in alphabet
N_B	No. of complex samples/burst
N_D	No. of time dilation bins
N_E	No. of complex samples between receiver input vectors
N_G	No. of symbol positions/burst
N_L	No. of bits/symbol ($N_L = \log_2 N_A$)
N_M	No. of integer line searches ($N_M = N_D \cdot N_W$)
N_Q	System Q
N_S	No. of complex samples/symbol
$N_{T\emptyset}$	No. of fractional line searches/integer line
N_W	No. of line searches/time dilation bin

[REDACTED]

■ In some applications, the single N_B - long burst described in Reference 1 will not be sufficient to transmit the necessary information. That is, the desired message length is greater than $N_L \cdot N_G$ bits. To accommodate such applications, the M7 system can be logically extended by constructing the transmission from N_Z consecutive N_B -long blocks, where each N_B -long block has the same structure as the original block, but is based on a different random bit stream. This allows $N_Z \cdot N_L \cdot N_G$ bits to be transmitted in a single burst without introducing any structure into the transmission. At the receiver, primary synchronization is performed on the first block only, later blocks being synchronized by the equivalent of the secondary synchronization search. The current implementation, for research purposes, is limited to the single block mode ($N_Z = 1$).

■ The discussion of computer requirements versus system parameters can become an abstract exercise very quickly. To provide a tangible basis for this discussion, two current versions of the M7 system will be considered relative to two existing hardware configurations. The implementation approach considered will be that of the existing implementation - other approaches may be worth pursuing, but the one given here appears straightforward.

■ The two versions of the M7 system considered in the examples are sketched in Table 2. The M7BX3 version is directed at investigating the tactical submarine to submarine communication problem and has a moderate bit rate and a moderate range capability. The M7BX4 version

Table 2: M7BX3 and M7BX4 Characteristics

(Table classified [REDACTED])

<u>Characteristic</u>	<u>System</u>	
	<u>M7BX3</u>	<u>M7BX4</u>
Application	Tactical	Strategic
Center frequency, Hz	204.8	150
Bandwidth, Hz	51.2	50.0
Burst duration, sec	80.0	819.2(13.7 min)
Block WT product	4096	4096
Modulation	64-ary biorthogonal	64-ary biorthogonal
Symbol Duration, sec	8.0	40.96
Symbol WT product	409	2048
Bit rate, bits/sec	.750	.146
Bits per burst	60	120
Doppler uncertainty, Kt	± 21.5	$\pm .25$
Nominal Range, nm	100	500
Operating (S/N) dB for P_E (BIT) = .0001, estimated from simulation data	-8.0	-10.0

██████████ is intended to approximate a strategic, low bit rate, long range communication system. Here, the desired message length requires $N_z = 10$. Consequently, M7BX4 as described in Table 1 is not implementable in full on the existing system.

██████████ The two versions of the hardware considered in the examples are based on existing Acoustic Communication Studies equipment. Consequently, a great deal of solid information concerning execution times, program size, etc. is available for both. Table 3 gives the salient information for a system based on the Texas Instruments 980A computer and for the same system when a Floating Point Systems AP-120B array processor is added. The 980A alone system represents roughly the typical minicomputer based organization, the 980A with AP system represents the typical minicomputer plus array processor organization.

2.0 Hardware Requirements ██████████

██████████ The M7 system employs large time-bandwidth product signals and operates with substantial time/frequency of arrival uncertainty. These features place stringent requirements on the computation speed and memory size of the hardware. The sections below describes each of these requirements.

2.1 Speed Requirements ██████████

██████████ In order to synchronize with the incoming signal, that is to detect its presence and estimate its time and frequency of arrival, a large number of calculations must be performed in real time. Once synchronization has been obtained, further extensive calculations are required to determine the transmitted message. Each operation imposes

Table 4a: Hardware Configurations of ACS

Computers (This table) (Software Development Equipment Excluded from this Table)

Characteristic	System	
	980A Alone	980A/AP-120B
<u>Hardware Arithmetic Speed: (μS)</u>		
Double Precision Integer Add	4.0	4.0
Single X Single Integer Multiply	7.25	7.25
Floating Point Add	150	150
Floating Point Multiply	240	240
Floating Point Add	—	~ .166
Floating Point Multiply	—	~ .166
<u>Software Speed: (ms)</u>		
Arithmetic	16 bit block, floating point	38 bit floating point
Complex Array Multiply/Point	.303	.001
Complex FFT N = 1024	1240	6.93
2048	2680	16.68
4096	5847	33.16
8192	--	77.31
<u>Memory Configuration (words)</u>		
CPU Memory (16 bit)	65536	65536
Moving Head Disk (16 bit)	1120000	1120000
Main Data (38 bit)	--	40960
Table (38 bit)	--	3072
Program Source (64 bit)	--	1024

its own requirements on the computer speed.

2.1.1 Synchronization Speed Requirements

Only the primary search in the synchronization process is significant in terms of calculation speed. As indicated in Reference 1, each primary search consists of $N_M \cdot N_{T\phi}$ Doppler bin searches over an N_B long input vector. For real-time operation these searches must be completed in $N_E/N_B \cdot T_B$ seconds where N_E is the number of complex samples between consecutive input vectors and T_B is the time duration of a block of N_B complex samples,

$$T_B = N_B \frac{N_Q}{f_R} \quad (1)$$

Each Doppler bin search requires the following minimal calculations:*

1. Array multiply between $X_o(f)$ and $A(f)$
2. Inverse Fast Fourier Transform (FFT) to yield $y(j, k)$
3. Calculation of $z(j, k)$ (Ref 1, Eqn 29)
4. Calculation of l_o (Ref 1, Eqn 30)

with existing software steps 3 and 4 occupy a time equivalent to an array multiply. Thus the calculations per Doppler bin are equivalent to one FFT and two array multiples.

To provide a simple, but useful bound on computer speed for synchronization, the maximum allowable time for an N_B -long FFT, T_{SYNCH}^* , will be computed based on the assumption that the time for the two array multiplies can be neglected. This bound is particularly convenient because it is close to the actual time for most versions of the M7 system

*All operations performed by the receiver are over complex array variables.

($2 \ll \log_2 N_B$) and calculation times for a given size FFT can often be found from manufacturer's data. Note, however that T_{SYNCH}^* is a strict upper bound, a computer which performs an N_B -long FFT in exactly T_{SYNCH}^* can not operate in real time.

■ To perform $N_M \cdot N_{T0}$ Doppler bin searches each of duration T_{SYNCH}^* in $N_E/N_B T_B$ seconds, the following equation must hold:

$$T_{\text{SYNCH}}^* = \frac{N_E}{N_B} \frac{T_B}{N_M \cdot N_{T0}} \quad (2)$$

where N_M is the number of line spacings ($\text{DFLINE} = 1/T_B$) required for the Doppler search as described in Reference 1.

■ Equation 2 becomes more useful when N_M is written as a function of the Doppler uncertainty, $|V|$. The frequency offset, DF , as a function of $|V|$ is given by:

$$DF = \frac{|V|}{C} f_R \quad (3)$$

From equation 28 of Reference 1,

$$DF_{\text{RANGE}} \text{ (Hz)} = \frac{f_R}{N_Q \cdot N_B} N_M \quad (4)$$

$$= 2 \cdot DF \quad (5)$$

since the search range is two sided and symmetric about f_R . Solving for N_M yields

$$N_M = 2 |V| / C N_Q \cdot N_B \quad (6)$$

Then equation 2 becomes

$$T_{\text{SYNCH}}^* = \frac{C}{2|V|} \frac{N_E}{N_B} \frac{1}{N_{T0}} \frac{1}{f_R} \quad (7)$$

If the search strategy implemented in M7BX3 is applied, the above equation can be simplified further. In M7BX3, a 50% overlap in the time domain ($N_E/N_B = \frac{1}{2}$) and a $\frac{1}{2}$ line spacing frequency search interval ($N_{T\phi} = 2$) are incorporated in the primary search. Further, take $C = 5000$ ft/sec. Then Equation 7 becomes

$$T_{\text{SYNCH}}^* = \frac{370.041}{f_R} \frac{1}{|V|} \quad (8)$$

where $|V|$ is expressed in Knots (Kt). Note that N_B does not appear explicitly in Equation 11, but that by definition T_{SYNCH}^* is the time to perform an N_B -long FFT.

The values for T_{SYNCH}^* for the M7BX3 and M7BX4 systems of Table 1 are 84 ms (milliseconds) and 9.87 seconds respectively. Since 84 ms is greater than the published 4096 transform time for the 980A/AP system of Table 3, M7BX3 is implementable on that hardware. M7BX3 is not implementable on the 980A alone hardware. In the case of the M7BX4 version, it is implementable with ease on the 980A/AP hardware and may be implementable on the 980A alone hardware.

Since the Doppler range for the M7BX3 system has been deliberately set as the maximum implementable by the 980A/AP hardware, further conclusions can be drawn. Since T_{SYNCH}^* for the M7BX3 system is about 2.5 times greater than the published 4096 transform time (33 ms) a crude, but useful estimate of the actual required 4096 transform time for the M7BX4 system can be obtained by dividing the corresponding T_{SYNCH}^* by 2.5. This yields a requirement for a 4096 transform time no longer than 3.95 seconds for the M7BX4 system and attempts to include the many overhead calculations necessary in an

actual system. Since 3.95 seconds is less than the published transform time (5.85 sec) for the 980A above hardware, an implementation of M7BX4 on that hardware may not be possible, contrary to the T_{SYNCH}^* calculations of the proceeding paragraph.

2.1.2 Information Decoding Speed Requirements

Because the information decoding operation of the M7 system takes place only after a detection by the synchronization operation, its time constraints are more flexible. If transmitted messages are known to be separated by some minimum time interval or if the arrival of more than one message in an interval is unlikely, the receiver can simply ignore its input after the detection takes place and devote its entire calculational resources to information decoding. This yields an interval, T_{BLANK}^* after each correct detection or false alarm in which an incoming signal will be ignored as the receiver is effectively "blanked out". With current thresholds set to yield less than one false alarm in 36 hours, blanking due to false alarms will be negligible for most applications. Of course, sufficient computer speed eliminates the need for blanking.

The information decoding operation is somewhat complicated and consequently an explanation of each sub-operation is beyond the scope of this paper. Three computationally important components of the information decoding operation are listed below along the number of FFT's required:

<u>Component</u>	<u>Transforms Required</u>
Secondary Search	$2 \cdot DF \cdot NT1$
Doppler removal/probe extraction	105
Symbol filtering	$2 \cdot N_A \cdot N_G$

Again in deriving a timing bound, the time required for array multiplies will be neglected. The above figures do include transforms for the bootstrapping operation, however. For a secondary search equivalent to that of M7BX3 ($DF = 1$, $NT1 = 5$), the total number of transforms becomes $115 + 2 \cdot N_A \cdot N_G$, with the relative importance of the first and second terms dependent on the size of the signalling alphabet, N_A , and the number of symbols per block, N_G .

For real-time operation with no blanking, the $115 + 2 \cdot N_A \cdot N_G$ N_B -long transforms must be performed in T_B seconds. Let T_{INFO}^* be the transform time for an N_B -long transform, then the following equation must hold:

$$T_{INFO}^* = \frac{N_G \cdot N_B}{(115 + 2N_A \cdot N_G) f_R} \quad (9)$$

If the transform time on a machine is greater than T_{INFO}^* , some amount of blanking of the receiver input will be required. Let T_{FFT} be the actual time required for an N_B -long transform, then the minimum length of the post-detection blanking interval, T_{BLANK}^* , is given by

$$T_{BLANK}^* = (T_{FFT} - T_{INFO}^*) (115 + 2N_A \cdot N_G) N_Z \quad (10)$$

Because of the array multiplies and other necessary overhead calculations, the actual blanking interval will be larger than T_{BLANK}^* .

■ For the M7BX3 and M7BX4 systems of Table 1, T_{INFO}^* is 57.3 ms and 221 ms respectively. The transform times of Table 3 then indicate that M7BX3 can not implement real-time on the 980A alone configuration, but can be implemented on the 980A/AP configuration. The M7BX4 system cannot be implemented in real-time on the 980A alone configuration either, while it can be implemented with ease on the 980A/AP configuration. The required minimum blanking intervals T_{BLANK}^* on the 980A above configuration are of the order of hours. Consequently, inclusion of a blanking interval is of value only if T_{FFT} is near T_{INFO}^* . In fact, when M7BX3 is run on the existing 980A/AP configuration, a blanking interval of 80 seconds is required due to overhead calculations.

2.2 Memory Requirements ■

■ The second major hardware requirement for the M7 system is for memory space. Five major functional requirements for storage can be designated:

1. KFILE storage
2. Input Buffer
3. Synchronization Files
4. Working Areas
5. Program storage

A variety of approaches to satisfying these requirements can be considered in implementing the system. Generally, a trade-off opportunity between speed of execution and memory size/cost can be made. The trade-offs indicated in the following discussion again parallels that of the current implementation.

2.2.1 KFILE Storage

■ The structure of the M7 system is based on a sequence of random bits, known as the KFILE. This sequence must be available to the receiver in order to synchronize and decode the transmission. The number of bits in the KFILE, N_{KB} , is given by

$$N_{KB} = N_Z N_B (1 + N_A/2) \quad (11)$$

For the M7BX3 and M7BX4 systems, N_{KB} is 135, 168 and 1,351,680 bits respectively. In terms of 16 bit computer words, a more useful measure, these values are 8,448 and 84,480 words respectively.

■ In the current implementation of the M7 system, KFILE's are generated by a laboratory noise generator and stored on a moving head disk file. This file, which contains other vectors needed by the receiver, is called the VFILE. In an operational system the KFILE (and consequently the VFILE) would probably be changed in a periodic basis. Consequently a means for entering as well as storing the KFILE would be necessary.

■ One approach to these problems is to interface the system to an approved cryptologic sequence generator and have it produce the needed bits on command. If an approved sequence generator cannot be used, alternative algorithms in conjunction with devices such as the National Bureau of Standards Data Encryption Standard (DES) might be satisfactory. Thus the KFILE storage requirement can be satisfied by providing the necessary storage and input capability or by interfacing KFILE generation hardware.

2.2.2 Input Buffer

Because the receiver operates asynchronously with the input data, the input must be buffered to ensure the necessary data is available to the receiver. The extent of this buffer depends on the speed of the receiver in performing both the synchronization and information decoding tasks. In general, a shorter input buffer becomes acceptable as the receiver speed increases. Determination of the minimum size of the input buffer is an involved problem which has not been pursued. The current implementation has an input buffer of $3N_B$ complex pairs ($6N_B$ real words) maintained on a moving head disk file. This buffer size has been sufficient for existing versions of the system having $N_Z = 1$. If N_Z is greater than 1, a longer buffer may be necessary.

2.2.3 Synchronization Files

The M7 receiver synchronization process requires a search over N_D time dilation bins where each time dilation bin is centered on a time-distorted replica of the transmitted probe component. With the exception of the central bin, the construction of the time-distorted replicas requires a substantial amount of calculations. Consequently, in the current implementation all of these time-distorted replicas are pre-computed and stored as synchronization files, a component of the VFILE on the moving-head disk unit. With this approach N_D vectors of N_B complex words or $2 \cdot N_D \cdot N_B$ real words are required. For M7BX3, 122,880 real words are required for the synchronization files.

■ If $N_D = 1$, that is, if N_M is less than about 16, then only the central time dilation bin is searched. In this case, which applies to the M7BX4 versions, no need for a pre-computed replica exists and the synchronization file can be eliminated.

2.2.4 Working Areas ■

■ The vector operations performed by the M7 receiver require substantial working areas in memory. For example, in the synchronization process, the transform of the input data, $X(f)$, is multiplied by the time-dilated replica's transform, $A_j(f)$, then inverse transformed to the time domain to yield $y(i, j)$. Because $X(f)$ and $A_j(f)$ are needed for each of N_W pure frequency offsets within a time dilation bin, at least $3 N_B$ -long complex vectors must be resident in the work area. In fact, an additional N_B -long complex vector is used in the current implementation to allow an 18% speed-up in the inverse FFT. Similarly, the Doppler removal algorithm requires at least $4 N_B$ -long complex vectors. The equivalent of another N_B -long complex vector is needed for scalars and miscellaneous tables, bringing the total requirement to $10 N_B$ words in the working areas. For either M7BX3 or M7BX4, this means 40,960 words should be available.

■ In the current implementation on the 980A/AP hardware, the working areas are located in the array processor main data memory. An additional 3072 words of random access table memory serve as storage for trigonometric constants, etc. Because the words of either of these memories are composed at 38 bits each, the size of the work and constant storage areas in the array processor (1.67×10^6 bits) is greater than that of the 980A itself (1.05×10^6 bits). Thus neither M7BX3 nor M7BX4

■ could be implemented with floating point arithmetic on the 980A alone hardware. Implementation with 16 bit integer arithmetic on the 980A alone hardware would be very difficult as only 21,504 words would be available for the program itself. Consequently, these versions are implementable only on machines with an effective address space significantly larger than 32,768, or with an array processor having approximately 44,000 words of data memory.

■ In the present implementation of the system two additional N_B -long working areas have been incorporated into the 980A memory. These areas are necessary to speed the transfers of vectors on the moving head disk file to the array processor and to facilitate the bootstrapping operation. If the KFILE synchronization files were directly accessible by the array processor, one of these vectors could be eliminated. The other vector is used in the re-construction of the transmitted signal during bootstrapping and could be eliminated if the re-construction algorithm was readily performed in the array processor. Consequently, limitations on either hardware or software may increase the working space requirements beyond those indicated above.

2.2.5 Program Storage Requirements

The software program which implements the M7 system also requires space in the computer memory. Perhaps more than any other requirement, an estimate of the extent of computer memory needed is dependent on the particular machine selected and the details of the program organization. Nevertheless, the discussion below will be helpful in estimating the memory requirements for program storage, as long as a resolution beyond about 16K 16 bit words is not sought.

The present implementation of the M7 system consists of a disk initialization program (VSET) which precalculates the necessary VFILE vector and a real time program (RECVR) which does the actual reception. Because the disk initialization program is performed only once prior to system operation, it will not be considered further.

Six functional groups into which the program memory space can be partitioned are:

1. Monitor System Software
2. General Purpose Subroutines
3. Input Buffer Manager
4. Receiver Tasks and Subroutines
5. Large Arrays
6. Miscellaneous Arrays

The first group includes non-specific operator interaction, hardware device servicing and task control functions. The second group contains subroutines of a general nature, mostly arithmetic. Software in groups one and two is not specific to the communication problem and, ideally, would be provided as a standard product by the hardware manufacturer. The input buffer manager allows the real-time input data to be processed

in a convenient manner. Although specific to real-time applications, it is not peculiar to the communication problem. Group four contains all tasks and subroutines which are specific to the communication problem - no part of group four is likely to be available from other sources. Groups five and six cover working areas in the mainframe. The space requirements of group five could potentially be eliminated under certain hardware conditions as discussed at the conclusion of the preceding section. The space requirements of group six represent the size of miscellaneous array storage required to run M7, beyond the working areas already discussed.

Table 4 below gives the current size in 16 bit words of each of the six software groups.

Table 4: Software Storage Requirements

(Based on RECVR/26 Oct 78A) (Table

<u>Group</u>	<u>Contents</u>	<u>Storage (16 bit words)</u>
1	Monitor system software	7,247
2	General purpose routines	9,453
3	Input buffer manager	9,377
4	Receiver tasks and subroutines	11,171
5	Large arrays	16,384
6	Miscellaneous arrays	<u>3,086</u>
	Total	56,718
	Group 5	- <u>16,384</u>
	Total (less Group 5)	40,334

Several cautions must be considered in conjunction with Table 4. First, the monitor system available is extremely memory and time efficient. A general purpose system such as provided by a manufacturer to all users would probably be larger. Second, the input buffer routines are for a single channel only and do not perform any filtering function. Third, although some space is devoted to statistical functions associated with the research purposes of the system, an operational system would almost certainly require further storage for purposes such as interference rejection, error detecting-correcting algorithms, message handling etc. These considerations lead to a first estimate of at least 65K words for program alone for an operational, single channel system.

2.2.6 Summary of Memory Requirements

The results of the preceding memory requirements discussion are summarized in Table 5. Two hardware configurations, different from those considered previously are given. Configuration A assumes memory

Table 5: Memory Requirements Summary (16 bit words)

System (Table classified)

<u>Requirement</u>	<u>M7BX3</u> <u>Configuration</u>		<u>M7BX4</u> <u>Configuration</u>	
	<u>A</u>	<u>B</u>	<u>A</u>	<u>B</u>
KFILE storage *	8448	-	84,480	-
Input buffer *	24,576	24,576	24,576	24,576
Synchronization files *	122,880	122,880	-	-
Working areas	44,000	44,000	44,000	44,000
Program Storage	<u>56,718</u>	<u>40,334</u>	<u>56,718</u>	<u>40,334</u>
Totals	256,622	231,790	209,744	108,910

* This storage is implemented in bulk storage moving head disk in the current system.

usage comparable to the present system and can be considered pessimistic (i.e. larger than absolutely necessary). Configuration B is based on the assumption of an on-line KFILE generator and homogeneous memory in the hardware and consequently has a much smaller memory requirement. Both the M7BX3 and M7BX4 versions of the system are shown.

■ The most significant result from Table 5, is that the M7 system requires far more memory than is directly addressable with current 16-bit minicomputers. Consequently any hardware on which the M7 system is to be implemented must have either a larger address space or a convenient memory paging feature. Alternatively, a trade-off between execution speed and addressability could be made by incorporating a bulk storage device. Probably the best solution is simply to have a large homogeneous address space. If this is not available, a partitioning into two memory units, one of which has a larger address space would be suggested. Only as a last resort would the paging capability associated with a bulk storage device be appropriate, due to the resulting software complexity and loss of execution speed.

3. Software development requirements ■

■ Implementation of the M7 system has two major elements: hardware and software. While hardware presents significant bounds on the maximum possible capability of the system, i.e. Doppler range, software determines how close to these bounds the system will actually operate. Perhaps the most important area of application for the above statement is in reliability. A communication system with an error rate of .001 can have its performance degraded by a factor of two due to an error in programming which occurs only once in a thousand operations.

Detection of such errors in systems with stochastic inputs can be extremely difficult unless the software is generated and evaluated with extreme care.

■ The following sections discuss the requirements for generation and evaluation for the M7 system. Before going into these requirements a brief comment on the size and complexity of the present software implementation will be presented as a point of reference.

3.1 Size and Complexity of the Present M7 Implementation

The size of a software task is important in determining the approach to accomplishing it. For example, the software for a microwave oven controller can be efficiently generated with less sophisticated tools than those for a ballistic missile defense system. In the first case, programming in machine code and testing by near-exhaustion may be appropriate. In the latter, high level languages and intricate software verification programs are necessary. The software for the existing M7 communication system clearly falls in between these extremes, and some measure of the size and complexity of the software is necessary to select appropriate software development techniques.

In section 2.2.5, the program size of the M7 system (less large arrays, Group 5) was given as 40,334 16 bit words. This is one very crude measure of the extent of the software task. Alternatively, consider the breakdown of that same program in terms of number entry points and lines of source code as indicated in Table 6 below. Each entry point signifies a piece of the overall software mass, so that in a rough sense, about 210 identifiable software modules must be interconnected. Each line of source code represents one line of program printout which must be carefully designed, test and maintained.

Table 6: Existing M7 Software Composition;

(26 Oct 78A) (Table

Group	Type	Entry Points	Language	Source Code Length (Lines)
1	System	61	980 A.L.	(6602)*
2	G.P. Routines			
	980A	73	980 A.L.	--
	FAP-G.P.	21	FAP A.L.	--
	FAP Special	9	FAP A.L.	382**
3	Buffer Task & Routines	18	F	1581
	Comm. Tasks	4	F	1143
4	Comm. Routines	15	F	1860
		4	980 A.L.	626***
	Support Programs	5	F	2458
			A.L.	1008 12.5%
			F	7042 87.5%
	Total	210	Total	8050

* Normally provided by manufacturer, not counted in total below.

** 64 bit microcode word/line approximately 4 times more difficult than 980A A.L.

*** 446 lines of A.L. format conversion routines, remainder writable in Fortran.

■ Although various technical definitions of program complexity have been proposed, the concept of complexity considered here is more qualitative - given an anomaly or software "Glitch" the complexity of the program is a measure of the time required to find the cause of the problem. The present system has been developed via the traditional method of independent subroutine development and testing followed by staged integration of the routine into the system. This approach is an excellent one, but its fundamental weakness is that the subroutine can not be adequately tested independently, as the variety of inputs is too great. Consequently, the union of a number of verified subroutines can be a program that works on only a small subset of inputs. More importantly, with stochastic inputs the particular input causing an anomaly may be infrequent and hard to detect. Thus, the complexity of the system, as implemented, is at least moderate; an operational system would be more complex.

3.2 Software Development Tools: ■

■ The reliability of the software for an implementation will depend on the quality of the tools of its development as well as the programmer's skill. Only three major and essential tools will be discussed here: operating system, high level programming language and program development software.

3.2.1 System Software: ■

■ Because the manufacturer of the existing 980A system did not provide an interrupt driven operating system until very recently, a special purpose system, more correctly called a monitor system, has been developed beginning in 1973. The present version of this system occupies 7,247 16 bit computer words and involves 6602 lines of source

code. Although the present system works very well, its development, testing and maintenance has been time consuming. For example, in the summer of 1978, a re-entrancy problem was found in the interrupt servicing routines which caused the system to crash mysteriously at a rate of about 2 crashes per month. Such problems are hard to detect - at that rate a hardware failure or power glitch would be suspected.

■ To avoid such difficulty, the computer selected for implementation of the M7 system should have a flexible and reliable operating system provided with it. It should be flexible in the sense that no modification of the fundamental system should be necessary to accommodate the implementation of the communication system. Driver modules for special hardware modules, of course, will be necessary, but they should be short and follow the canonical structure used by the operating system. The operating system should be already well-evaluated for reliability, where the only acceptable indication of this reliability is successful application to real-time problems by a number of independent users, over a period of years.

3.2.2 High Level Language: ■

■ Although the M7 system software could theoretically be developed in assembly language (or even machine code), a high-level language would certainly be used by the vast majority of software designers. Indeed, the military is beginning to require use of a high level language for all systems beyond the development stage. The present M7 implementation, exclusive of the monitor system, has 88% of its source code in FORTRAN IV. The remaining 12% of the source code lines are in assembly language for reasons of necessity (i.e. microcode for the array processor), compatibility (i.e. executable by the transmitter

without the FORTRAN library) and convenience (i.e. radix 40 packing and unpacking). If necessary all but 5% of the software (the array processor microcode) could be written in FORTRAN.

■ FORTRAN is only one of a variety of high level languages suitable for implementing the M7 system and other languages can offer even further advantages. The only critical requirements for such a language is that it should be flexibly interfaced to the operating system and have only moderate overhead. Specifically, all peripheral devices should be handled within the normal syntax of the language, i.e. READ/WRITE statements in FORTRAN. Some languages are so powerful in notation they may not meet the latter requiremen.. For example, a program written in BASIC might treat the statement

$$A = B + C$$

has a matrix equation, even for scalar variables. The resulting overhead in execution time would probably be unacceptable. Both these requirements will normally be satisfied by software available from the computer manufacturer.

3.2.3 Program Development System: ■

■ To test, modify and maintain the 200 plus modules requires convenient program development system including editors, linkers and subroutine libraries. One measure of the convenience of such a program development system is the time required to change a software module, document the change and the execute the resulting system for evaluation purposes. The program development system from which the current M7, implementation was constructed is implemented on the same hardware (980A) the M7 system runs on and requires about 30 minutes to insert a fully

documented change. Strangely, the majority of this time (20 min) is spent in linking the object modules together.

■ A key problem with the existing program development system is the lack of automatic source and object dating. In a system with a large number of modules, care must be taken that all of the modules included in an executable program be of the most recent revision level. Enormous difficulties arise when subroutines of a lower revision level are inadvertently mixed into an otherwise correct program. In the present program development system, revision-level dating is performed by the programmer and great care is required to ensure the program uses only current modules. Program development systems on other manufacturer's system should include automatic source and object dating, eliminating this problem.

3.3 Software Evaluation: ■

■ An essential component of software development for the M7 system is careful evaluation of the system against both known and stochastic signals. This is because of the inherent non-linearity of the processing (superposition does not apply), the wide variety of allowable inputs during operation at sea, and the need for reliability against infrequent, but erroneous events. Only by extensive testing and statistical examination of selected "internal" parameters can the full capabilities of the system be realized.

■ In order to perform the required evaluation the software must be developed on a system with more peripherals than required by the operational hardware. Specifically, the software development hardware should include a noise source, one or more tape drives, and high-speed printer or display device. The need for each of these items is

discussed below.

Once traditional evaluation of the M7 subroutines and main program against fixed inputs is completed, evaluation over carefully controlled stochastic inputs must be performed. The most natural approach to this evaluation is to construct digital synthetic data tapes for the receiver and statistically observe its performance. In the development of the present system, these synthetic data tapes contain signal and noise at precisely controlled signal to noise ratios. The signals included can be at arbitrary Doppler shifts and are passed through pre-specified linear time invariant channels. Further, the time of arrival is randomized to assure adequate synchronization testing. To accomplish this type of evaluation requires a digital tape peripheral and noise source.

Measurement of error performance alone with synthetic data is not sufficient to verify the receiver operation or locate the source of observed problems. Instead, a number of "internal" parameters or their statistics should be available for examination. An "internal" parameter is one which would not normally be available to the operator of a military system, but which checkpoints the performance of the program's components. For example, in the present implementation of the M7 system, about 50 internal parameters are analysed statistically about every 20 bursts. To provide a means of printing these and similar results, a high-speed printer or plotter is necessary.

The above techniques and equipment yielded significant improvements in the present M7 system. In the time interval since the system was "completed" in June 1978 to the present, February 1979,

several subtle software errors have been discovered and system improvements made. These changes have improved the error performance of a system which seemed to be operating correctly by a factor of at least two. Although much of the experience gained in the interval need not be repeated, a similar test program and associated equipment is necessary for any future implementation.



PART 3

COMMENTS ON THE MACS
COHERENCE TIME MEASUREMENTS ■

21 MAY 1979




1. Introduction

The Mobile Acoustic Communications Study (MACS) described in References 1, 2, 3 and 4 represents the largest and most geographically diverse collection of experimental results available for the design of underwater acoustic communication systems. Because interpretation of these results will effect the design of Navy systems for many years, a critical discussion of the results is appropriate. This paper addresses the coherence time measurements of the MACS data.* Subsequent sections show that the MACS coherence times are attributable to either inter-platform motion or to time of arrival compensation error; so that the measured values are not those for the actual acoustic medium. The performance of large time-bandwidth (TW) systems under comparable inter-platform motions is then analyzed, with the important result that large TW systems can operate successfully with burst duration longer than the MACS coherence time.

If the MACS coherence times are a result of inter-platform motion rather than the acoustic channel, a simple relation between system center frequency and permissible burst duration is available. Indeed the apparent coherence time at 200 Hz will be 2.5 times larger than that measured by MACS at 500 Hz. This means that large TW systems are applicable even when motional effects are present, provided that the center frequency is chosen low enough. Because a large TW system offers significant

* Since the frequency smear is the transform of the time correlation function, the comments given are applicable to that result as well.



(~ 10dB) performance advantages over the conventional incoherent tonal system, this result deserves consideration.

■ Section 2 reviews the MACS coherence time measurement as presented in Reference 1. The effects of sinusoidal phase modulation on the coherence time is studied in Section 3. Two sources of potential phase modulation: inter-vessel motion and time of arrival estimation error are shown to yield coherence times in the same range as those obtained by MACS. Section 4 analyses the performance of large TW channel measurement systems assuming equivalent phase modulation. Finally, Section 5 provides recommendations for the users of MACS data and suggests a more suitable transmission waveform for future experiments.

2. MACS Coherence Time Measurement ■

■ A summary of the MACS coherence technique described in Reference 1 and in Section 2.1 of References 3 and 4 will be given for convenience.

■ The basic transmission for the MACS data was a Gaussian pulse of duration 8.839 ms between 3dB points having a bandwidth of 99.848 Hz between 3dB points.* Such a pulse has the minimum theoretical TW product of 1.253. Pulses were transmitted at a variety of frequencies from 500 to 3500 Hz, however, this paper considers only the 500 Hz data. These pulses were sent periodically at a rate of about one per second, with a typical interval containing 1000 - 4000 pulses over 15-60 minutes.

* Equivalently: 12.5 ms between 6dB points in time, 141.207 Hz between 6dB points in frequency.

Received pulses were coherently demodulated to a complex baseband waveform and sampled, yielding complex pairs with 4.096 ms between pairs. Note that the sample interval, 4.096 ms, is equivalent to a 720° phase rotation at 500 Hz. The received pulses are windowed to give $S_n(\tau)$, the uncorrected channel response to the n-th pulse.

The collection of pulse responses $S_n(\tau)$, in a given data interval is processed to remove "deterministic" changes in arrival time.

The term "Deterministic" is used here to designate these arrival time changes caused by non parallelism of the actual ships tracks: the time scale of these changes is large compared to the time scales of stochastic fluctuations of the medium, and the separation is effected on the basis of that criterion. (Reference 1, page 9).

Correction is accomplished by calculating the cross-correlation function $C_{n,k}(\beta)$ of the envelope squared of the n-th and k-th pulses. The point of maximum correlation between the first and nth pulse, $\hat{\tau}_n$, is the input to the correction process. Here $\hat{\tau}_n$ is necessarily quantized at the sampling interval 4.096 ms because $C_{n,k}(\beta)$ is an incoherent measurement. Thus the input to the time of arrival correction algorithm is quantized in 720° phase steps.

The measured values of $\hat{\tau}_n$ are fitted with a 4th degree polynomial over an interval of 300 seconds.* A weighting technique is applied at cusps in arrival time occurring between two polynomially-fitted intervals. The points on the resulting smooth curve are designated \hat{t}_n where \hat{t}_n is not quantized. The n-th received pulse $S_n(\tau)$ is shifted in time and phase by t_n to yield $\hat{S}_n(\tau)$, the corrected received pulse response. All subsequent analysis is performed on $\hat{S}_n(\tau)$.

A set of complex points $\hat{H}_n(o)$ representing the complex value of the channel transfer $\hat{H}_n(f)$ of the carrier frequency is computed:

$$\hat{H}_n(f) = \int \hat{S}_n(\tau) e^{-2\pi f\tau} d\tau \quad (2.1)$$

$$\hat{H}_n(o) = \int \hat{S}_n(\tau) d\tau \quad (2.2)$$

where the integration takes place over the previously selected window. The magnitude of $\hat{H}_n(o)$ is shown in the top center plot of the MACS data.** The power spectrum, F_k , of the series $H_n(o)$ ($n = 1 \dots N$) is called the frequency smear and is shown in top right plot of the MACS data.*** The discrete Fourier transform of F_k is called the time correlation function, $R_{HH}(i)$, and is normalized by $R_{HH}(o)$ to yield the normalized correlation function, $\rho_{HH}(i)$.

* References 1 and 2 use a 6-th degree polynomial and presumably the same interval size. Where differences exist between References 1, 2 and References 3, 4 the text describes the most recent data.

** In the old format of References 1 and 2, $\hat{H}_n(o)$ is in the upper right corner of the data (Plot A).

*** Top center (Plot B) in References 1 and 2.

The magnitude of the normalized correlation function is shown in the middle plot of the right hand column in the MACS data.*

The MACS coherence time is defined as the time offset τ^* corresponding to i^* so that

$$|\rho_{HH}(i^*)| = .4 \quad (2.3)$$

In rare instances more than one solution to Equation 2.3 may be available. In such cases, the minimum value of τ^* is taken as the coherence time. In principle, two pulses separated by τ^* suffer a correlation loss of 4dB ($10 \log_{10} .4$) relative to a constant channel.

3. Consequences of Phase Modulation on the MACS Coherence Time

Phase modulation of the MACS data would occur if either the inter-platform distance varied or if the time-of-arrival correction algorithm was unsuccessful. This section first shows the consequences of a general phase modulation under the assumption that the medium itself is time invariant. Then the specific case where the phase modulation is sinusoidal is examined. Realistic examples are given in which coherence times comparable to those of the MACS data are obtained solely due to inter-platform motion or correction errors.

Consider the situation where the actual response function, $H_n(\omega)$, of the acoustic channel is time invariant.

* Bottom center (Plot C) in References 1 and 2.

$$H_n(o) = H(o) \quad (3.1)$$

for all n in the data interval. Let the measured channel be the product of the actual response function with a sequence of complex numbers z_n over the same interval

$$\hat{H}_n(o) = H(o)z_n \quad (3.2)$$

Then the normalized time correlation function, $\rho_{\hat{H}\hat{H}}(i)$ is simply the normalized auto-correlation function of the sequence z_n , $\rho_{zz}(i)$.

$$\rho_{\hat{H}\hat{H}}(i) = \frac{\sum_{j=0}^{N-1} H(o)z_j (H(o)z_{j+i})^*}{\sum_{j=0}^{N-1} |H(o)|^2 |z_j|^2} \quad (3.3)$$

$$= \rho_{zz}(i) \quad (3.4)$$

That is, if the channel is time invariant, but subject to a modulating sequence z_n , the measured coherence time is effectively that of the modulating sequence.

(U) For convenience, the continuous time equivalents of the preceding functions will be considered. Since adequacy of the MACS sampling technique is not in question, no difficulty need arise.

Assume $z(t)$ is a sinusoidally phase modulated waveform:

$$z(t) = e^{jh_p} \cos(2\pi t/T_p) \quad (3.5)$$

where h_p is the maximum phase excursion in radians and T_p is the period of the modulating waveform. Since $z(t)$ is periodic of period T_p , $\rho_{zz}(\tau)$

will also be periodic of period T_p .

The normalized autocorrelation of $z(t)$, $\rho_{zz}(\tau)$ is then given by

$$\rho_{zz}(\tau) = \frac{1}{T_p} \int_{-T_p/2}^{+T_p/2} z(t) z^*(t + \tau) dt \quad (3.6)$$

$$= \frac{1}{T_p} \int_{-T_p/2}^{+T_p/2} e^{j h_p \cos \frac{2\pi t}{T_p}} e^{-j h_p \cos \frac{2\pi(t + \tau)}{T_p}} dt \quad (3.7)$$

From trigonometric identities (Reference 5, No. 4.3.37) the exponent can be simplified.

$$h_p \left[\cos \frac{2\pi t}{T_p} - \cos \frac{2\pi(t + \tau)}{T_p} \right] = -2 h_p \sin \frac{2\pi t}{T_p} \sin \frac{\pi \tau}{T_p} \quad (3.8)$$

Then

$$\rho_{zz}(\tau) = \frac{1}{T_p} \int_{-T_p/2}^{+T_p/2} e^{-j(2 h_p \sin \frac{\pi \tau}{T_p}) \sin \frac{2\pi t}{T_p}} dt \quad (3.9)$$

$$= J_0 \left(2 h_p \sin \frac{\pi \tau}{T_p} \right) \quad (3.10)$$

where $J_0(u)$ is the zero-th order Bessel function of the first kind and the transition from Equation 3.9 to Equation 3.10 is by Lommel's formula (Reference 5, No. 9.1.21). $J_0(u)$ is a decaying, oscillatory function of u as shown in Reference 5, Figure 9.1. Thus for a simple model of the phase modulation, an analytic result for the time correlation function is obtained.

The MACS coherence time, τ^* , then satisfies

$$.4 = J_0(2h_p \sin \pi \tau^*/T_p) \quad (3.11)$$

From linear interpolation of the Table 9.1 of Reference 5,

$$2 h_p \sin \pi \tau^*/T_p = 1.696 \quad (3.12)$$

for Equation 3.11 to be valid, that is $h_p \geq .848$. If $h_p < .848$, then $\rho_{HH}(\tau)$ never goes as low as .4 and consequently no MACS coherence time can be defined. This result indicates the model is applicable only for maximum phase excursions greater than .848 radians (48.6°).

If $h_p \geq .848$ radians, Equation 3.12 can be solved to yield the MACS coherence time τ^* :

$$\tau^* = \frac{T_p}{\pi} \arcsin\left(\frac{.848}{h_p}\right) \quad (h_p \geq .848) \quad (3.13)$$

No small angle approximations have been made up to this point. If τ^*/T_p is less than .1, then the small angle approximation $\sin u = u$ provides a more convenient form of Equation 3.13.

$$\tau^* \approx .270 T_p/h_p \quad \begin{matrix} (h_p \geq .848) \\ (\tau^*/T_p < .1) \end{matrix} \quad (3.14)$$

The second condition of Equation 3.14 will be satisfied if $h_p \geq 2.70$; which also satisfies the first condition. Thus the sinusoidal phase modulation model gives τ^* explicitly in terms of the modulation parameters h_p , T_p provided h_p is greater than 2.70 radians (155 degrees).

(C) Two potential sources of phase modulation must be considered in interpreting the MACS data. First, the intervessel distance might be

modulated by the helmsman or currents. Second, the time of arrival compensation algorithm may introduce significant phase errors at relatively short periods. The MACS data contained in References 1 through 4 does not discuss of the sensitivity of the coherence time measurements to these effects, nor does the presented data contain sufficient results to resolve these issues. The paragraphs below apply the trivial model given above to each situation and show that under realistic assumptions, the MACS coherence times could be determined by either effect. Obviously, other modulating waveforms, such as random noise, could be studied, however the discussion here will be instructive by itself.

Consider the situation in which one of the platforms follows a sinusoidal track about a specified heading and the other platform maintains its heading exactly. The inter-platform distance, $y(t)$, will then be sinusoidally modulated. Let

$$y(t) = \frac{a_{\max}}{2\pi} v T_p \cos 2\pi t/T_p + d \quad (3.15)$$

where a_{\max} is the maximum heading error in radians, v is the vessel speed and T_p is the period of the vessel motion. The maximum heading error, a_{\max} , is the largest angle between the actual and intended track, when the small angle assumption $\tan \theta = \theta$ is made. The maximum phase excursion, h_p , is then

$$h_p = a_{\max} v T_p f_0/c \quad (3.16)$$

where f_o is the center frequency and c is the speed of sound.

The MACS coherence time, τ^* , can be calculated from Equation 3.14

$$\tau^* = \frac{.270 c}{a_{\max} v f_o} \quad (3.17)$$

provided that $h_p \geq 2.70$ and a_{\max} is small ($a_{\max} < \pi/10$)*. For the 5 kt vessel speed and 500 Hz center frequency of the MACS data:

$$h_p = .015 a_{\max}^o \cdot T_p \quad (3.18)$$

where a_{\max}^o is the maximum heading error in degrees. If $\frac{a_{\max}^o \cdot T_p}{\pi} \geq 180$, then $h_p > 2.70$ and Equation 3.17 gives a coherence time τ^* of

$$\tau^* = \frac{18.3}{a_{\max}^o} \quad (3.19)$$

For a maximum heading error of two degrees and a motional period greater than 180 seconds Equation 3.19 yields a coherence time of 9.2 seconds, which is within the range of the MACS results. Heading errors of this magnitude are apparently not unusual.

The second potential source of phase modulation of the MACS data is the time of arrival compensation. Inspection of the "Reception Time" plots included in References 2 through 4 indicates substantial variance in the arrival time relative to the quantization step of 4.096 ms (720°). Because the scaling of both axes of these plots is automatically selected, this variance is sometimes difficult to judge.

Dr. Freese has indicated that the quantity labeled "Residual" in the lower center of these plots (Reference 4 only) is the root mean

* For convenience take $c = 5000$ ft/sec, 1 kt = 1.689 ft/sec.

squared difference between the measured arrival time and the arrival time estimated by the curve-fitting algorithm in milliseconds. Over the 84 time arrival plots of Reference 4, this quantity has a mean value of 6.3 milliseconds with a minimum of .95 ms (Blake 5/5) and a maximum of 22.5 ms (Shelf North 50/15). Translated into phase at 500 Hz, the "residual" has a mean of 3.08 cycles, a minimum of 167°, and a maximum of 11 cycles. Moreover, 53% of the plots have "residuals" greater than 720°, only 17% have residuals less than 360°. Consequently the effects of the time of arrival compensation algorithm are worth considering.

The difference between the measured and fitted arrival time is not sinusoidal, as can be seen from any of the "Reception Time" plots. If the actual arrival time is smoothly varying, however, the difference between the actual and fitted arrival times could appear sinusoidal. Under these conditions the model given earlier provides insight. Let E be the error between the actual and fitted arrival times. Then h_p is given by

$$h_p = 2\pi f_o E \quad (3.20)$$

and

$$\tau^* = .043 \frac{T_p}{E \cdot f_o} \quad (3.21)$$

where $h_p \geq 2.70$ must hold to apply Equation 3.21.

At 500 Hz, Equation 3.20 becomes

$$h_p = 3.14 E_{ms} \quad (3.22)$$

where E_{ms} is the error expressed in milliseconds. The condition for Equation 3.21 will be met if $E_{ms} > .86$ ms. Equation 3.21 is then

$$\tau^* = .086 \frac{T_p}{E_{ms}} \quad (3.23)$$

Assume that T_p is of the order of the interval size (300 seconds) divided by the degree of the fitting polynomial (4), that is 75 seconds. Then a one millisecond error between the actual and fitted arrival times yields a coherence time of 6.5 seconds. This is also within the range of the MACS coherence times.

The preceding discussion clearly does not prove that the MACS coherence time measurements result from either platform motion or time of arrival compensation errors. It does show, however, that these effects must be understood to properly interpret the MACS data.

4. Phase modulation of large TW systems

If inter-platform motion was the dominant factor in the MACS coherence time measurement, the same phase modulation will be present in large TW systems. The effect of this modulation on system performance will depend on the system center frequency, f_o , the signal duration, T_B , and the specific motional waveform. In this section, the performance of a large TW system under the sinusoidal phase modulation of the preceding section will be examined. The results of this examination show that the MACS coherence time τ^* is not the limiting value for T_B and that large TW systems have considerable resistance to such phase modulation. Further, the apparent differences in coherence

times measured by the MACS project (References 1 through 4) and those of the ACS project (References 6 and 7) will be explained.

For convenience, the M7 pseudo noise burst communications system and specifically its synchronization/channel response measurement algorithm will be considered. The analysis will be equally applicable to the periodic pseudorandom sequence techniques which have found wide application by ONR transmission measurement investigators.

Let $a(t)$, $|a(t)| = 1$, be the transmitted pseudonoise burst waveform of duration T_B in the probe component of the M7 system. In the system bandwidth, $a(t)$ is white

$$R_{aa}(\tau) \sim T_B \delta(\tau) \quad (4.1)$$

For pseudonoise systems with TW products greater than 1000, Equation 4.1 is an excellent approximation.

Assume the received signal, $y(t)$, is the sinusoidally phase modulated response of a linear, time invariant channel, $c(t)$, to the transmitted waveform, $a(t)$.

$$y(t) = e^{jh_p} \cos \frac{2\pi(t + t_0)}{T_p} \int a(u) c(t - u) du \quad (4.2)$$

Here h_p is the maximum phase excursion in radians, T_p is the motional period and t_0 indicates the starting time of the burst relative to the motional period. Although $y(t)$ will have a longer time duration than $a(t)$ due to the channel, its duration will still be of the order of T_B .

Before proceeding further, observe that if the burst duration T_B is small relative to the motional period, T_p , the phase modulation appears as a simple frequency shift. Assume $T_B < T_p/10$, then the small angle approximations $\sin u = u$, $\cos u = 1$ applied to Equation 4.2 yield

$$y(t) \sim e^{-jh_p \sin \frac{2\pi t_0}{T_p} - \frac{2\pi t}{T_p} + h_p \cos \frac{2\pi t_0}{T_p}} \int a(u)c(t-u)du \quad (4.3)$$

$T_B < T_p/10$

The first term in the exponent represents a pure frequency shift, the second represents a constant phase shift. A large TW system, such as the M7 communication system, includes automatic Doppler removal algorithms and would compensate for the motional effects under the assumption. The constant phase shift term would have no effect at all. Consequently, motional effects are important for large TW systems only when the burst duration T_B is near the motional period T_p .

The estimated channel response, $\hat{c}(t)$, is obtained by cross-correlating $y(t)$ with a replica of the transmitted signal, $a(t)$

$$c(t) = \int a^*(v)y(v+t)dv \quad (4.4)$$

$$= \int a^*(v) e^{\frac{jh_p \cos 2\pi(t_0 + t + u)}{T_p}} a(u)c(v+t-u)du dv \quad (4.5)$$

Let $v - u = w$, then

$$\hat{c}(t) = \int c(t+w) R_{aa}(-w, h_p, t_0, +t, T_p) dw \quad (4.6)$$

where

$$R_{aa}(-w, h_p, t', T_p) = \int e^{jh_p \cos \frac{2\pi(t'+u)}{T_p}} a(u)a^*(u+w)du \quad (4.7)$$

If no interplatform motion is present, then $h_p = 0$ and Equation 4.7 becomes

$$R_{aa}(-w, 0, t', T_p) = \int a(u)a^*(u+w)du \quad (4.8)$$

$$= R_{aa}(w) \quad (4.9)$$

$$\sim T_B \delta(w) \quad (4.10)$$

Then

$$\hat{c}(t) \sim T_B c(t) \quad (4.11)$$

by inserting Equation 4.10 into Equation 4.6. Thus, if no interplatform motion is present, the crosscorrelation procedure of Equation 4.4 gives the channel impulse response $c(t)$ multiplied by a processing gain T_B .

When h_p is non-zero, $R_{aa}(w, h_p, t', T_p)$ may be changed in two ways. First, it may no longer be impulsive as required in Equation 4.1. Second, its peak correlation value may be reduced to less than T_B . The first change would have the most drastic consequences, but will not occur unless the phase modulation is correlated with the pseudonoise transmission. That is,

$$R_{aa}(w, h_p, t', T_p) \sim 0 \quad |w| > 0 \quad (4.12)$$

Consequently, the following approximation for $R_{aa}(w, h_p, t', T_p)$ is appropriate:

$$R_{aa}(w, h_p, t', T_p) = z'(h_p, t', T_p) \delta(w) \quad (4.13)$$

where

$$z'(h_p, t', T_p) = \int_a e^{jh_p \cos \frac{2\pi(t' + u)}{T_p}} du \quad (4.14)$$

since $|a(t)| = 1$. The range of integration of Equation 4.14 is over the T_B long interval where $a(t)$ is non zero. The reduction in $z(h_p, t', T_p)$ relative to T_B as a function of the motional parameters h_p , t' and T_p is important and will be discussed below.

■ The following definition will be convenient:

$$z(h, a, b) = \frac{1}{2\pi b} \int_{2\pi a}^{2\pi a + 2\pi b} e^{j2\pi h \cos u} du \quad (4.15)$$

The function $z(h, a, b)$ has the following properties:

$$z(h, a, b) \sim 1 \quad \text{small } h, \text{ all } a \text{ or small } b, \text{ all } a \quad (4.16)$$

$$z(h, a + .5, b) = z(h, a, b) \quad (4.17)$$

$$z(h, a, .5n) = J_0(2\pi h) \quad \text{all } a \text{ and integer } n \quad (4.18)$$

Appendix A gives tables of $z(h, a, b)$ which have been verified via Equation 4.18 to be correct to 3 significant figures. Note that $z(h, a, b)$ is in general complex.

Equation 4.13 can be rewritten in terms of $z(h, a, b)$ as follows:

$$R_{aa}(w, h_p, t', T_p) = z(h, a, b) \cdot T_B \delta(w) \quad (4.19)$$

where

$$h = h_p/2\pi \quad (4.20)$$

$$a = t'/T_p \quad (4.21)$$

$$b = T_B/T_p \quad (4.22)$$

Thus $z(h, a, b)$ can be interpreted as the loss factor, relative to T_B , for a phase modulation parameterized by h , a and b . Here h represents the maximum phase excursion in cycles and equals the maximum spatial excursion in wavelengths. The parameter a gives the initial angle in cycles and b is the burst duration normalized by the national period.

Define the loss due to motion, $L(h, a, b)$ as follows:

$$L(h, a, b) = -10 \log_{10} |z(h, a, b)|^2 \quad (4.23)$$

This is the loss in signal to noise ratio experienced by the cross-correlation process expressed in decibels. In an actual system, the initial angle a would not be known, hence the following loss, L_{\max} , is of more value in system design:

$$L_{\max}(h, b) = \max_{0 \leq a < .5} L(h, a, b) \quad (4.24)$$

That is, L_{\max} is the maximum loss over all initial angles for a given h and b . Figure 4.1 depicts lines of constant L_{\max} over the h, b plane.

For small h or for small b L_{\max} is small as expected.

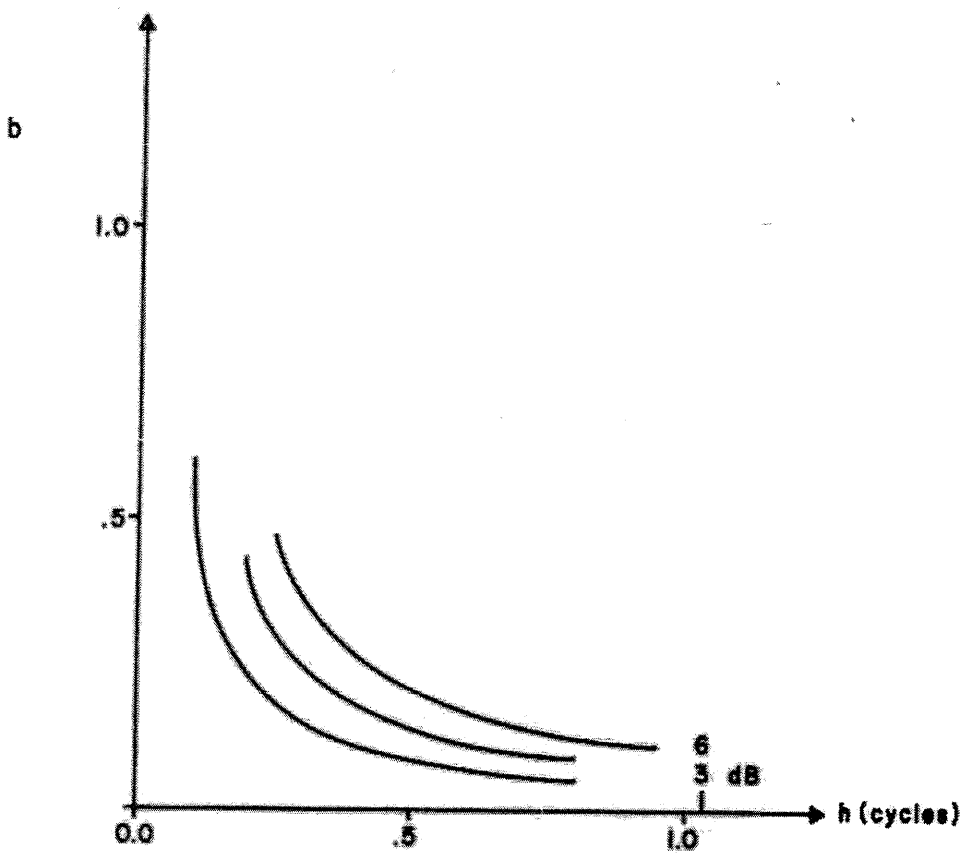


Figure 4.1: Lines of Constant L_{MAX}

(This figure [redacted])

The preceding analysis is immediately applicable to the synchronization and channel measurement processes in the M7 communication system. The effect of interplatform motion on the information demodulation process deserves further study, but appears to be small compared to the former. The loss experienced by the M7 synchronization and channel measurement processes will be equal to $L(h, a, b)$, but the performance measure $L_{\max}(h, b)$ is more convenient.

From Figure 4.1, curves of constant $L_{\max}(h, b)$ are seen to be nearly hyperbolic, that is,

$$h \cdot b \approx K_L \quad (4.25)$$

for a specified loss $L_{\max}(h, b)$ in decibels. This approximation fails for small h , as a specified $L_{\max}(h, b)$ may not occur for any b below a given value of h , designated h_L^* . That is, given a loss L ,

$$L_{\max}(h, b) < L \quad \text{for all } b \quad (4.26)$$

$$\text{if } h < h_L^*$$

Table 4.1 gives K_L and h_L^* for $L = 1, 3, 6$ and 10 dB. Further, for $b < .1$ the system's automatic Doppler removal algorithm will remove the motional effects as indicated in Equation 4.3. Subject to these constraints, Equation 4.25 provides insight into the M7 system performance.

Table 4.1. Limiting values of h

(This Table

Loss L, dB	K_L	h_L^*
1.	.044	.05
3.	.073	.15
6.	.109	.20
10.		.25

From Equations 3.16 and 4.20,

$$h = \frac{a_{\max}}{2\pi c} v T_p f_o \quad (4.27)$$

then Equation 4.25 becomes

$$\frac{a_{\max} v f_o T_B}{2\pi c} = K_L \quad (4.28)$$

where b was found from Equation 4.22. This gives a convenient relation between the platform motion indicated by a_{\max} and v and the burst characteristics T_B and f_o . For example, consider the 5Kt vessel speed and 2° heading error assumed in the preceding section. In order for the M7 system to have less than a 3 dB loss, the following relation from Equation 4.28 must hold:

$$f_o \cdot T_B \leq 7775 \quad (4.29)$$

At the current M7 center frequency of 204.8 Hz, this requires that $T_B \leq 40$ sec. At the 500 Hz center frequency of the MACS data, $T_B \leq 15.5$ sec. Note carefully that Equation 4.28 is valid only where the loss

curves are hyperbolic; that is, $h > h_L^*$, $b > .1$.

Equation 4.28 can be exploited further making use of Equation 3.17 to relate the MACS coherence time τ^* to a_{\max} .

$$\frac{.270}{2\pi} \frac{T_B}{\tau^*} = K_L \quad (4.30)$$

This can be rewritten to yield

$$T_B = 1.7 \tau^* \quad (4.31)$$

Here the value of K_L corresponding to a 3 dB loss has been taken from Table 4.1. Equation 4.31 holds only if the conditions of Equation 3.17 are valid, $h_p \geq 2.70$ ($h > .430$), a_{\max} small. The conditions of Equation 4.25, $b > .1$, $h > h_{3dB}^* = .15$, must also hold. The important result is that the burst duration corresponding to a 3dB loss, T_B by Equation 4.31, is larger than the MACS coherence time τ^* by 70%, under the sinusoidal phase modulation model. Consequently, the MACS coherence time by itself does not determine the time duration for a large TW system, even under an elementary motional model.

The preceding analysis is also helpful in understanding the coherence times measured by the ACS project as described in References 6 and 7. These results indicate the medium decorrelates approximately 3 dB in 210 seconds, but the measurement technique is significantly different from the MACS project.

In the ACS technique, channel impulse response measurements $\hat{c}_i(t)$ are computed from several disjoint input signal vectors $x(t + iT_B)$, $0 \leq t < T_B$, $i = 0, 1, \dots$, using a large TW product wave-

form. The normalized crosscorrelation function $\rho_i(\tau)$ is computed for each interval $i > 0$.

$$\rho_i(\tau) = \frac{1}{\sqrt{\int |\hat{c}_0(t)|^2 dt \int |\hat{c}_i(t)|^2 dt}} \int \hat{c}_0^*(t) \hat{c}_i(t + \tau) dt \quad (4.32)$$

In general $\rho_i(\tau)$ is complex. Then the following correlation coefficient is found.

$$\rho_i = \max_{\tau} |\rho_i(\tau)| \quad (4.33)$$

The purpose of the maximization is to eliminate the effects of time of arrival changes between the 0-th and i-th interval. Plots of ρ_i versus the time offset, iT_B , are generated and the coherence time is found by interpolation of the resulting plots. The processing also employs a Doppler removal algorithm.

Because motional effects reduce the size of $\hat{c}_i(t)$ by $z(h_i, a_i, b_i)$ and do not change its shape, the normalization indicated in Equation 4.32 eliminates the motional effects completely. Indeed if $c_i'(t)$ is the actual channel response in the ith interval then

$$\rho_i(\tau) = \rho_{c_0' c_i'}(\tau) \quad (4.34)$$

that is, $\rho_i(\tau)$ is the normalized cross correlation for the actual channel. The only consequence of the interplatform motion will be in the reduction of the signal to noise ratio in the estimated channel response $\hat{c}_i(t)$. All ACS measurements included algorithms which calculated $\rho_i(\tau)$ only if both

$\hat{c}_0(\tau)$ and $\hat{c}_1(\tau)$ had signal to noise ratios greater than 10 dB. Thus the ACS coherence time measurements are insensitive to motional effects.*

5. Conclusions and Recommendations

The MACS coherence time measurement is sensitive to both interplatform motion and errors in arrival time compensation. Under the assumption of a sinusoidal variation in interplatform distance with a maximum heading error of 2° on one platform the coherence time is limited to 9.2 seconds even if the medium is actually time invariant. Similarly a 1 millisecond error in arrival time with a period of 75 seconds yields a maximum coherence time of only 6.5 seconds. Since both of these results are in the same range as those of the MACS data, the MACS coherence times may be attributable more to platform motion or the time of arrival compensation technique than to actual changes in the acoustic medium.

If the MACS coherence times are highly influenced by interplatform motion, these motional effects must be understood in detail to design improved communication systems. Ideally, continuous and coherent data on interplatform motion should be obtained. This data should be capable of indicating fractional wavelength variations in distance and could be obtained by coherent demodulation of a tonal component in the transmission. Unfortunately, the MACS data lacks such a component and the

* All ACS experiments had transmissions with substantial carrier lines. Consequently, information on interplatform motion could be obtained by analysis of carrier phase.

[REDACTED]

necessary information on vessel motion may not be obtainable from the existing data.

■ Performance of large TW product systems, such as the M7 communication system, depends on the specifics of the interplatform motion. For the sinusoidal distance variation considered here, the large TW systems are less sensitive to motional effects than the MACS measurement technique. For example, under the same conditions a large TW system can use a burst duration 70% larger than the MACS coherence time and achieve only a 3 dB loss. If the motional period is large relative to the burst duration, the losses are even smaller.

■ The following recommendations are offered based on the above results. First, recipients of References 1 through 4 should be advised that the coherence times reported may be due to platform motion or time of arrival compensation error. Such a notice is needed because the MACS documents do not consider these effects and represent the coherence time as a measurement of the medium itself. Second, the MACS data should be reprocessed to extract better information on interplatform motion, if that is possible. Third, future MACS experiments should include a tonal component adequate to resolve interplatform motions.

[REDACTED]

[REDACTED]

REFERENCES

1. Freese, H. A., Description of Processing of MACS Sea Trip Data, Naval Underwater Systems Center, New London, Connecticut, 06320, TM No. 771198, 23 Sept. 1977.
 2. Ellinthorpe, A. W. and H. A. Freese, MACS Transmission Data: Results from the June 1976 Sea Trip (U), Naval Underwater Systems Center, New London, Connecticut 06320, TM No. 771061 (two parts), 23 Sept. 1977. (CONF).
 3. Ellinthorpe, A. W. and H. A. Freese, MACS Transmission Data: Results from the November 1976 Sea Trip (U), Naval Underwater Systems Center, New London, Connecticut, 06320, TM No. 781050 (two parts), 7 March 1978. (CONF).
 4. Ellinthorpe, A. W., H. A. Freese and G. J. O'Brien, MACS Transmission Data: Results of the January 1977 Sea Trip (U). Naval Underwater Systems Center, New London, Connecticut, 06320, TM No. 781194 (three parts), 13 Oct. 1978. (CONF).
 5. Abramowitz, M. and I. A. Stegun, Handbook of Mathematical Functions, National Bureau of Standards, Applied Mathematics Series, No. 55, U.S. Government Printing Office, Washington, D.C. 20402, June 1964.
 6. Kimball, C. V., Acoustic Communication Studies (U), Journal of Defense Research, Series B: Tactical Warfare, Vol. 7B, No. 2, Advanced Research Projects Agency, Washington, D.C., Summer 1975. (CONF).
 7. Kimball, C. V., Personal Communication to Dr. A. O. Sykes, Office of Naval Research, Code 222, dated 27 May 1976.
- [REDACTED]



APPENDIX A

TABLE OF $Z(h, a, b)$ ■

$\eta = .1, (.1), 1.$

$a = \text{worst } a \text{ for } a = 0., (.05), .45$

$b = .05, (.05), 1$

THIS TABLE IS ■.



DELTA = 0.010000

H, A, AND B IN TABLE BELOW ARE IN FRACTIONS OF A CYCLE. H = 0.63 RADIAN.
FIRST LOSS ENTRY IS MAXIMUM LOSS, SECOND IS AVERAGE LOSS OVER A.
A = 0, 1 * 0.050, 0.450

H	AMAX	B	ZR	ZI	MAG Z	ANG Z	/Z/##2	LOSS(DB)	
0.10	0.250	0.050	0.804	-0.572	0.987	-35.4	0.974	-0.1	-0.1
0.10	0.200	0.100	0.817	-0.581	1.003	-35.4	1.005	-0.0	-0.0
0.10	0.200	0.150	0.824	-0.561	0.997	-34.3	0.994	-0.1	-0.1
0.10	0.150	0.200	0.848	-0.530	1.000	-32.0	1.000	-0.2	-0.1
0.10	0.150	0.250	0.867	-0.479	0.991	-28.9	0.982	-0.3	-0.2
0.10	0.100	0.300	0.886	-0.416	0.979	-25.1	0.958	-0.5	-0.2
0.10	0.050	0.350	0.904	-0.342	0.967	-20.7	0.935	-0.5	-0.3
0.10	0.050	0.400	0.910	-0.265	0.947	-16.2	0.897	-0.7	-0.4
0.10	0.000	0.450	0.911	-0.187	0.930	-11.6	0.864	-0.8	-0.4
0.10	0.000	0.500	0.903	-0.116	0.911	-7.3	0.829	-0.9	-0.5
0.10	0.450	0.550	0.897	-0.052	0.898	-3.3	0.807	-0.9	-0.6
0.10	0.450	0.600	0.889	0.000	0.889	0.0	0.790	-1.0	-0.7
0.10	0.450	0.650	0.885	0.040	0.886	2.6	0.785	-1.1	-0.7
0.10	0.400	0.700	0.887	0.068	0.890	4.4	0.792	-1.1	-0.8
0.10	0.400	0.750	0.891	0.082	0.895	5.3	0.801	-1.1	-0.8
0.10	0.350	0.800	0.899	0.083	0.903	5.3	0.815	-1.0	-0.8
0.10	0.350	0.850	0.904	0.073	0.907	4.6	0.822	-1.0	-0.9
0.10	0.300	0.900	0.906	0.053	0.908	3.4	0.824	-1.0	-0.9
0.10	0.250	0.950	0.907	0.028	0.907	1.8	0.823	-0.9	-0.9
0.10	0.250	1.000	0.903	0.000	0.903	0.0	0.816	-0.9	-0.9

TABLE OF Z(H,A,B) - 08 MAY 79

DELTA = 0.010000

H, A, AND B IN TABLE BELOW ARE IN FRACTIONS OF A CYCLE. H = 1.26 RADIAN.
FIRST LOSS ENTRY IS MAXIMUM LOSS, SECOND IS AVERAGE LOSS OVER A.
A = 0, 1 * 0.050, 0.450

H	AMAX	B	ZR	ZI	MAG Z	ANG Z	/Z/##2	LOSS(DB)	
0.20	0.250	0.050	0.324	-0.932	0.987	-70.8	0.973	-0.2	-0.1
0.20	0.200	0.100	0.329	-0.947	1.003	-70.8	1.005	-0.2	-0.1
0.20	0.200	0.150	0.364	-0.926	0.995	-68.5	0.990	-0.5	-0.3
0.20	0.150	0.200	0.434	-0.891	0.991	-64.0	0.982	-0.8	-0.4
0.20	0.150	0.250	0.513	-0.818	0.966	-57.9	0.932	-1.3	-0.7
0.20	0.100	0.300	0.588	-0.714	0.925	-50.6	0.855	-1.8	-0.9
0.20	0.050	0.350	0.645	-0.584	0.871	-42.2	0.758	-2.2	-1.2
0.20	0.050	0.400	0.668	-0.445	0.803	-33.7	0.645	-2.8	-1.5
0.20	0.000	0.450	0.666	-0.309	0.734	-24.9	0.538	-3.3	-1.9
0.20	0.000	0.500	0.642	-0.189	0.670	-16.4	0.448	-3.8	-2.2
0.20	0.450	0.550	0.614	-0.085	0.620	-7.8	0.385	-4.2	-2.5
0.20	0.450	0.600	0.590	0.000	0.590	0.0	0.348	-4.6	-2.8
0.20	0.450	0.650	0.578	0.068	0.532	6.7	0.339	-4.7	-3.0
0.20	0.400	0.700	0.583	0.119	0.595	11.6	0.354	-4.9	-3.3
0.20	0.400	0.750	0.599	0.147	0.617	13.8	0.380	-4.8	-3.5
0.20	0.350	0.800	0.624	0.159	0.641	13.5	0.411	-4.8	-3.6
0.20	0.350	0.850	0.643	0.130	0.656	11.4	0.431	-4.5	-3.7
0.20	0.300	0.900	0.654	0.093	0.660	8.1	0.436	-4.4	-3.8
0.20	0.250	0.950	0.653	0.047	0.655	4.1	0.429	-4.1	-3.8
0.20	0.250	1.000	0.642	0.000	0.642	0.0	0.413	-3.8	-3.8

DELTA = 0.010000

H, A, AND B IN TABLE BELOW ARE IN FRACTIONS OF A CYCLE. H = 1.88 RADIAN. FIRST LOSS ENTRY IS MAXIMUM LOSS, SECOND IS AVERAGE LOSS OVER A. A = 0. , I * 0.050 , 0.450

H	AMAX	B	ZR	ZI	MAG Z	ANG Z	/Z/**2	LOSS(DB)	
0.30	0.250	0.050	-0.275	-0.947	0.986	-106.2	0.973	-0.2	-0.2
0.30	0.200	0.100	-0.280	-0.962	1.002	-106.2	1.005	-0.5	-0.2
0.30	0.200	0.150	-0.220	-0.968	0.993	-102.8	0.985	-1.1	-0.6
0.30	0.150	0.200	-0.104	-0.971	0.977	-96.1	0.954	-2.0	-1.0
0.30	0.150	0.250	0.046	-0.924	0.925	-87.2	0.855	-3.0	-1.5
0.30	0.100	0.300	0.193	-0.817	0.840	-76.7	0.705	-4.3	-2.2
0.30	0.050	0.350	0.303	-0.660	0.726	-65.3	0.527	-5.5	-2.9
0.30	0.050	0.400	0.345	-0.485	0.596	-54.6	0.355	-7.9	-3.7
0.30	0.000	0.450	0.334	-0.323	0.464	-44.0	0.216	-8.7	-4.6
0.30	0.000	0.500	0.291	-0.192	0.349	-33.5	0.122	-10.7	-5.5
0.30	0.450	0.550	0.238	-0.036	0.253	-19.9	0.064	-11.9	-6.3
0.30	0.450	0.600	0.196	0.000	0.196	0.0	0.038	-14.2	-7.2
0.30	0.450	0.650	0.173	0.075	0.188	29.6	0.035	-14.5	-8.0
0.30	0.400	0.700	0.178	0.140	0.226	38.2	0.051	-16.3	-8.7
0.30	0.400	0.750	0.209	0.183	0.275	40.7	0.076	-15.3	-9.3
0.30	0.350	0.800	0.256	0.187	0.316	38.1	0.100	-15.7	-9.8
0.30	0.350	0.850	0.295	0.159	0.335	28.3	0.112	-14.1	-10.2
0.30	0.300	0.900	0.315	0.189	0.333	19.2	0.111	-13.3	-10.5
0.30	0.250	0.950	0.311	0.052	0.316	9.5	0.100	-11.8	-10.7
0.30	0.250	1.000	0.291	0.000	0.291	0.1	0.084	-10.7	-10.7

TABLE OF Z(H,A,B) - 08 MAY 79

DELTA = 0.010000

H, A, AND B IN TABLE BELOW ARE IN FRACTIONS OF A CYCLE. H = 2.51 RADIAN. FIRST LOSS ENTRY IS MAXIMUM LOSS, SECOND IS AVERAGE LOSS OVER A. A = 0. , I * 0.050 , 0.450

H	AMAX	B	ZR	ZI	MAG Z	ANG Z	/Z/**2	LOSS(DB)	
0.40	0.250	0.050	-0.773	-0.612	0.986	-141.6	0.972	-0.3	-0.2
0.40	0.200	0.100	-0.786	-0.622	1.002	-141.6	1.004	-0.9	-0.4
0.40	0.200	0.150	-0.724	-0.673	0.989	-137.1	0.978	-2.0	-1.0
0.40	0.150	0.200	-0.593	-0.751	0.957	-128.3	0.916	-3.6	-1.8
0.40	0.150	0.250	-0.392	-0.776	0.870	-116.8	0.756	-5.6	-2.9
0.40	0.100	0.300	-0.179	-0.709	0.731	-104.2	0.535	-8.5	-4.2
0.40	0.050	0.350	-0.022	-0.554	0.555	-92.3	0.308	-11.8	-5.8
0.40	0.050	0.400	0.032	-0.376	0.377	-85.2	0.142	-17.8	-7.7
0.40	0.000	0.450	0.006	-0.224	0.224	-88.4	0.050	-22.8	-9.8
0.40	0.000	0.500	-0.055	-0.124	0.136	-113.7	0.018	-25.3	-10.5
0.40	0.450	0.550	-0.122	-0.056	0.134	-155.5	0.018	-17.4	-10.0
0.40	0.450	0.600	-0.176	0.000	0.176	180.0	0.031	-15.1	-9.9
0.40	0.450	0.650	-0.209	0.060	0.218	164.1	0.047	-13.2	-10.1
0.40	0.400	0.700	-0.209	0.126	0.244	148.9	0.059	-12.5	-10.8
0.40	0.450	0.750	-0.168	0.176	0.243	133.6	0.059	-12.3	-11.8
0.40	0.150	0.800	-0.100	0.182	0.213	117.3	0.045	-13.9	-13.4
0.40	0.100	0.850	-0.042	0.156	0.161	105.0	0.026	-17.4	-15.7
0.40	0.050	0.900	-0.016	0.098	0.100	99.5	0.010	-22.6	-18.1
0.40	0.000	0.950	-0.026	0.041	0.049	122.1	0.002	-23.7	-23.7
0.40	0.000	1.000	-0.055	0.000	0.055	179.7	0.003	-25.3	-25.2

TABLE OF Z(H,A,B) - 08 MAY 79



DELTA = 0.010000

H, A, AND B IN TABLE BELOW ARE IN FRACTIONS OF A CYCLE. H = 3.14 RADIANS.
 FIRST LOSS ENTRY IS MAXIMUM LOSS, SECOND IS AVERAGE LOSS OVER A.
 A = 0. , I * 0.050 , 0.450

H	AMAX	B	ZR	ZI	MAG Z	ANG Z	/Z/**2	LOSS(DB)	
0.50	0.250	0.050	-0.984	-0.051	0.986	-177.0	0.972	-0.5	-0.3
0.50	0.200	0.100	-1.000	-0.052	1.002	-177.0	1.003	-1.4	-0.7
0.50	0.200	0.150	-0.973	-0.147	0.984	-171.4	0.968	-3.2	-1.6
0.50	0.150	0.200	-0.879	-0.310	0.932	-160.5	0.868	-6.1	-3.0
0.50	0.150	0.250	-0.674	-0.437	0.803	-147.0	0.645	-9.9	-4.8
0.50	0.100	0.300	-0.422	-0.440	0.610	-133.6	0.372	-17.2	-7.4
0.50	0.050	0.350	-0.238	-0.312	0.393	-127.4	0.154	-25.7	-10.7
0.50	0.050	0.400	-0.190	-0.155	0.246	-140.8	0.060	-17.7	-9.8
0.50	0.000	0.450	-0.235	-0.049	0.241	-168.2	0.058	-12.8	-8.8
0.50	0.000	0.500	-0.304	-0.010	0.304	-178.1	0.092	-10.3	-8.3
0.50	0.350	0.550	-0.369	-0.005	0.369	-179.3	0.136	-8.9	-8.2
0.50	0.250	0.600	-0.420	0.000	0.420	180.0	0.176	-8.9	-8.3
0.50	0.200	0.650	-0.458	0.026	0.459	176.8	0.211	-11.3	-8.8
0.50	0.150	0.700	-0.468	0.081	0.475	170.2	0.226	-14.7	-9.5
0.50	0.150	0.750	-0.428	0.139	0.449	162.0	0.202	-15.4	-10.2
0.50	0.100	0.800	-0.347	0.159	0.381	155.4	0.145	-16.6	-10.5
0.50	0.100	0.850	-0.277	0.129	0.303	156.1	0.092	-14.5	-10.5
0.50	0.050	0.900	-0.254	0.064	0.261	165.9	0.068	-12.9	-10.4
0.50	0.000	0.950	-0.271	0.018	0.272	176.2	0.074	-11.4	-10.4
0.50	0.000	1.000	-0.304	0.000	0.304	180.0	0.092	-10.3	-10.3

TABLE OF Z(H,A,B) - 08 MAY 79

DELTA = 0.010000

H, A, AND B IN TABLE BELOW ARE IN FRACTIONS OF A CYCLE. H = 3.77 RADIANS.
 FIRST LOSS ENTRY IS MAXIMUM LOSS, SECOND IS AVERAGE LOSS OVER A.
 A = 0. , I * 0.050 , 0.450

H	AMAX	B	ZR	ZI	MAG Z	ANG Z	/Z/**2	LOSS(DB)	
0.60	0.250	0.050	-0.832	0.528	0.985	147.6	0.971	-0.6	-0.4
0.60	0.200	0.100	-0.845	0.537	1.001	147.6	1.002	-2.1	-1.0
0.60	0.200	0.150	-0.882	0.424	0.978	154.3	0.957	-4.8	-2.4
0.60	0.150	0.200	-0.879	0.202	0.902	167.0	0.814	-9.7	-4.6
0.60	0.150	0.250	-0.728	-0.025	0.728	-178.0	0.530	-17.8	-8.0
0.60	0.100	0.300	-0.478	-0.109	0.490	-167.2	0.240	-23.9	-10.8
0.60	0.000	0.350	-0.295	-0.018	0.296	-176.5	0.087	-14.1	-9.2
0.60	0.000	0.400	-0.273	0.101	0.292	159.7	0.085	-10.8	-8.2
0.60	0.000	0.450	-0.340	0.141	0.368	157.4	0.136	-8.9	-7.7
0.60	0.000	0.500	-0.402	0.107	0.416	165.9	0.173	-7.9	-7.5
0.60	0.200	0.550	-0.443	0.048	0.446	173.8	0.199	-9.4	-7.7
0.60	0.200	0.600	-0.475	-0.000	0.475	-180.0	0.226	-12.7	-8.1
0.60	0.200	0.650	-0.512	-0.015	0.513	-178.3	0.263	-14.0	-8.4
0.60	0.150	0.700	-0.538	0.018	0.538	178.0	0.290	-14.1	-8.4
0.60	0.150	0.750	-0.511	0.080	0.517	171.1	0.267	-12.2	-8.2
0.60	0.050	0.800	-0.420	0.108	0.442	165.9	0.195	-10.6	-8.1
0.60	0.150	0.850	-0.358	0.071	0.365	168.8	0.133	-10.0	-8.0
0.60	0.150	0.900	-0.345	0.015	0.345	177.5	0.119	-9.3	-8.0
0.60	0.100	0.950	-0.372	-0.011	0.373	-178.4	0.139	-8.6	-7.9
0.60	0.100	1.000	-0.402	-0.000	0.402	-180.0	0.161	-7.9	-7.9



DELTA = 0.010000

H, A, AND B IN TABLE BELOW ARE IN FRACTIONS OF A CYCLE. H = 4.40 RADIAN.
 FIRST LOSS ENTRY IS MAXIMUM LOSS, SECOND IS AVERAGE LOSS OVER A.
 A = 0. , I * 0.050 , 0.450

H	AMAX	B	ZR	ZI	MAG Z	ANG Z	/Z/XX2	LOSS(DB)	
0.70	0.250	0.050	-0.372	0.912	0.985	112.2	0.970	-0.8	-0.5
0.70	0.200	0.100	-0.377	0.927	1.001	112.1	1.001	-2.9	-1.4
0.70	0.200	0.150	-0.486	0.841	0.971	120.0	0.944	-6.3	-3.4
0.70	0.150	0.200	-0.608	0.620	0.868	134.5	0.754	-15.6	-6.9
0.70	0.150	0.250	-0.561	0.326	0.649	149.8	0.421	-24.7	-11.3
0.70	0.050	0.300	-0.351	0.174	0.391	153.6	0.153	-14.2	-9.4
0.70	0.050	0.350	-0.196	0.233	0.304	130.1	0.093	-10.5	-8.2
0.70	0.050	0.400	-0.218	0.310	0.379	125.1	0.144	-9.5	-7.6
0.70	0.000	0.450	-0.302	0.280	0.412	137.2	0.170	-9.0	-7.6
0.70	0.000	0.500	-0.342	0.185	0.389	151.6	0.152	-9.3	-7.9
0.70	0.200	0.550	-0.346	0.083	0.356	166.5	0.127	-11.8	-8.4
0.70	0.200	0.600	-0.348	-0.000	0.348	-180.0	0.121	-13.8	-8.7
0.70	0.200	0.650	-0.375	-0.052	0.379	-172.1	0.143	-12.0	-8.8
0.70	0.100	0.700	-0.418	-0.045	0.421	-173.8	0.177	-10.8	-8.8
0.70	0.050	0.750	-0.415	0.014	0.415	178.0	0.173	-10.7	-8.9
0.70	0.000	0.800	-0.344	0.050	0.348	171.7	0.121	-11.1	-9.0
0.70	0.200	0.850	-0.282	0.013	0.283	177.3	0.080	-11.0	-9.1
0.70	0.450	0.500	-0.287	-0.035	0.289	-173.1	0.084	-10.8	-9.2
0.70	0.400	0.950	-0.323	-0.036	0.325	-173.7	0.106	-10.2	-9.3
0.70	0.100	1.000	-0.342	-0.000	0.342	-179.9	0.117	-9.3	-9.3

TABLE OF Z(H,A,B) - 08 MAY 79

DELTA = 0.010000

H, A, AND B IN TABLE BELOW ARE IN FRACTIONS OF A CYCLE. H = 5.03 RADIAN.
 FIRST LOSS ENTRY IS MAXIMUM LOSS, SECOND IS AVERAGE LOSS OVER A.
 A = 0. , I * 0.050 , 0.450

H	AMAX	B	ZR	ZI	MAG Z	ANG Z	/Z/XX2	LOSS(DB)	
0.80	0.250	0.050	0.225	0.958	0.984	76.8	0.968	-1.0	-0.6
0.80	0.200	0.100	0.229	0.973	1.000	76.7	1.000	-3.9	-1.9
0.80	0.200	0.150	0.073	0.961	0.964	85.6	0.929	-9.7	-4.7
0.80	0.150	0.200	-0.168	0.814	0.831	101.6	0.690	-34.1	-11.2
0.80	0.050	0.250	-0.251	0.512	0.570	116.1	0.325	-16.5	-10.0
0.80	0.000	0.300	-0.105	0.320	0.337	108.2	0.113	-11.6	-8.5
0.80	0.050	0.350	0.003	0.365	0.365	89.5	0.134	-10.3	-7.9
0.80	0.050	0.400	-0.070	0.407	0.413	99.8	0.171	-11.4	-8.0
0.80	0.000	0.450	-0.161	0.320	0.358	116.7	0.129	-12.5	-8.6
0.80	0.000	0.500	-0.169	0.195	0.258	131.0	0.066	-15.4	-9.6
0.80	0.450	0.550	-0.132	0.087	0.158	146.7	0.025	-16.0	-10.6
0.80	0.450	0.600	-0.103	-0.000	0.103	-180.0	0.011	-19.8	-11.3
0.80	0.450	0.650	-0.113	-0.072	0.134	-147.4	0.018	-17.5	-11.9
0.80	0.400	0.700	-0.168	-0.034	0.193	-150.8	0.037	-18.2	-12.7
0.80	0.400	0.750	-0.196	-0.041	0.201	-168.1	0.040	-15.2	-13.4
0.80	0.450	0.800	-0.143	0.001	0.143	179.4	0.021	-16.9	-14.0
0.80	0.450	0.850	-0.092	-0.036	0.104	-159.8	0.011	-19.6	-14.6
0.80	0.200	0.900	-0.125	-0.073	0.144	-149.7	0.021	-19.4	-15.1
0.80	0.150	0.950	-0.165	-0.050	0.172	-163.2	0.030	-17.5	-15.3
0.80	0.150	1.000	-0.169	-0.000	0.169	-179.8	0.029	-15.5	-15.5

TABLE OF Z(H,A,B) - 08 MAY 79



DELTA = 0.010000

H, A, AND B IN TABLE BELOW ARE IN FRACTIONS OF A CYCLE. H = 5.65 RADIANs.
 FIRST LOSS ENTRY IS MAXIMUM LOSS, SECOND IS AVERAGE LOSS OVER A.
 A = 0. , I * 0.050 , 0.450

H	AMAX	B	ZR	ZI	MAG Z	ANG Z	/Z/**2	LOSS(DB)	
0.90	0.250	0.050	0.738	0.650	0.983	41.4	0.967	-1.2	-0.7
0.90	0.200	0.100	0.750	0.660	0.999	41.3	0.998	-5.1	-2.5
0.90	0.200	0.150	0.597	0.745	0.955	51.3	0.912	-13.7	-6.4
0.90	0.200	0.200	0.289	0.736	0.790	68.6	0.625	-21.5	-11.2
0.90	0.050	0.250	0.083	0.490	0.497	80.3	0.247	-12.9	-9.2
0.90	0.100	0.300	0.160	0.295	0.335	61.5	0.112	-11.3	-8.3
0.90	0.050	0.350	0.219	0.350	0.413	58.0	0.170	-12.7	-8.4
0.90	0.050	0.400	0.099	0.368	0.361	74.9	0.145	-17.6	-9.6
0.90	0.000	0.450	0.018	0.248	0.249	86.0	0.062	-22.0	-11.5
0.90	0.000	0.500	0.045	0.132	0.139	71.2	0.019	-27.0	-12.5
0.90	0.450	0.550	0.110	0.059	0.135	28.2	0.016	-13.1	-12.0
0.90	0.450	0.600	0.162	-0.000	0.162	-0.0	0.026	-15.8	-12.3
0.90	0.400	0.650	0.173	-0.070	0.186	-22.2	0.035	-14.6	-13.4
0.90	0.250	0.700	0.115	-0.116	0.164	-45.2	0.027	-18.0	-15.2
0.90	0.000	0.750	0.059	-0.070	0.093	-52.5	0.009	-21.3	-17.2
0.90	0.400	0.800	0.090	-0.028	0.094	-17.5	0.009	-22.7	-18.6
0.90	0.350	0.850	0.117	-0.066	0.124	-29.6	0.018	-27.3	-19.7
0.90	0.300	0.900	0.069	-0.090	0.114	-52.5	0.013	-33.7	-21.8
0.90	0.000	0.950	0.032	-0.049	0.058	-56.6	0.003	-29.0	-24.7
0.90	0.250	1.000	0.045	-0.000	0.045	-0.5	0.002	-27.0	-26.9

TABLE OF Z(H,A,B) - 08 MAY 79

DELTA = 0.010000

H, A, AND B IN TABLE BELOW ARE IN FRACTIONS OF A CYCLE. H = 6.28 RADIANs.
 FIRST LOSS ENTRY IS MAXIMUM LOSS, SECOND IS AVERAGE LOSS OVER A.
 A = 0. , I * 0.050 , 0.450

H	AMAX	B	ZR	ZI	MAG Z	ANG Z	/Z/**2	LOSS(DB)	
1.00	0.250	0.050	0.977	0.102	0.983	6.0	0.966	-1.5	-0.8
1.00	0.200	0.100	0.993	0.103	0.998	5.9	0.997	-6.5	-3.1
1.00	0.200	0.150	0.904	0.275	0.945	16.9	0.894	-20.4	-8.5
1.00	0.050	0.200	0.612	0.430	0.748	35.1	0.559	-17.1	-10.3
1.00	0.000	0.250	0.324	0.292	0.436	42.0	0.190	-11.9	-8.8
1.00	0.100	0.300	0.346	0.125	0.368	19.9	0.135	-13.6	-8.7
1.00	0.050	0.350	0.366	0.209	0.422	29.7	0.178	-18.7	-10.2
1.00	0.050	0.400	0.217	0.215	0.306	44.7	0.093	-31.5	-12.6
1.00	0.000	0.450	0.163	0.092	0.187	29.3	0.035	-17.3	-11.5
1.00	0.000	0.500	0.220	0.021	0.221	5.3	0.049	-13.2	-10.9
1.00	0.350	0.550	0.292	0.009	0.292	1.8	0.085	-11.2	-10.8
1.00	0.100	0.600	0.349	-0.000	0.349	-0.0	0.122	-11.1	-11.3
1.00	0.100	0.650	0.378	-0.047	0.361	-7.1	0.145	-15.9	-12.0
1.00	0.250	0.700	0.332	-0.108	0.350	-18.0	0.122	-15.2	-12.2
1.00	0.150	0.750	0.255	-0.084	0.268	-18.2	0.072	-15.1	-12.4
1.00	0.100	0.800	0.265	-0.034	0.271	-7.2	0.074	-19.3	-12.9
1.00	0.100	0.850	0.281	-0.074	0.290	-14.7	0.084	-19.1	-13.3
1.00	0.050	0.900	0.219	-0.084	0.235	-21.1	0.055	-17.4	-13.3
1.00	0.000	0.950	0.193	-0.033	0.196	-9.7	0.038	-14.9	-13.2
1.00	0.000	1.000	0.220	-0.000	0.220	-0.0	0.048	-13.2	-13.1



APPENDIX B

DR. ELLINTHORPE'S REPLY ■

BY MUTUAL AGREEMENT, THE LETTER
GIVEN IN THIS APPENDIX IS CLASSIFIED ■■■■■.



NAVAL UNDERWATER SYSTEMS CENTER
HEADQUARTERS
NEWPORT, RHODE ISLAND 02840

NEWPORT, R. I. 02840
AREA CODE 401
841 - EXT.
AUTOVON 948 + EXT.
NEW LONDON, CONN. 06320
AREA CODE 203
442 - 0771 - EXT.
AUTOVON 636 + EXT. 4179

IN REPLY REFER TO:
3103:AWE:bj
9460/MACS
Ser 93103-67
8 June 1979

Dr. Christopher V. Kimball
University of Miami
School of Marine and Atmospheric Science
4600 Rickenbacker Causeway
Miami, Florida 33149

Ref: (a) "Comments on the MACS Coherence Time Measurements" by C. V. Kimball
dated 21 May 1979
(b) Your letter dated 22 May 1979

Dear Chris:

- This is a response to reference (a) which was forwarded by reference (b).
- The MACS measurements were undertaken with the foreknowledge that they could examine only limited regions of the multi-dimensional space which is needed to describe underwater acoustic propagation, but with the expectation that the results could be extended by physical explanations to span the global regions of interest for tactical ship to ship links. The reports cited by reference (a) are deliberately restricted in their contents to a recitation of the empirical results; the generalizations through physical theories cannot be conducted on a piecemeal basis but must incorporate the whole of the data and a great deal of other work besides, and that phase of the work is far from complete.
- Reference (a) deals with only one parameter, time coherence; asserts the reported results to be due to either platform motion or improper processing procedures; proposes that a cautionary statement be distributed to warn of there "defects"; and asserts that the inclusion of tone transmissions would have remedied the matter.
- My first concern is the narrowness of reference (a)'s considerations in both its overall viewpoint and in several of its details. The history of underwater sound work is bedevilled by similar failures to confront the fact that the processes being studied result from a complex coupling of many effects whose disentanglement is a difficult and delicate task; to overlook that coupling is an impermissible and grossly misleading simplification.
- For example, the restriction of interest to time coherence leads to reference (a)'s recommendation that tones be included as a means of cleansing the MACS defects. They were in fact included but the results have not been

3103:AWE:bj
9460/MACS
Ser 93103-67

- reported because of the obscurity of their significance, a property which is a consequence of the inability to discern multipath effects in tone data. In other words, the time and frequency domains cannot be decoupled. This disagreeable fact is reflected in the prescriptions of channel characterization theory which are that measurement probes can be constructed of sequences of pulses, or groups of tones, or their union in the form of pseudo-noise; and the three are formally equally efficient. (It was convenient to use pulses in the MACS work.)
- Reference (a) is, of course, correct in pointing out that platform motion perturbations contribute to the observed coherence time results. Other contributions, ignored by reference (a), are; the modulations imposed by reflection from a stormy surface; the effects of platform motion coupling with scattering (from rough bottom topography, from within bottom sediments, or from within the volume); and the effects of internal wave motion. Our responsibility is to define all of these contributions quantitatively, in both physical terms and in their effects on system performance.
- As a matter of possible interest, platform motion perturbations are caused by helmsman behavior and are frustratingly non-stationary, depending on the time within the watch and on the particular watchstander. The worst case magnitude is about 1° to 2° rms (as reference (a) correctly assumes) with a time constant of about 100 seconds. That magnitude is similar to the magnitude of the minimum spread induced by a single reflection from a rough bottom. (The minimum occurs at the extreme range attainable by a single reflection where the grazing angle is minimized.) Multiple bottom reflections (encountered at greater ranges) or steep angle reflections (encountered at shorter ranges) produce larger spreads by a factor of two or more. The time constant of the bottom reflection process is about two orders of magnitude shorter than that of the motional perturbations at speeds and frequencies of operational interest. The surface induced effects are even worse.
- Thus, reference (a) is broadly correct in its discussion of the effects of motional perturbations, but in ignoring the other more important phenomena it misrepresents reality; motional perturbations are a minor factor.
- In the matter of the procedures used to remove the gross motional effects, reference (a)'s algebra is correct but its premises aren't. The issue (not addressed by reference (a)) is a problem inherent to measurements made between moving ships, the situation that the Navy is all about. It is that the velocity vectors cannot be closely controlled; the two ships can find themselves in different current fields, or have different gyro errors, or have different errors in their speed sensors. As a result, the path length varies in both a stochastic manner and, as a result of corrective action by the receiving ship (where bearing and travel time information are available), in a deterministic manner. The time scales associated with these trends are in the hundreds of seconds whereas thousands of seconds of data are needed to obtain adequately low variance estimates of the propagation parameters.

3103:ANE:bj
9460/MACS
Ser 93103-67

■ Thus the trends have to be removed, and in a way which doesn't corrupt the results. The procedure that has been followed has been to fit a polynomial to the arrival times, and a key issue is the choice of time constant for the polynomial. If it is too small then some of the real propagation changes will be inadvertently removed, and if it is too large then spurious doppler effects will be leaked into the data. The time constant has been chosen at around 100 seconds, in part on the twin grounds that it is smaller than the gross path length changes and is of the order of the time duration of operational use for either tactical communications or echo ranging.

■ The notion of transit time in a fading channel is beset by the problem that in the presence of a fade there can be no definition of any such quantity. The issue is a fundamental one, having to do with the definition of group or energy velocity which itself collapses at transmission nulls. (Stratton's book treats the matter carefully.) Thus a plot of arrival time is, by any measure, certain to exhibit spikes whenever the signal amplitude falls to zero. One cannot in fact speak of anything more than the arrival time obtained by averaging over some suitable interval because, in general, the several modes fade independently. The choice of about 100 seconds in the fitting procedure was therefore based on having many pulse arrivals to form this average, in addition to the other considerations cited earlier.

■ Reference (a) ignores these points and assumes that the variance in the arrival time estimates represents an error in fitting procedure and, having set up that straw man, proceeds to show that such an error would be intolerable. Of course it would be, but it is not such an error and reference (a)'s discussion of this matter is thus irrelevant.

■ In addition to the above generalities, reference (a) contains a number of particular points that are objectionable:

● In the sentence which begins at the foot of page 1 and terminates at the top of page 2 it is asserted that -- "a large TW system offers significant (~ 10 dB) performance advantages --". The basis for this remark is unclear. The criterion for gauging system performance is commonly accepted to be the minimization of the energy required to transmit a unit of information, and that criterion is not satisfied by maximizing the single parameter, integration time. Even in that simplistic case the unique figure 10 dB is not discernible; the allowable coherent time is simply inversely proportional to center frequency and there are no discontinuities.

● The last sentence of the first complete paragraph on page 2 says that - 'a more suitable transmission waveform -- ' will be suggested. As explained earlier this is a false claim.

3103:AWE:bj
9460/MACS
Ser 93103-67

• In the paragraph at the top of page 3 and in several subsequent paragraphs mention is made of the fact that the sampling interval was equivalent to 2 carrier periods at 500 Hz. This citation appears to reflect an ignorance of the sampling theorem; the sampling rate was 2.5 times the bandwidth. (It was also equivalent to 20 carrier periods at 5000 Hz, a number that is more striking than 2.)

• The discussion of section 4 shows that a slowly varying phase modulation is easily overcome. This is true but irrelevant because of the other time constants already noted.

Sincerely,



A. W. ELLINTHORPE

